Dissertations, Theses, and Masters Projects   Theses, Dissertations, & Master Projects

1999

Nitrate reduction at the groundwater - salt marsh interface

Craig -1967 Tobias
College of William and Mary - Virginia Institute of Marine Science

INFORMATION TO USERS

This manuscript has been reproduced from the microfilm master. UMI films the text directly from the original or copy submitted. Thus, some thesis and dissertation copies are in typewriter face, while others may be from any type of computer printer.

The quality of this reproduction is dependent upon the quality of the copy submitted. Broken or indistinct print, colored or poor quality illustrations and photographs, print bleedthrough, substandard margins, and improper alignment can adversely affect reproduction.

In the unlikely event that the author did not send UMI a complete manuscript and there are missing pages, these will be noted. Also, if unauthorized copyright material had to be removed, a note will indicate the deletion.

Oversize materials (e.g., maps, drawings, charts) are reproduced by sectioning the original, beginning at the upper left-hand corner and continuing from left to right in equal sections with small overlaps. Each original is also photographed in one exposure and is included in reduced form at the back of the book.

Photographs included in the original manuscript have been reproduced xerographically in this copy. Higher quality 6" x 9" black and white photographic prints are available for any photographs or illustrations appearing in this copy for an additional charge. Contact UMI directly to order.

UMI®

NITRATE REDUCTION AT THE GROUNDWATER - SALT MARSH INTERFACE

A Dissertation
Presented to
the Faculty of the School of Marine Science
of the College of William and Mary

in Partial Fufillment
of the Requirements for the Degree of
Doctor of Philosophy

----

by

Craig Robert Tobias

1999

UMI Number: 9942559

UMI
300 North Zeeb Road
Ann Arbor, MI 48103
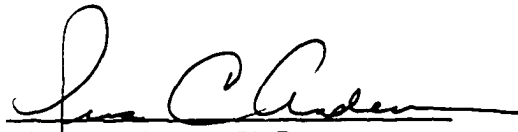
APPROVAL SHEET
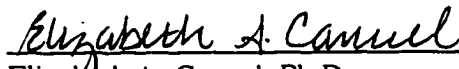
This dissertation is submitted in partial fulfillment of the requirements for the degree of

Doctor of Philosophy
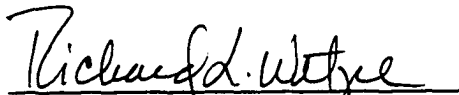
Craig Robert Tobias
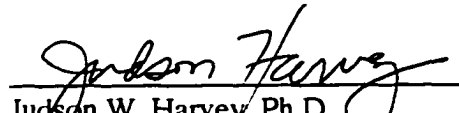
Approved, June 28, 1999
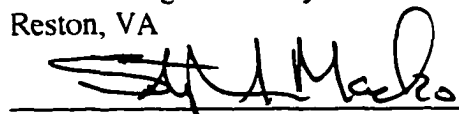
Iris C. Anderson, Ph.D.
Committee Co-Chair/Advisor

Elizabeth A. Canuel, Ph.D
Committee Co-Chair/Advisor

Hugh, W. Ducklow, Ph.D

Richard L. Wetzel, Ph.D

Judson W. Harvey, Ph.D
U.S. Geological Survey
Reston, VA

Stephen A. Macko, Ph.D
Department of Environmental Science
University of Virginia
Charlottesville, VA

DEDICATION

This dissertation is dedicated to my parents, without whom I would neither be alive, nor

care about the way the world works.

TABLE OF CONTENTS

SECTION III. Tracking the Fate of a High Concentration Groundwater Nitrate Plume Through a Fringing Marsh: A Combined Natural Gradient Tracer and In Situ Isotope Enrichment Study

ACKNOWLEDGEMENTS

LIST OF TABLES

LIST OF FIGURES

ABSTRACT

The influence of groundwater discharge on the hydrology and biogeochemical cycling of nitrogen (specifically nitrate reduction) in a fringing intertidal wetland was studied through the estimation of seasonal groundwater discharge, the determination of nitrogen cycling rates in isolated cores, and characterization of *in situ* nitrate reduction pathways using combined[15]N enrichment and natural gradient tracer techniques.

Groundwater discharge into a fringing mesohaline saltmarsh was estimated by three independent methods including Darcy's Law, a combined water and salt mass balance over an annual cycle, and a subsurface tracer test during a period of high flow. Seasonal patterns of discharge predicted by both Darcy's Law and the water and salt balance yielded similar seasonal patterns with discharge maxima and minima in April and September, respectively. Water inputs to the wetland subsurface were dominated by horizontal groundwater flux in the Spring and tidal infiltration in the Autumn. Water export from the subsurface was dominated by drainage to the estuary for the entire year except August when evapotranspiration was the major route of loss. Darcy's Law calculations indicated up to twice the discharge compared with the mass balance estimates during high flow (Spring), and less than half the mass balance derived estimates at low flow (Autumn). Based upon the comparison with tracer results and estimates of error, we suggest that water and salt mass balance provided the more reasonable estimate of groundwater flux at high flows, and Darcy techniques were better estimates of flow at lower flux magnitudes at our site. Tracer test results performed at high discharge agreed with the mass balance estimates of discharge at that time. The high discharge and the high percentage of groundwater flux to the total water budget from February to May indicated a seasonal purging of porewater and solutes from the marsh to the estuary, and suggests that any marsh processing of groundwater derived solute loads are likely to occur only during this period.

Multiple N-cycling processes were quantified in isolated cores collected under conditions of negligible groundwater-derived nitrate loading. Rates of mineralization, nitrification, potential denitrification (DNF), and potential dissimilatory nitrate reduction to ammonium (DNRA) were estimated along with porewater concentrations of oxygen, sulfide, and conductivity during periods of high (May 1997) and low (October 1997) groundwater discharge. All N cycling processes were confined to the upper 1-1.5 meters of marsh where organic matter and ammonium were most abundant. Depth integrated rates for mineralization, nitrification, DNRA, and DNF ranged between 0.97 -11.20, 0.00 - 2.16, 0.88 -6.13, and 1.84 -17.62 mmoles N m^{-2} hr^{-1} respectively. Mineralization, measured in cores using the isotope dilution technique, was the dominant process, exceeding nitrification by 3 - 20 fold. Natural abundance $\delta^{15}N$ measurements of the ammonium, particulate organic nitrogen, nitrate, and molecular nitrogen pools suggested that in situ nitrification rates were of similar magnitude (relative to mineralization) as determined by core experiments, and that coupled nitrification - denitrification was a sizeable sink for mineralized N. During Spring discharge (May) marsh porewater

PROJECT OVERVIEW

NITRATE REDUCTION AT THE GROUNDWATER - SALT MARSH INTERFACE

BACKGROUND AND JUSTIFICATION

Groundwater has been recognized as an important non-point source of freshwater and nitrogen to nearshore ecosystems yet there is only cursory knowledge of the patterns of groundwater discharge into estuaries, and little is understood about the behavior of nitrogen at the aquifer - estuary interface. Nitrogen budgets constructed for New England marshes and bays (Howes et al. 1996; Valiela et al. 1992; Wieskel and Howes 1991), Chesapeake Bay and its sub-estuaries (Libelo et al. 1990; Simmons 1989; Bachman 1994), Long Island Sound, NY (Capone and Bautista 1985), and Tomales Bay, CA (Oberdorfer and Smith 1990) have suggested the importance of groundwater in the overall nitrogen mass balance. With the exception of budgets constructed from surface water base-flow measurements (Bachman 1994), or validated with porewater concentrations (Giblin and Gaines 1990; Brock et al. 1982), groundwater nitrogen input estimates have been constructed historically by coupling water flux calculations (based on hydraulic head and conductivity, seepage rates, or soil moisture budgets) with nitrate concentrations measured in aquifers or springs, or estimated from nitrogen application rates. Consequently the nitrate transport through the aquifer - estuary interface is often assumed to be conservative. Estimates which have not considered potential changes in speciation and concentration of nitrogen upon discharge may tend to over-emphasize the importance of groundwater-borne nitrogen.

One such discharge interface exists at the ecotone between the aquifer and marsh-fringed estuaries. Because of density differences between fresh groundwater and saline estuarine water, discharge into the coastal environment, excluding base flow into non-tidal streams, is concentrated in intertidal or nearshore subtidal zones (Reilly and Goodman 1985; Bokuniewicz 1992). Along the eastern North American coast, these zones consist of either intertidal / nearshore sediments, or fringing wetlands. In particular, emergent

wetlands occupy 79 % of Virginia's 8195 km shoreline Hobbs 1979). These ecosystems are therefore positioned within the landscape to potentially receive much of the groundwater discharge prior to entry into adjacent estuaries. Nitrate is usually the dominant nitrogen species in shallow oxidized groundwater (Fetter 1993), and marshes typically demonstrate a large capacity to process allochthonous nitrate (Kaplan et al. 1979). Consequently, they have been suggested as important buffers for groundwater derived nitrogen loads (Harvey and Odum 1990; Howes et al. 1996), and thus, regulators of estuarine water quality.

Although the potential of marshes to buffer estuaries against groundwater nitrogen loads has received some attention, the importance of this function remains in question (Howes et al. 1996; Portnoy et al. 1998). In order for these ecosystems to significantly attenuate groundwater nitrogen loads they must both: 1) receive a large proportion of the total groundwater discharged to the estuary and 2) process and export the groundwater N out of the estuarine landscape.

Groundwater discharge into wetlands is driven by multiple factors including: water table elevation, sediment hydraulic conductivity, frequency of tidal inundation, and evapotranspiration (Winter and Woo 1990; Harvey and Odum 1990; Nuttle and Harvey 1995). Given this complexity, few confident estimates of groundwater discharge into tidal marshes have been derived, and temporal variability has not been addressed.

As groundwater contacts anaerobic marsh sediments, nitrate can be attenuated through macrophyte uptake, assimilatory nitrate reduction into bacterial biomass, dissimilatory reduction to ammonium ($NO_3^- \rightarrow NH_4^+$), or denitrification ($NO_3^- \rightarrow N_2$). Of these, denitrification, is the only mechanism which insures that N will not be exported to the estuary. Although most previous studies have considered denitrification as the

primary nitrate reduction process operating in marshes, reduction to ammonium, in some organic-rich sediments can be the favored pathway of nitrate reduction (Koike and Sorenson 1988). Determining the relative proportion of nitrate reduced via denitrification vs. dissimilatory reduction to ammonium is critical for estimating the amount of groundwater derived N exported to the atmosphere or retained in the ecosystem.

Most of the investigations of the interaction between groundwater and marshes focussed on groundwater discharge that was anthropogenically enriched in nitrate (Howes et al. 1996). However, not all groundwater contains elevated nitrogen concentrations, and the effects of discharge on the internal cycling of autochthonous nitrogen in marshes, and implications for marsh function or sustainability within the landscape have been largely overlooked. In addition to their potential role in anthropogenic N attenuation, intertidal wetlands must balance accretion and subsidence to keep pace with eustatic sea level rise (Stevenson et al. 1986). The high production observed in marshes is maintained by tight cycling and conservation of nitrogen within the ecosystem, and the influence of fresh groundwater inputs on these processes has not been well documented. Consequently, it is not known if groundwater discharge increases, or decreases, the sustainability of marshes within the estuarine landscape.

Therefore, uncertainties in estimating total groundwater flux through wetlands, as well as the magnitude and mechanisms of nitrogen processing during discharge need to be resolved before any unifying conclusions about the nature of marsh-groundwater interactions can be reached. It is essential that these interactions be assessed both from a water quality perspective (do marshes acting as buffers against groundwater N loads?), and from a marsh ecology perspective (does groundwater, with or without N, affect nitrogen cycling, storage, and export in the marsh?).

The objectives of this dissertation were to: 1) examine seasonal patterns of groundwater discharge within a marsh discharge zone, 2) characterize autochthonous N cycling in the discharge zone during a period of low, and high groundwater discharge, and 3) determine the fate of groundwater-derived NO_3^- during discharge through the marsh. Each of these objectives will be addressed individually in the following three sections.

LITERATURE CITED

Bachman, L.J. 1994. Nitrogen loads to Chesapeake Bay from groundwater. Chesapeake Bay Research Conference - toward a sustainable coastal watershed: The Chesapeake Experiment. p. 53

Bokuniewicz, H. J. 1992. Analytical descriptions of subaqueous groundwater seepage. Estuaries. 15: 458-464.

Brock, T.D., D.R. Lee, D. James, and D. Winek. 1982. Groundwater seepage as a nutrient source to a drainage lake: Lake Mendota, Wisconsin. Water Research. 16: 1255-1263.

Capone, D.G., and M.F. Bautista. 1985. A groundwater source of nitrate in nearshore sediments. Nature. 313: 214-216.

Fetter, C.W. 1993. Contaminant Hydrogeology. Macmillan Publishing.
Giblin, A.E., and A.G. Gaines. 1990 Nitrogen inputs to a marine embayment: the importance of groundwater. Biogeochemistry. 10: 309-328.

Harvey, J.W., and W.E. Odum. 1990. The influence of tidal marshes on upland groundwater discharge to estuaries. Biogeochemistry. 10: 217-236.

Hobbs, C.H. 1979. Summary of shoreline situation reports of Virginia's Tidewater localities. Special Report: Appl. Mar. Sci and Ocean Eng. 209

Howes, B.L., P.K.Weiskel,D.D. Goehringer, and J.M. Teal. 1996. Interception of freshwater and nitrogen transport from uplands to coastal waters: the role of saltmarshes. p. 287-310. *In* K.F. Nordstrom and C.T. Roman [eds.] Estuarine shores: evolution, environments and human alterations. John Wiley and Sons.

Kaplan, W., I. Valiela, and J.M. Teal. 1979. Denitrification in a salt marsh ecosystem. Limnol. and Oceanog. 24: 726-734.

Koike, I., and J. Sorenson. 1988. Nitrate reduction and denitrification in marine sediments, p. 251-270. *In* T. Blackburn and J. Sorenson [eds.], Nitrogen cycling in the coastal marine environments. John Wiley and Sons.

Libelo, E.L., W.G. MacIntyre, and G.H. Johnson. 1990. Groundwater nutrient discharge to the Chesapeake Bay: Effects of near-shore land use preactices. New perspectives in the Chesapeake System: A research and management partnership. 613-622.

Nuttle, W.K., and J.W. Harvey. 1995. Fluxes of water and solute in a coastal wetland sediment. 1. The contribution of regional groundwater discharge. J. Hydrol. 164: 89-107.

Oberdorfer, J.A., M.A. Valentino, and S.A. Smith. 1990. Groundwater contribution to the nutrient budget of Tomales Bay, California. Biogeochemistry 10: 199-216.

Portnoy, J.W., B.L. Nowicki, C.T. Roman, and D.W. Urish. 1998. The discharge of nitrate-contaminated groundwater from a developed shoreline to a marsh-fringed estuary. Wat. Res. Res. 34: 3095-3104.

Reilly, T.E., and A.S. Goodman. 1985. Quantitative analysis of saltwater-freshwater relationships in groundwater systems--A historical perspective. J. Hydrol. 80: 125-160.

Simmons, G.M. 1989. The Chesapeake Bay's hidden tributary: submarine groundwater discharge. p. 9-29. *In* Proceedings of groundwater issues and solutions in the Potomac River Basin / Chesapeake Bay Region.

Stevenson, J.C., L.G. Ward, and M.S. Kearney. 1986. Vertical accretion in marshes with varying rates of sea level rise. *In*: Estuarine Variability, Academic Press. 241-259.

Valiela, I., K. Foreman, M. LaMontage, D. Hersh, J. Costa, P. Peckol, B. DeMeo-Andreson, C. D'Avanzo, M. Babione, C. Sham, J. Brawley and K. Lajtha. 1992. Couplings of watersheds and coastal waters: sources and consequences of nutrient enrichment in Waquoit Bay, Massachussettes. Estuaries. 15: 443-457.

Weiskel, P.K., and B.L. Howes. 1992. Differential transport of sewage-derived nitrogen and phosphorous through a coastal watershed. Env. Sci. Tech. 26: 352-360.

Winter, T.C., and M.K. Woo. 1990. The hydrology of lakes and wetlands. *In*: M.G. Wolman, and H.C. Riggs [eds.], Surface Water Hydrology. Geologic Society of North America.

SECTION I

Estimating Groundwater Discharge Through Riparian Wetlands to Estuaries: A
Comparison of Methods and Implications for Marsh Function†

ABSTRACT

Fringing wetlands have long been considered critical in the regulation of nutrient exchange with the estuary both as a potential source of materials, and as a filter attenuating watershed nutrient fluxes. Because groundwater has become recognized as a potentially important nutrient source to coastal systems, defining the degree of interaction between groundwater and these ecosystems is essential. Groundwater discharge into a fringing mesohaline saltmarsh was estimated by three independent methods including Darcy's Law, a combined water and salt mass balance over an annual cycle, and a subsurface tracer test during a period of high flow. Seasonal patterns of discharge predicted by both Darcy's Law and the water and salt balance yielded similar seasonal patterns with discharge maxima and minima in April and September, respectively. Water inputs to the wetland subsurface were dominated by horizontal groundwater flux in the Spring and tidal infiltration in the Autumn. Water export from the subsurface was dominated by drainage to the estuary for the entire year except August when evapotranspiration was the major route of loss. Darcy's Law calculations indicated up to twice the discharge compared with the mass balance estimates during high flow (Spring), and less than half the mass balance derived estimates at low flow (Autumn). Based upon the comparison with tracer results and estimates of error, we suggest that water and salt mass balance provided the more reasonable estimate of groundwater flux at high flows, and Darcy techniques were better estimates of flow at lower flux magnitudes at our site. Tracer test results performed at high discharge agreed with the mass balance estimates of discharge at that time. The high discharge and the high percentage of groundwater flux to the total water budget from February to May indicated a seasonal purging of porewater and solutes from the marsh to the estuary, and suggests that any marsh processing of groundwater derived solute loads are likely to occur only during this period. The observed seasonal dominance of

groundwater in the subsurface water balance concurrent with the groundwater-driven export of solutes, and the wetland's potential to modify groundwater prior to discharge, suggests that groundwater may be an important link between these ecosystems and estuarine water quality.

INTRODUCTION

Wetlands have been suggested as potential regulators of nutrient fluxes with nearby coastal systems acting both as sources of, and sinks for, organic and inorganic nitrogen and phosphorous (Jordan et al. 1983). Hydrological balances mediate chemical fluxes between the marsh and the adjacent estuary, but often all components of the water balance are not well characterized (Yelverton and Hackney 1986; Whiting and Childers 1989). LaBaugh (1986) suggested that uncertainties in wetland chemical flux budgets arise primarily from uncertainties in the water balance.

The magnitude and pattern of groundwater discharge through intertidal riparian wetlands may also be instrumental in structuring macrophyte ecology and regulating nutrient inputs to adjacent estuaries. Porewater salinity, controlled in part by groundwater discharge, has been shown to be a good co-predictor for the distribution of common marsh halophytes. The dominant saltmarsh macrophyte (*Spartina spp*) demonstrates increased productivity in response to heightened porewater flushing and lower porewater salinities (Hackney et al. 1996; Bradley and Morris 1991; Wiegert et al. 1983).

The nature of the hydrological interaction between groundwater fluxes of nitrogen and riparian intertidal wetlands has been particularly difficult to define. Marshes typically demonstrate a high potential for nitrogen attenuation through denitrification or uptake, and occupy much of the temperate intertidal shoreline of trailing continental edges (eg. 79% of Virginia's 8195 km shoreline is bordered by emergent wetlands; Hobbs 1979). Intertidal and nearshore subtidal areas tend to be the zones of maximal groundwater discharge along coastal margins not dominated by karst features (Bokuniewicz 1992; Reilly and Goodman 1985; Cable et al. 1997). Consequently the importance of fringing wetlands in attenuating

groundwater derived nitrogen loads has been suggested (Harvey and Odum 1990). There is however, mounting evidence that groundwater often passes underneath wetland sediments and discharges directly to adjacent creek bottoms or through erosional creekbends which cut into the aquifer (Portnoy et al. 1997, Bohlke and Denver 1995, Anderson et al. 1997) Therefore, quantifying the groundwater flux directly to the wetland (relative to the total groundwater discharge to the estuary) becomes the critical element in assessing the relative importance of marshes in buffering the estuary against groundwater nitrogen loads. Despite the potential importance of this flux, there is only cursory knowledge of the magnitude and patterns of discharge and few attempts have been made to quantify the groundwater flux into intertidal wetlands on an annual cycle.

The two approaches most often used to estimate groundwater discharge into wetlands are based on Darcy's Law; or based on mass balances of water or solutes. Darcy's Law estimates are derived from measurements of hydraulic head, and estimates of hydraulic conductivity. Calculating a water flux using this approach often assumes homogeneity in sediment properties, and steady flow conditions. Errors include those that arise due to sediment heterogeneity, macropore flow, and tidally fluctuating heads encountered in most intertidal wetlands (Harvey and Nuttle 1995; Winter 1981; Hemond and Fifield 1982). Models that solve time-varying equations of groundwater flow are useful in situations where tidal fluctuations cause rapid changes in the magnitude and direction of groundwater fluxes (Harvey et al. 1987). Nevertheless, resulting groundwater discharge estimates often contain large errors, and probably do not represent the flow of solely fresh groundwater into the system.

Mass balance methods have the advantage that errors are typically smaller than erors in estimating hydraulic conductivity. However, a greater number of parameters typically

need to be estimated for the mass balance method. Uncertainties in individual terms of the water balance propogate through the calculation and increase the uncertainty of the groundwater flux estimate when it is calculated by difference. Water and solute mass balances can yield groundwater discharge estimates whose total error is less than that of Darcy derived fluxes alone (Hunt et al. 1996; Gehrels and Mulamoottil 1990). The combined mass and water balance approach shows the greatest utility when the system is well-mixed, the number of inputs and outflows is limited, and steady state assumptions can be made (Harvey et al. 1995; Morris 1995, Hunt et al. 1996). Still, in some wetlands, one or more terms of the water balance need to be derived from a Darcy derived flux calculation (Harvey and Odum 1990).

To our knowledge, a coupled water and solute mass balance approach has not previously been used to estimate transient and seasonal groundwater fluxes through riparian intertidal wetlands. In this study, we used three independent methods to estimate the groundwater flux into a mesohaline marsh near the upland/marsh border. Gradient - conductance calculations (Darcy's Law) and coupled water and solute balance approaches were used to provide estimates of groundwater discharge over an annual cycle, and a conservative tracer injection was used to empirically estimate the discharge rate during a period of high flow. This study was conducted as part of a larger project designed to examine the role of biogeochemical processes in modifying groundwater nitrate loads.

SITE DESCRIPTION AND METHODS

The study site is located in the Colonial National Historical Park (37° 16' 42" N , 76° 35' 16" W) on the Ringfield Peninsula near the confluence of King Creek and the York River in southeastern Virginia (Figure 1). The forested upland slope of approximately 1:1 grades through a mixed community of *Spartina cynosuroides* and *Spartina alterniflora* (short form) into a monotypic *S. alterniflora* (short form) fringing marsh approximately 25 meters in width. Upland geology and marsh evolution near the site are discussed in Libelo et al. (1990) and Finkelstein and Hardaway (1988), respectively. The small scale marsh stratigraphy consists of the upper 30 -80 cm of sandy marsh peat underlain by a semi-continous layer (10-20 cm thick) of lower permeability glauconitic silty sand. Below 150-200 cm the glauconitic deposits grade into cleaner oxidized iron-rich sands and shell hash of pre-Holocene origin. The study area borders the mesohaline portion of the York River (salinity range 12-21 ppt). Subsurface porewater conductivity decreases with depth and the conductivity is lowest during the Spring (Figure 2). Research instrumentation consisted of four upland water table wells and four parallel transects of multilevel piezometers extending perpendicular from the upland marsh border twenty meters out into the marsh (Figure 1). The multilevel piezometers were arranged into clusters of four-five with the depths at the base of the screens ranging from 50 -250 cm in 50 cm intervals (Figure 1). Piezometers and upland wells were installed with a 7.6 cm diameter auger, placement of a fine sandpack around the screens, sealed with a bentonite plug above the sandpack, and backfilled with auger cuttings. All piezometers and wells were constructed of 1" pvc with a screened interval of 50 cm using 0.01" slot screen. Boardwalks were constructed over the marsh between piezometer clusters.

Figure 1. Site location and schematic showing multi level piezometer grid. Outer transects and the upland piezometer were used for water level and salinity measurements. The inner two transects were sampled for salinity only

Chesapeake Bay

78°W   77°W   76°W   75°W   74°W

YORK RIVER

N

King Creek

Ringfield
Peninsula

PLAN VIEW
not to scale

Marsh   Upland

piezometer clusters

CROSS SECTION
not to scale

Marsh   border   Upland

PLAN VIEW
not to scale

● = piezometer
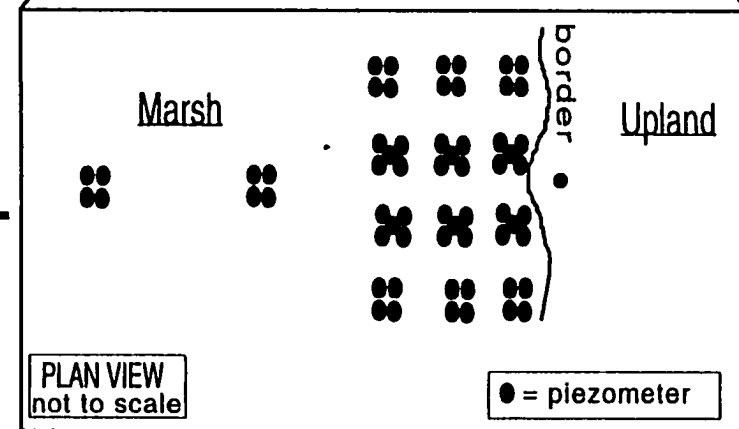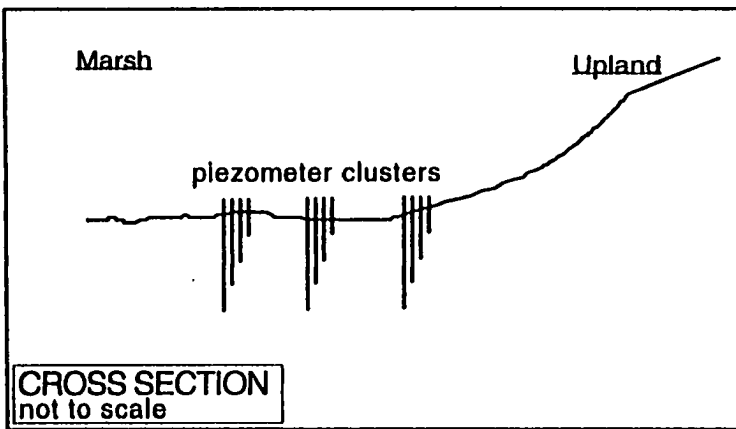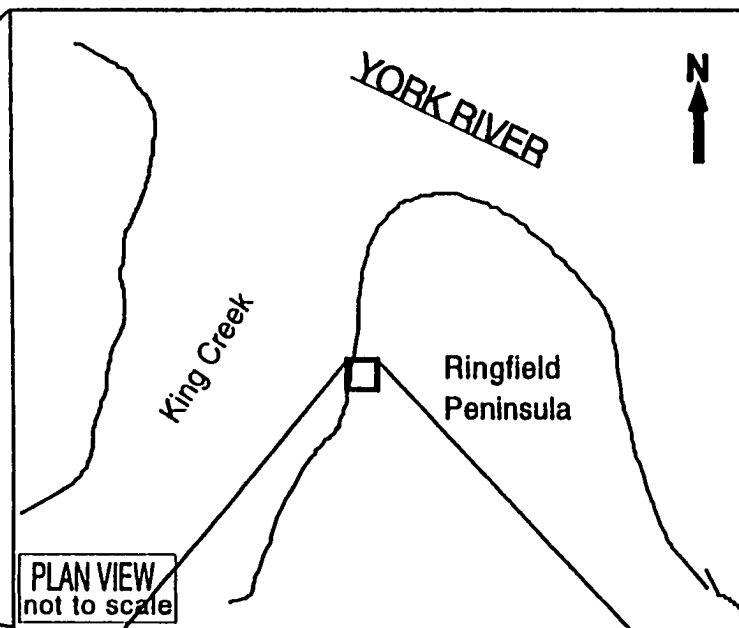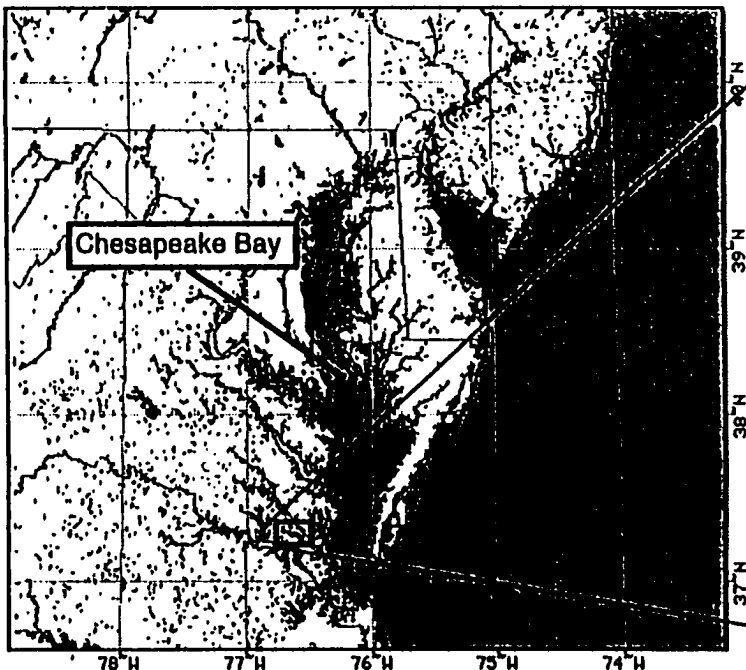
Figure 2. Distribution of subsurface conductivity at periods of high (May 1997) and low

(October 1997) groundwater flow. Positive "shore normal" distance is marshward. Shore

normal distance is equal to zero at the upland border. Sampling point locations (squares)

indicate the depth of the center of the 50 cm piezometer screen. The conductivity of tidal

water was 23.2 and 34.6

mS cm^{-1} for May and October, respectively.
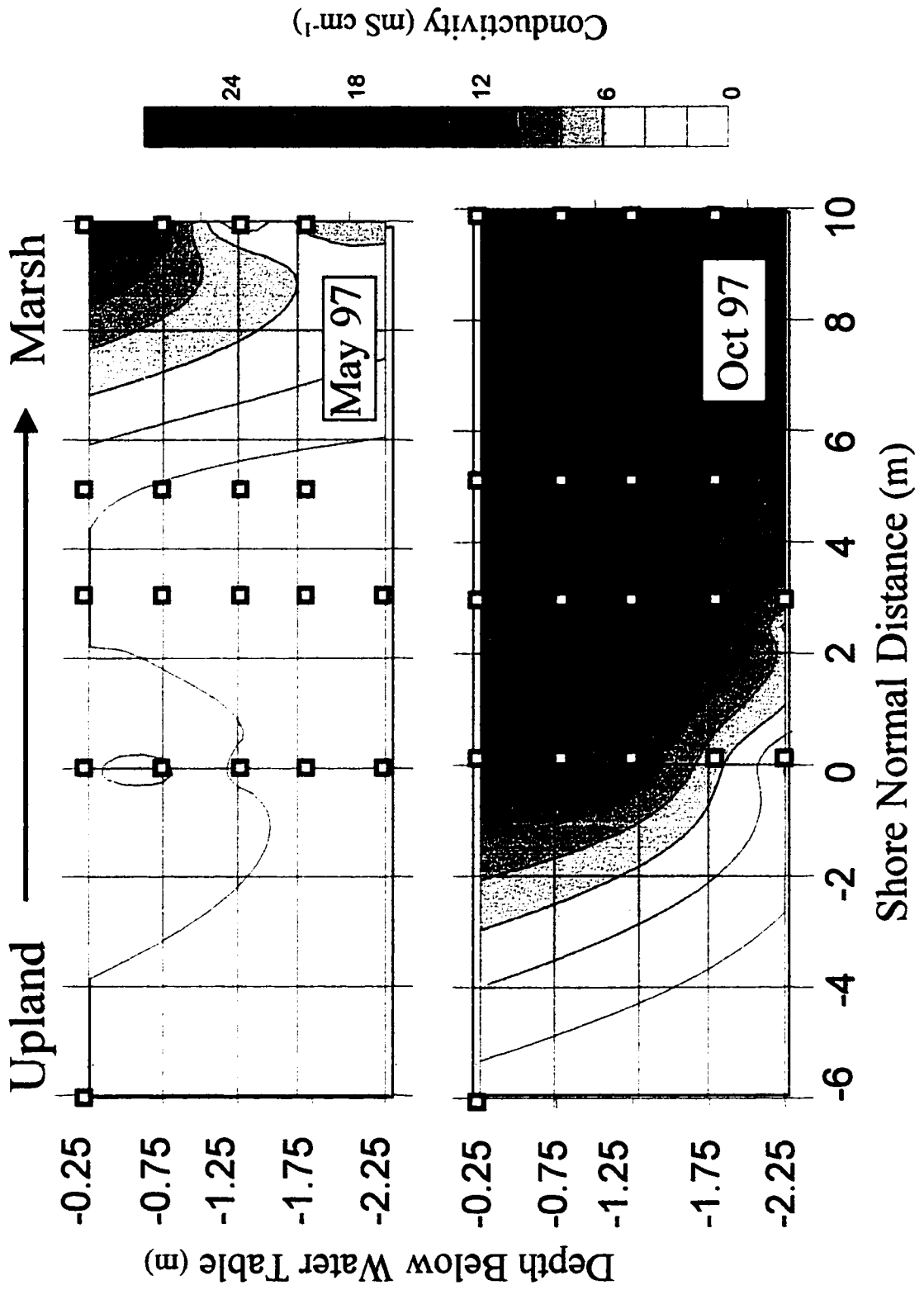
Methods of Estimating Groundwater Discharge

Darcy's Law, a combined water and salt mass balance model, and an *in situ* subsurface tracer test were used to estimate groundwater discharge into the upper 1 meter of marsh sediment within 2 meters of the upland forest border. The upper 1 meter of sediment demonstrated the greatest seasonal fluctuation in subsurface conductivity and was the zone of maximal biogeochemical activity. Consequently a control volume of 1 m^3 was chosen for cross method comparison. The upper boundary of this control volume is the sediment surface, the lower boundary is at one meter, and horizontal boundaries are located between the upland border and 2 meters into the marsh respectively. The Darcy and mass balance estimates were derived from pooled measurements from the eight piezometer clusters (2 per transect) nearest the upland border, and were spatially averaged over an approximate 10 m^2 marsh area.

Darcy's Law Calculations

Horizontal and vertical groundwater discharge into the marsh were calculated from hydraulic head and sediment hydraulic conductivity measurements according to :

$$q = -K_{h,v} \frac{dh}{dl} \qquad (1)$$

where q is the specific discharge of groundwater, $K_{h,v}$ is the average hydraulic conductivity (vertical (K_v) or horizontal (K_h)) of the saturated sediment between piezometers, h is the hydraulic head measured in the piezometers and l is the linear distance between the midpoints of the piezometer screens. Hydraulic conductivity of the marsh

sediment was determined in 1996 from slug tests (Hvorslev 1951) performed in all

piezometers. Head measurements were taken at slack high and slack low tides on the peak

spring and neap tides for 18 months. Horizontal discharge was calculated from average

head gradients and K_h values between the nearest upland well and each of the eight

piezometers (50 and 100 cm depths) located within 2 meters of the upland border.

Individual calculations for the 50 and 100 cm horizons were averaged. Vertical discharge

was calculated using average vertical gradients and K_v values from piezometers screened at

2 m and 1m depth. Because K_h:K_v ratios typically vary from 2 - 20 in many types of

sediments, K_v was estimated to be 0.1 x K_h (Fetter 1993). The sum of the horizontal and

vertical dicharge flux described above therefore characterizes groundwater flow into a

control volume at the landward edge of the fringing marsh.

Subsurface Water and Salt Balance

A mass balance model for water and salt was used to estimate the flux of fresh

groundwater into the same control volume as defined in the Darcy estimates. Model inputs

included head and salinity measurements in piezomters and estimates of evapotranspiration

and precipitation. Monthly means for all model input parameters were determined prior to

solving for the average monthly influx.

Conservation of subsurface water in the wetland sediment is expressed as:

$$\frac{dV}{dt} = Q_{GW} + Q_P + Q_T - Q_{ET} - Q_D \tag{2}$$

where dV/dt is the change in water storage volume over a month, Q_{GW}, Q_P, Q_T are the

monthly mean inputs of groundwater, precipitation, and tidal infiltration flux, respectively.

Q_{ET} and Q_D are the mean monthly export fluxes of evapotranspiration and drainage,

respectively. Conservation of salt in the wetland sediment is expressed as:

$$\frac{dS}{dt} = Q_{GW}C_{GW} + Q_PC_P + Q_TC_T - Q_{ET}C_{ET} - Q_DC_W, \tag{3}$$

where dS/dt is the rate of change in salt mass in the control volume ($S = C_W \cdot V$) within a month and C_{GW}, C_P, C_T, C_{ET}, and C_W are the monthly mean salt concentrations (g salt liter^{-1}) associated with the fluxes Q_{GW}, Q_P, Q_T, Q_{ET}, Q_D, described above. Rearranging [2] and substituting into [3] yields the combined equation for conservation of water and salt:

$$\frac{dS}{dt} = Q_{GW}\,C_{GW} + Q_PC_P + Q_TC_T - Q_{ET}C_{ET} - (Q_{GW} + Q_P + Q_T - Q_{ET} - \frac{dV}{dt})C_W. \tag{4}$$

Solving [4] for Q_{GW} and simplifying by setting C_{ET}, C_p, and C_{GW} equal to zero due to negligibly low salt concentrations yields the governing equation for the mass balance model:

$$Q_{GW} = \frac{(-Q_TC_T + Q_PC_W + Q_TC_W - Q_{ET}C_W - \frac{dV}{dt}C_W + \frac{dS}{dt})}{-C_W} \tag{5}$$

Defintion of Model Input Terms

Tidal Infiltration (Q_T)

   Calculation of the infiltration of river water into the control volume at high tide followed the procedure presented in Harvey and Odum (1990) and Harvey et al. (1995). The equation used to compute the infiltration flux is:

$$Q_T = N(Z_{SED} - h_{MIN})\,S_y \tag{6}$$

where (N) is the frequency of innundation (number of times the site is flooded per day), $(Z_{SED}-h_{MIN})$ is the difference between the elevation of the sediment surface and the average minimum head (water level) beneath the marsh, and S_y is the specific yield (0.12) of marsh sediment as determined from measured head changes following known volume additions to replicate cores collected from the study area (Harvey et al. 1995). Q_T was computed for each piezometer cluster and averaged. Since the site is irregularly flooded, (N) was determined by summing the number of tidal events per month whose maximum tidal height exceeded the sediment elevation at each well cluster. The monthly sum was normalized to an average value per day. Tidal elevations recorded at the Gloucester Point, VA York River NOAA tide gauge were used to determine N after groundtruthing the site for specific flooding events.

Evapotranspiration (Q_{ET})

Evapotranspiration of water out of the control volume was assumed to be equal to the average monthly potential evapotranspiration rate (P_{ET}) derived from air temperature and daylength (Hamon 1961):

$$P_{ET} = \frac{[0.021 \, (H_t^{\,2} \, e_{sat})]}{(T_t + 273)} \tag{7}$$

where H_t is the average number of hours of daylight per day in the month, T_t is the monthly average air temperature (°C), and e_{sat} is the relative humidity estimated from air temperature as defined by Bosen (1960):

$$e_{sat} = 33.86[(.00738T_t + .8072)^8 - .000019(1.8T_t + 48) + .001316] \tag{8}$$

Monthly Q_{ET} was normalized to a per day rate (liters m^{-2} day^{-1}) for input to the model. Air

temperature from Newport News, Virginia (located approximately 10 km from the site) was used to estimate P_{ET}.

Precipitation (Q_p)

Precipitation inputs to the control volume were estimated from meteorological data collected at the Virginia Institute of Marine Science located approximately 9 km from the study site according to:

$$Q_p = P - Px \qquad (9)$$

where (P) is the total monthly precipitation, and (x) is the fraction of the total rainfall that fell on the marsh when NOAA tidal records predicted that the marsh was flooded. Q_p was normalized to a daily flux prior to input into the model.

Salt Concentration (C_w)

The porewater salt concentration in the control volume (C_w) was derived by averaging measurements in the eight paired clusters of piezometers. Each paired cluster consisted of a 50 and 100 cm piezometer. Four clusters were sampled 4-8 times per month but were not purged prior to sampling. Later testing determined that unpurged piezomters provided unreliable estimates of salinity because water and salt were stored in the body of the piezometer above the screen. The remaining four clusters were purged prior to sampling and sampled once every 2-3 months. For those piezometers, salinity estimates for missing months were determined by linear interpolation. We attempted to minimize the effect of well storage artifacts on measured salinity in the nonpurged wells by averaging the salinity estimates from the purged piezometers with salinity values recorded at the nonpurged wells for those months

Intramonthly Changes in Volume and Salt (dV/dt, dS/dt)

The rate of change of water storage in the control volume was calculated from the equation:

$$\left(\frac{dV}{dt}\right)_i = \left(\frac{\Delta V}{\Delta t}\right)_i = \frac{\Delta h \cdot A \cdot Sy}{\Delta t} \tag{10}$$

where Δh is the average difference between hydraulic heads in the piezometers measured on or near the first and last days of month (i), A is the area of the control volume ($1m^2$), Sy is the specific yield, and Δt is the number of days between the head measurements.

The rate of change in salt mass in the control volume was calculated from the equation:

$$\left(\frac{dS}{dt}\right)_i = \left(\frac{\Delta S}{\Delta t}\right)_i = \frac{\left(S_f - S_0\right) \cdot V}{\Delta t} \tag{11}$$

where S_0 and S_f are the salt concentrations (g salt liter^{-1}) measured on or near the first and last days of month (i) respectively, V is the mean control volume (liters), and Δt is the number of days between salt measurements. The mean control volume is defined by:

$$V = \left[\, 1 - \left(\, Z_{SED} - h_{MIN}\,\right)\right] \cdot A \tag{12}$$

where the sediment thickness of the control volume is assumed to be 1 meter deep.

<u>Tracer Studies</u>

To empirically determine the groundwater discharge velocity into the marsh, a small scale tracer release was performed at a period of high groundwater discharge in March 1998. The tracer experiment protocol follows: 1.0 -1.5 M potassium bromide (KBr) solution was injected as a single slug into two adjacent injection wells (2" pvc) located at the upland marsh border. The injection and target wells were screened from 10 cm to 50 cm below the marsh surface. The target well array and the injection wells were sampled over the following 1 - 2 months. Br concentrations in samples were measured in the laboratory using an Orion 94-35 Br specific electrode following temperature equilibration. Bromide data were mapped into contour plots and the piezometers located nearest the center of mass were identified. Bromide breakthrough plots were generated for these piezometers and the discharge flux (Q_{GW}) was determined as:

$$Q_{GW} = (\frac{L}{t}) A \cdot n \qquad (13)$$

where L is the distance between the injection point and the target well(s) along the center of mass, t is the elapsed time from the injection start until the peak of the bromide breakthrough curve, A is the cross sectional area (defined as 1 m^2), and n is the average sediment porosity between 10 and 50 centimeters depth.

RESULTS

Darcy Estimates

The distribution of the horizontal (K_h) and vertical (K_v) hydraulic conductivities for the upland and shallow marsh strata used in the Darcy discharge estimates are shown in Table 1. The small range of K_h ($2 - 17 \times 10^{-4}$ cm sec^{-1}) supports the averaging of conductivity values between the upland and marsh piezometers used in the calculations. The range is typical of fine grained or silty sands and is within the values reported for marsh sediments determined by bail test methods for a nearby fringing marsh located on the York River (Harvey and Odum 1990). The hydraulic conductivity of the basal marsh deposits was generally lower ranging from. $0.4 - 5.0 \times 10^{-4}$ cm sec^{-1}, and the conductivity of the oxidized sands and shell hash composing the underlying aquifer was similar to that encountered in the upper meter of marsh strata ($1.8 - 12.0 \times 10^{-4}$ cm sec^{-1}). The pooled groundwater discharge estimate from each of the piezometers is shown in Figure 3. The standard deviation of the individual piezometer discharge estimates was proportional to the absolute value of the mean horizontal and vertical discharge at 39 % and 98 %, respectively. The groundwater flux estimates derived from the Darcy calculation followed a seasonal pattern with peak discharge in early spring near days 120 and 480 (Figure 3). The groundwater flow minimum was encountered in early autumn near days 240-300, and was accompanied by slight flow reversal into the aquifer. Vertical hydraulic gradients (dh/dl) were larger than horizontal gradients, but the estimated K_v was an order of magnitude lower than K_h. As a result, horizontal fluxes dominated the groundwater discharge during high flow periods in the spring by approximately 5:1, but were similar to vertical fluxes during periods of low discharge in the fall. Head data were not normalized to freshwater prior to calculation of the horizontal and vertical discharge fluxes. Given the observed salinities in piezometers used to calculate discharge, density correction of

hydraulic head would decrease the horizontal flux by a maximum of 2 %, and the vertical flux by less than 1%.

Table 1. Distribution of hydraulic conductivity at the Ringfield Site. K_h and K_v denote estimated horizontal and vertical conductivity respectively. (*) indicates depth below water table in October 1996. All other depths are below the marsh sediment surface.

Piezometer #	Location	Depth (cm)	K_h (x 10^{-4} cm sec^{-1})	K_v (x 10^{-4} cm sec^{-1})
RU - 4	Upland	0-50*	6.5	0.7
1-1	Marsh	0-50	14.0	1.4
1-6	Marsh	0-50	11.4	1.1
2-4	Marsh	0-50	14.2	1.4
2-8	Marsh	0-50	17.3	1.7
1-2	Marsh	50-100	5.1	0.5
1-5	Marsh	50-100	2.0	0.2
2-3	Marsh	50-100	2.7	0.3
2-7	Marsh	50-100	6.7	0.7

Figure 3. Horizontal and vertical groundwater discharge estimates derived from Darcy calculations. Negative values denote flow into the aquifer from the marsh. Standard deviation is proportional to the absolute value of the mean discharge estimate with coefficients of variation for horizontal and vertical fluxes at 39 % and 98 %, respectively.

Groundwater Discharge Flux (liters m^{-2} day^{-1})

Day

Horizontal Discharge
Vertical Discharge

Jan 1997

Jan 1998
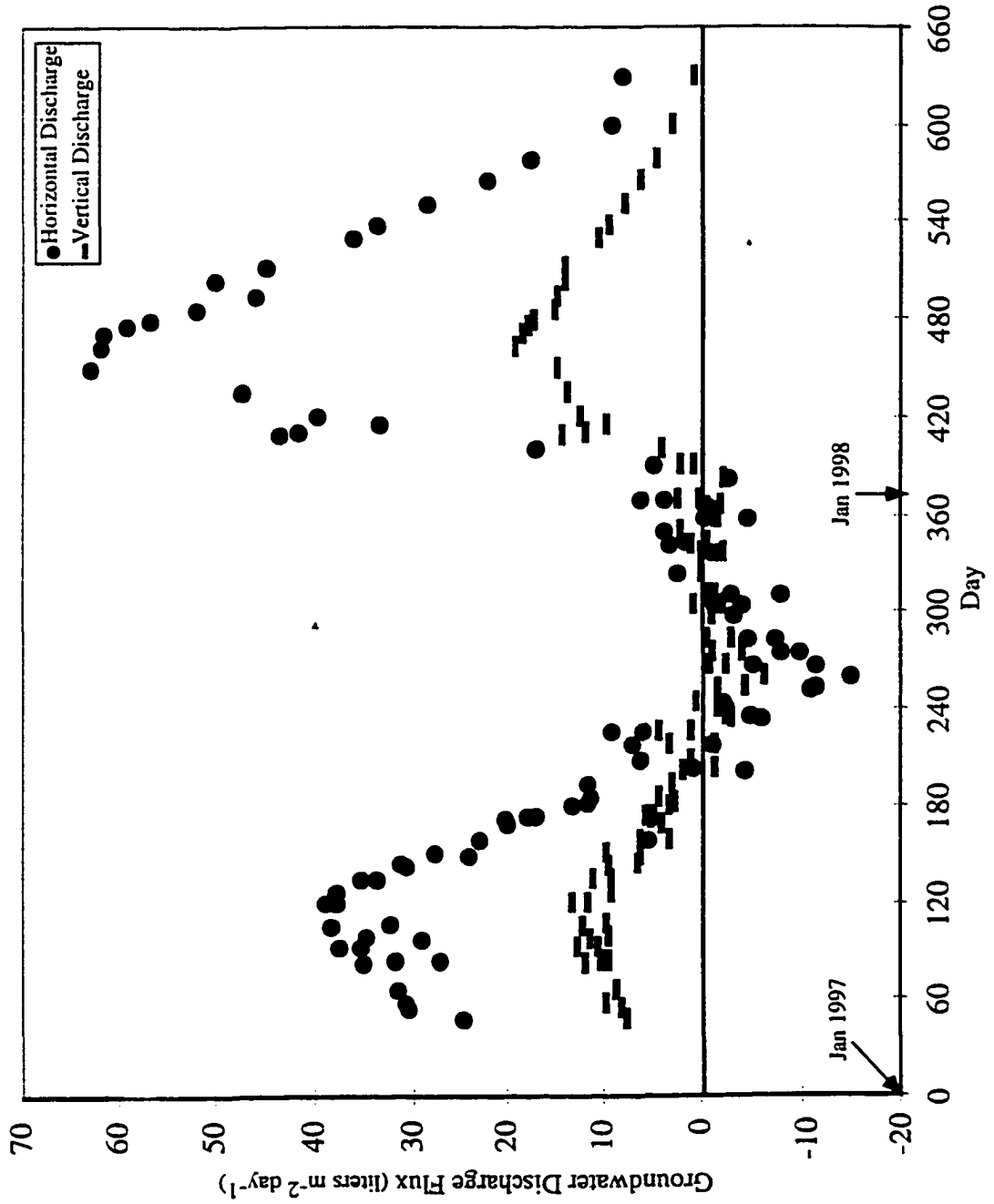
Water/Salt Balance Estimates

The annual pattern of subsurface salinity mimics the seasonal fluctuations in river salinity except that subsurface salinities are suppressed relative to river water by approximately 30-75% (Fig.4). Greater variations in salinity were encountered in piezometers that were purged before sampling. The 50 and 100 cm piezometers possessed a screen volume to total piezometer volume ratio of 0.33 and 0.25 respectively. Piezometer deadspace above the screen may have therefore dampened the response of unpurged piezometers to changing salinities surrounding the screen.

Table 2 shows the different components of the water and salt balance. Groundwater and tidal infiltration are the dominant inputs in spring and autumn, respectively. Drainage exceeds water loss via evapotranspiration for all months except August.

Figure 5 shows the estimates of fresh groundwater discharge derived from the water and salt balance model. Peak discharge occurred in April, and a minimum in August. The error bars represent standard deviations determined by a Monte Carlo simulation of the model manipulating the following parameters: $(Z_{SED} - h_{MIN})$; porewater salinity; daily mean temperature; and precipitation. The input parameters were used to derive Q_T, dV/dt, C_W, dS/dt and Q_{ET} in the model. The simulation simultaneously varied all input parameters within one standard deviation assuming a normal distribution. In addition to the Monte Carlo analysis, results from a sensitivity analysis performed on the model are shown in Table 3. From the raw data, monthly and annual means and standard deviations were determined for all input paramters. The annual average and (range) of the monthly coefficients of variation for each of the terms was: Q_T - 59% (22-157%); dV/dt - 84% (25 - 151%); C_W - 13.5% (2.1 - 23%); Q_{ET} - 40% (10-73%). On the basis of previous error

Figure 4. Average monthly porewater salinity in the upper 1 meter of marsh sediment, and of tidal flooding water. Error bars are standard error ($3 < n < 10$).
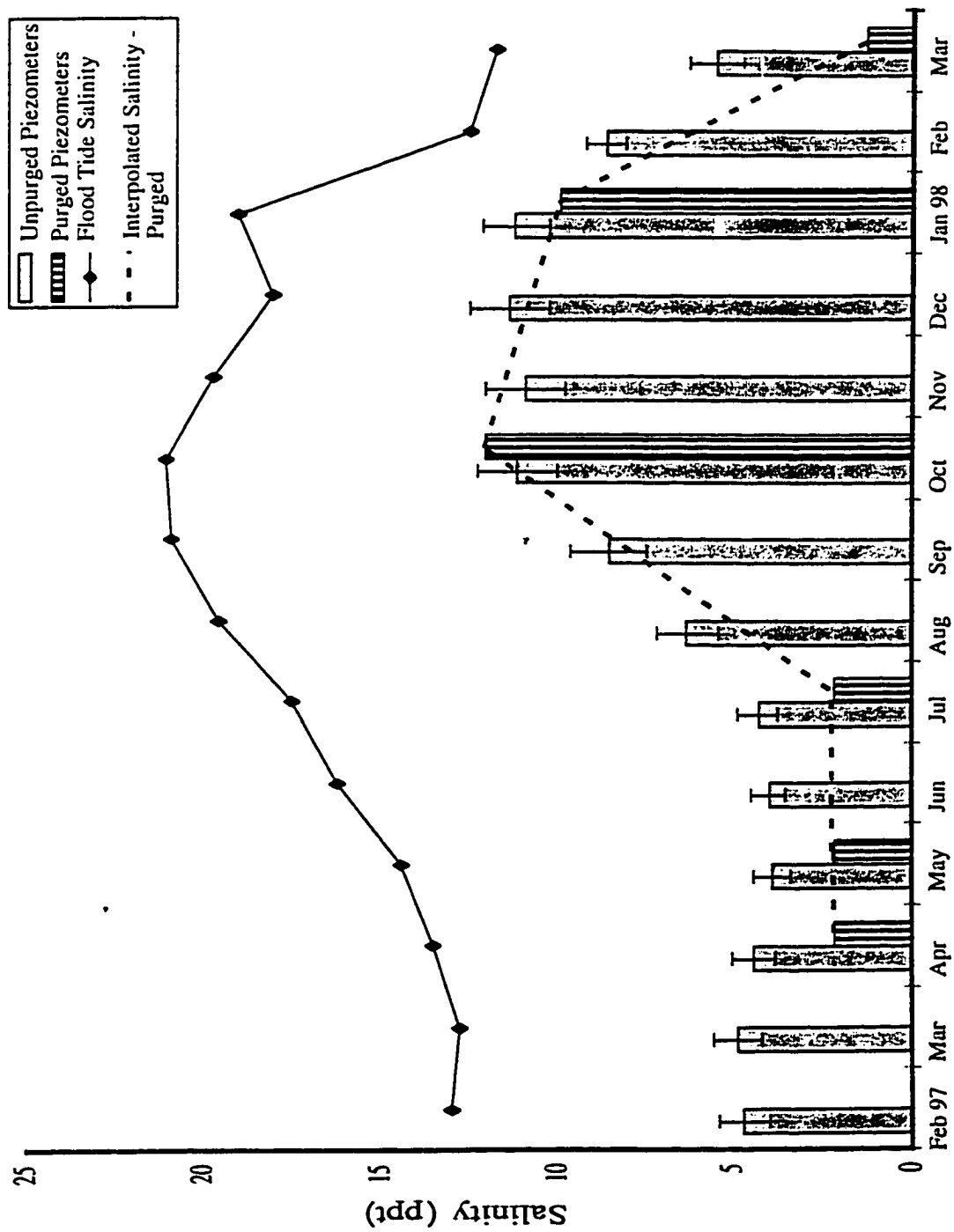
Table 2. Monthly accounting of the water fluxes derived from the water/salt balance. % Groundwater was calculated from $\{Q_{GW} / \sum (Q_T + Q_P + Q_{GW})\} \times 100$.

Month	Tidal Infiltration (Q_T) (l m^{-2} day^{-1})	Precipitation (Q_P) (l m^{-2} day^{-1})	Evapo-transpiration (Q_{ET}) (l m^{-2} day^{-1})	Change in Storage (dV/dT) (l m^{-2} day^{-1})	Groundwater (Q_{GW}) (l m^{-2} day^{-1})	Porewater Drainage (Q_D) (l m^{-2} day^{-1})	% Groundwater of all Inputs
Feb 97	2.7	3.3	0.9	0.0	4.2	9.3	41
Mar	2.1	1.9	1.4	0.0	9.0	9.5	69
Apr	3.5	0.8	1.8	0.0	12.2	19.2	74
May	2.6	0.4	2.8	0.0	16.5	11.4	85
Jun	4.2	0.6	4.2	0.1	11.5	14.3	70
Jul	4.3	6.0	5.0	0.1	6.8	10.5	40
Aug	4.4	1.2	4.0	0.0	0.6	3.3	10
Sep	7.3	0.7	2.8	0.1	1.0	9.3	11
Oct	9.8	3.3	1.8	0.0	6.0	14.3	31
Nov	8.9	4.0	0.9	0.1	2.7	14.9	17
Dec	5.1	0.0	0.6	0.1	4.0	9.0	44
Jan 98	5.8	2.8	0.7	0.1	3.1	14.4	26
Feb	1.7	2.2	0.9	0.1	13.1	14.2	77
Mar	1.7	2.2	1.4	0.0	22.6	22.7	85

Figure 5. Groundwater flux estimate derived from the water/salt balance model. Error

bars are standard deviations estimated from monte carlo simulations (n=50) of the model.

Figure: Bar chart of Groundwater Discharge (liters m^{-2} day^{-1}) versus Month, from feb 1997 to mar. The y-axis ranges from -10 to 25.
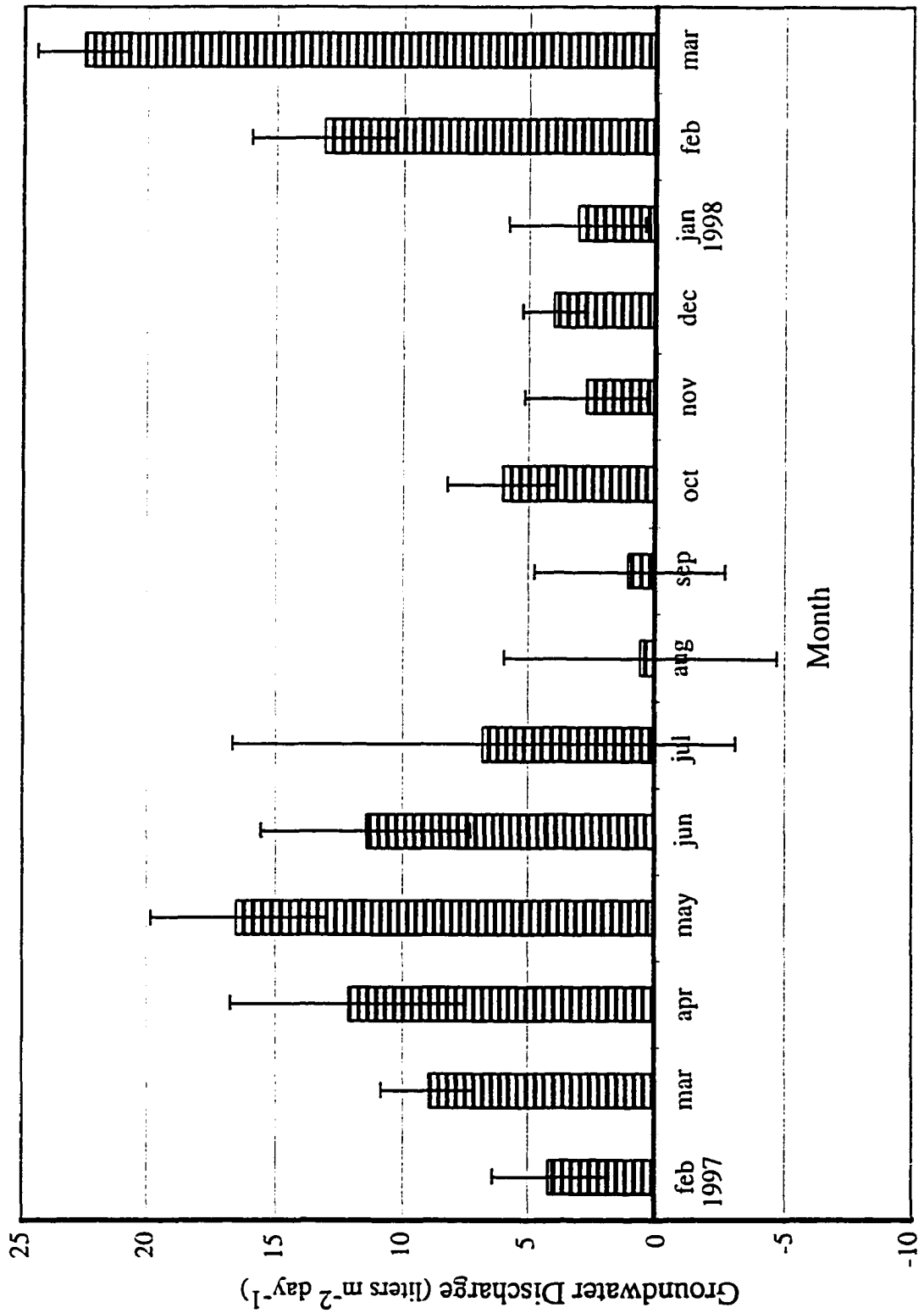
Table 3. Sensitivity analysis of the water/salt model to a two standard deviation increase (+) or decrease in model input parameters. Months and parameters which were most sensitive (i.e. greater than a 2 fold change in output) are shaded.

Month	Q_{gw} Nominal (l m^{-2} day^{-1})	Q_T +	Q_T -	Cw +	Cw -	Q_P +	Q_P-	Q_{et} +	Q_{et} -	dV/dT +	dV/dT -
		N-fold Change From Nominal Case									
Feb 97	4.2	1.71	-1.72	-1.03	1.03	2.19	1.79	1.19	-1.08	1.00	1.00
Mar	9.0	1.57	-1.45	-1.14	1.21	-1.31	1.21	1.09	-1.06	1.00	1.00
Apr	12.2	1.99	-1.88	-1.26	1.47	-1.09	1.06	1.07	-1.05	1.00	1.00
May	16.5	2.03	-1.59	-1.22	1.43	-1.03	1.02	1.08	-1.05	1.00	1.00
Jun	11.5	2.03	-1.92	-1.16	1.21	-1.06	1.04	1.29	-1.17	-1.01	1.00
Jul	6.8	5.00	-2.96	-1.31	1.44	2.52	1.88	1.23	-1.18	-1.01	-1.01
Aug	0.6	30.60	-15.7	3.77	5.44	-3.00	3.00	5.54	-2.22	1.06	-1.03
Sep	1.0	10.22	-9.78	3.44	5.04	2.03	1.68	2.06	-1.79	1.08	-1.05
Oct	6.0	1.66	-2.02	-1.31	1.41	-1.82	1.54	1.22	-1.13	1.00	1.00
Nov	2.7	3.62	-3.04	-1.13	1.14	3.59	2.66	1.16	-1.12	-1.03	-1.03
Dec	4.0	1.82	-1.80	-1.23	1.29	-1.03	1.02	1.06	-1.04	1.02	1.02
Jan 98	3.1	3.90	-2.52	-1.52	1.74	-2.35	1.90	1.22	-1.09	-1.06	1.05
Feb	13.1	1.16	-1.07	-1.25	1.65	-1.24	1.16	1.04	-1.03	1.01	1.00

analysis in wetlands (Winter 1981), a coefficient of variation for Q_P of 75% was used in this analysis. Model sensitivity to the terms (Q_T, C_W, Q_P, Q_{ET}, and dV/dt) was determined by increasing and decreasing each term individually by 2 standard deviations in each month. Since changes in dS/dt are determined by variation in C_W model sensitivity to dS/dt was determined as a response to the manipulation of C_W. Although Q_P, dV/dt, Q_T, Q_{ET}, and C_W are the terms with the highest individual variance (in descending order), the model was most sensitive to changes in Q_T, followed by C_W, Q_P, Q_{ET}, and lastly dV/dt. Results from the sensitivity analysis indicated that the model was most sensitive to changes in any parameters in late summer (July - September).

Tracer Estimate

Figure 6 contains a contour plot of the bromide plume generated following the tracer injection in March 1998. A bromide breakthrough curve (Figure 7) was constructed for the piezometers located on the axis along which the center of mass was travelling for the plume. The mean transport time in March was 2.84 cm day^{-1} (linear velocity), which corresponds to a groundwater discharge of 22.4 ± 7.5 l m^{-2} d^{-1}.

Comparison of Methods

Annual patterns of Darcy-derived and water and salt balance-derived discharge are similar although the water and salt balance estimates are 2-7 times lower than Darcy estimates for January through May (Figure 8). Darcy and water and salt balance discharge estimates are similar for June - August, and Darcy estimates fall below water and salt balance discharge values for the late summer and autumn. With the exception of July, August, and January, observed variability was lower using the water and salt derived estimates than discharge values calculated using Darcy's Law. Estimated error in the Darcy groundwater flux increased proportionally with the absolute value of the mean discharge.

Uncertainty in the Darcy estimate approaches 100% at the maximum flow observed in April 1998. Tracer derived estimates of discharge are closer to the trend and range of average values predicted by the water and salt balance method in March and out of the range of error associated with the Darcy method. Error for the March tracer derived groundwater flux is based on averaging transport times for the different piezometers identified as being near the center of mass and estimated at ± 4 liters m^{-2} day^{-1}.

Figure 6. Bromide contour plot of the marsh subsurface following the March 1998 tracer test. Shore normal distance is equal to zero at the upland border. Plot represents day 14 and post injection. Solid ellipses denote piezometers near the center of mass of the plume used in the calculation of groundwater discharge. The numbered open ellipses denote piezometers used in the calculation of discharge.
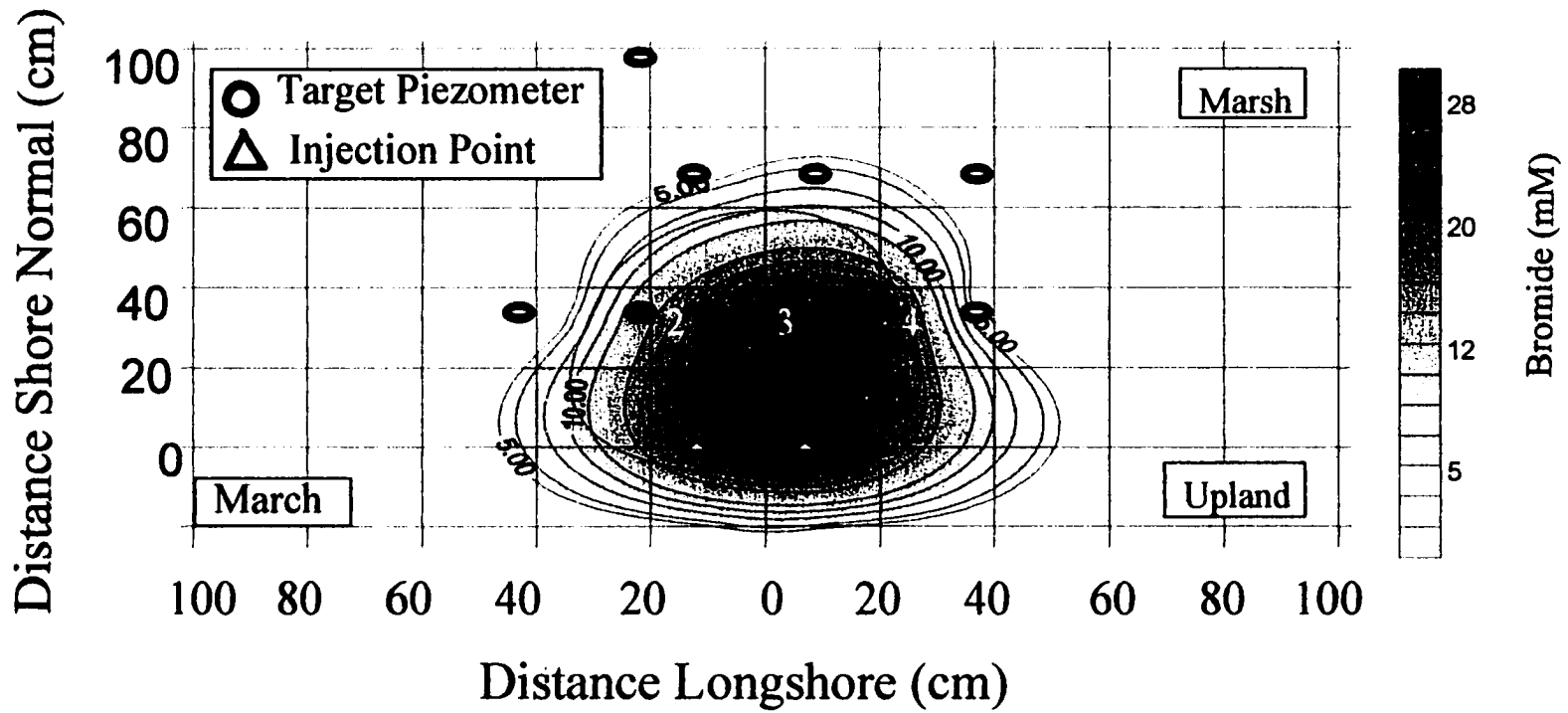
Figure 7. Bromide breakthrough curve of piezometers (2,3, and 4) used to calculate groundwater velocity and discharge for the March tracer tests. See Figure 6 for piezometer locations.

Figure: Bromide (mM) versus Days Post Inject. March 1998. piezometers 2, 3, 4.
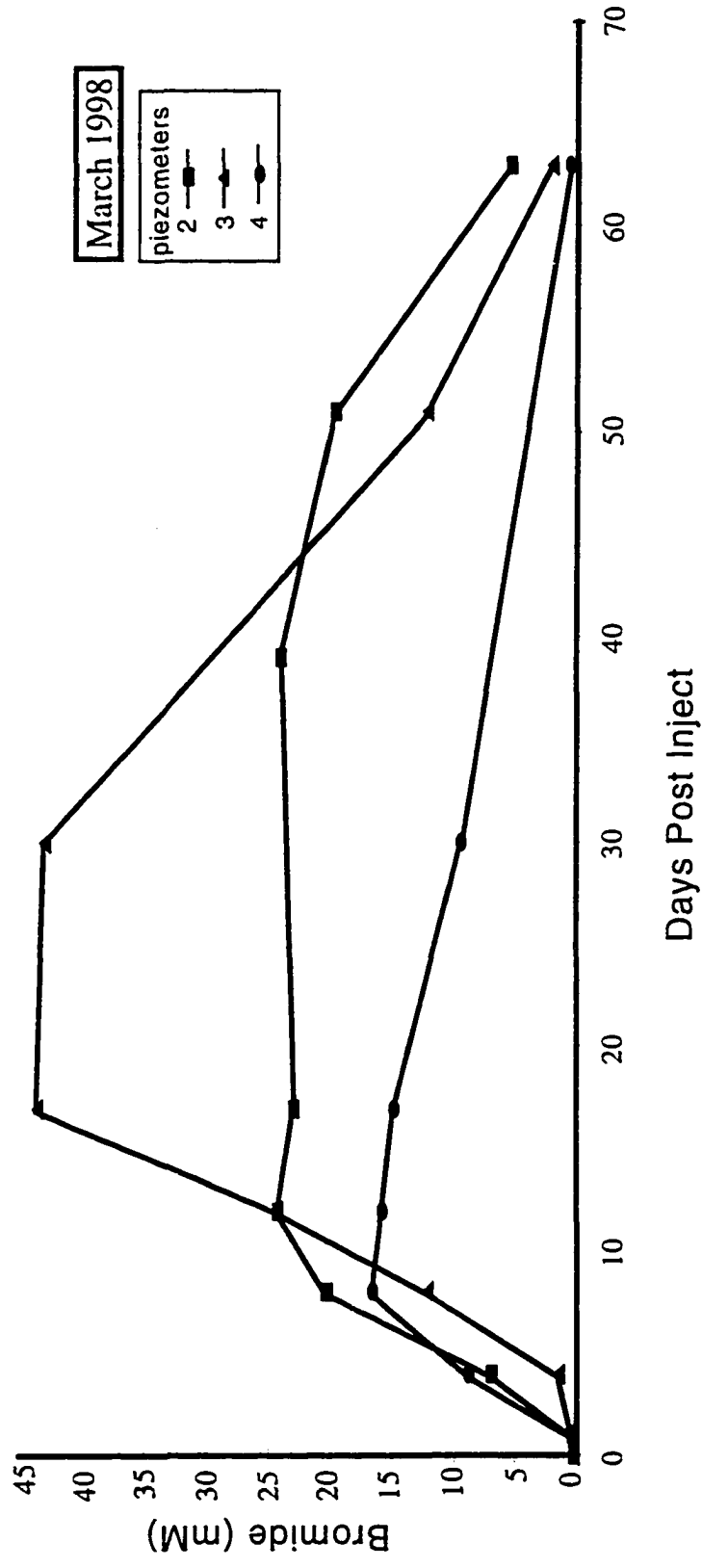
Figure 8. Comparison of groundwater discharge estimates: Darcy; water/salt balance; and

tracer test. The size of the vertical bars represents the range of estimates. The range

presented for the Darcy estimate is the sum of minimum horizontal and vertical estimates

(min) and the sum of the maximum horizontal and vertical estimates (max). Minimum or

maximum estimates were determine by subtraction or addition of the standard deviations to

the individual means. Determination of the range for the water/salt balance estimate was

derived from standard deviations estimated from the Monte Carlo simulation. Coefficient

of variation for the March tracer test estimate is 0.38. The height of the circle denotes the

standard deviation ($7.5 \ l \ m^{-2} \ d^{-1}$) of tracer discharge estimates calculated from piezometers

2,3, and 4.
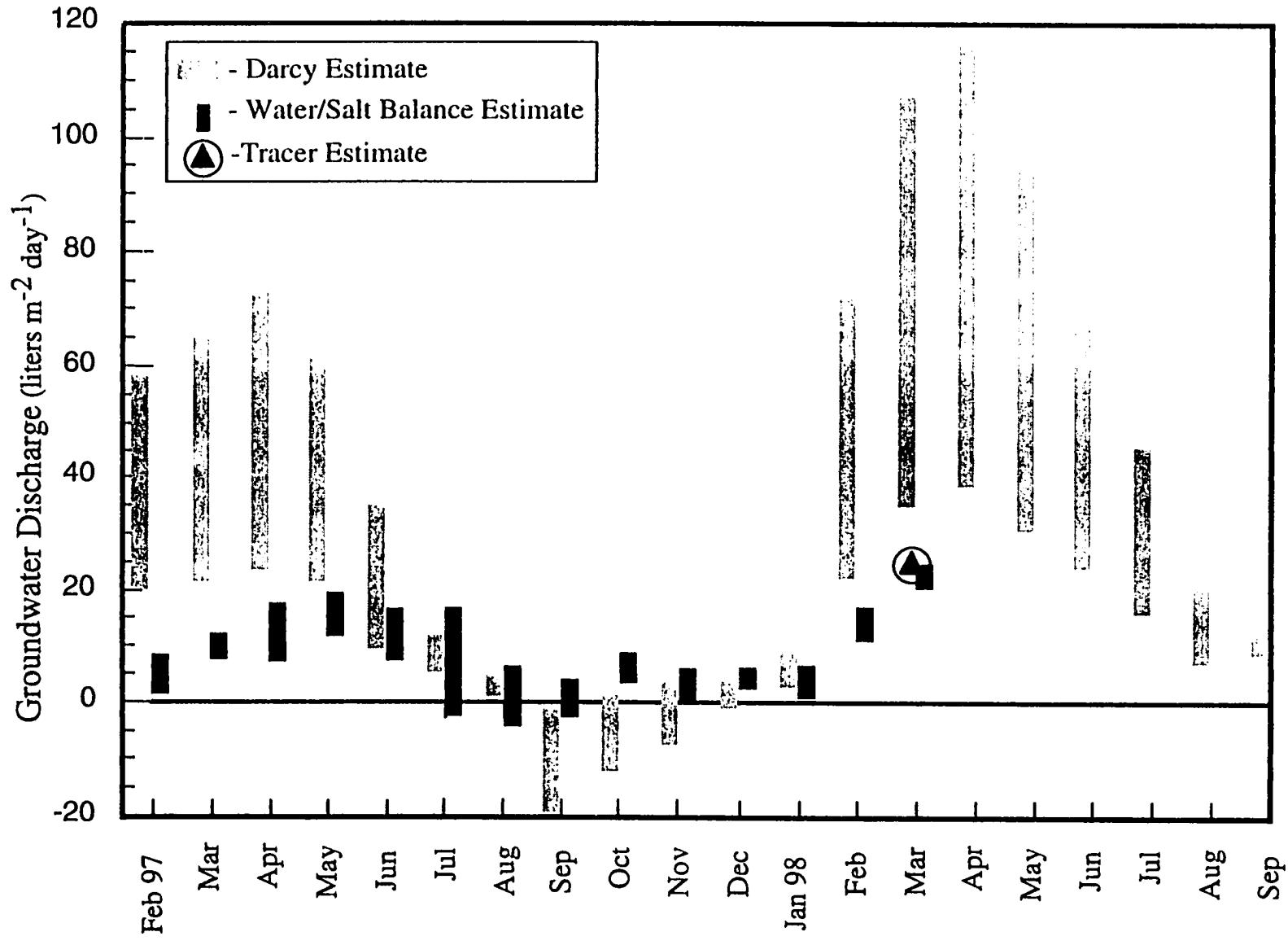
DISCUSSION

Few studies characterizing the hydrology of tidal marshes on an annual cycle are available for comparison with this work. Most attempts at a Darcy-estimated or water balance-derived groundwater flux have been conducted over shorter timescales during the summer months only.

Darcy Estimates

The seasonal pattern of discharge including the slight flow reversal out of the marsh in the late summer and early fall closely mimicked intra-annual fluctuations in upland hydraulic head. August groundwater fluxes were nearly identical to values estimated using the Darcy approach at the nearby Carter Creek marsh by Harvey and Odum (1990) and are nearly 100 times larger than groundwater fluxes reported for a subarctic coastal marsh (Price and Woo 1988). In this study, the summertime Darcy flux is near lower estimates of groundwater discharge for marshes and small compared to reported subtidal fluxes (Harvey and Odum 1990; Staver and Brinsfield 1996; Cable et al. 1997). Large errors for the Darcy estimates were derived primarily from variability in measuring hydraulic head at infrequent intervals against a background of tidally- fluctuating water levels, and variability in measured hydraulic conductivity between piezometers. Assessing the uncertainty in vertical hydraulic conductivity estimates was beyond the scope of the study. However, the estimated K_v would have to be increased 4 fold in order for the vertical groundwater flux to rival horizontal groundwater flux during periods of high discharge. Winter (1981) estimated an approximate 50-100% error in measuring hydraulic conductivity in anisotropic sediments and hydraulic conductivity error has been identified as a likely source of the disparity between groundwater fluxes estimated using K and those calculated from estimates of specific yield (Nuttle and Harvey 1995; Chambers et al. 1992). Within the

seasonal pattern of Darcy estimated discharge, existed a shift in the relative importance of the horizontal and vertical flow components through the year. There is greater total groundwater flow through the upper marsh strata when water table height exceeds the elevation of the hydraulically less conductive basal marsh deposits in the late winter and spring. This subsurface horizontal discharge may be supplemented by hillslope discharge in the form of springs or seeps when the water table is sufficiently high (Focazio 1997). Previously, the horizontal component has been considered negligible in regions similar to the study site which are far from creekbanks or which experience sporadic flooding (Nuttle and Hemond 1988; Nestler 1997; Nuttle and Harvey 1995). As upland head decreases into the summer, the Darcy calculation predicted that some discharge to the marsh still occured but became increasingly less dependent on the horizontal component until July and August when the vertical and horizontal flux vectors were approximately equal. This shift likely results from both a decrease in the upland head and an increase in the effect of evapotranspiration on vertical piezometric head during this time (Hemond and Fifield 1982; Dacey and Howes 1984). Because most previous studies have looked at the hydrologic balance in marshes within the context of macrophyte ecology, they were performed during the growing season in the summer when groundwater inputs were low. Consequently, vertical fluxes have come to be considered the dominant flowpath for fresh groundwater entry into these systems. The importance of vertical groundwater transport in July and August at our site is consistent with previous work performed during these periods of high evapotranspiration in the summer (Nuttle and Harvey 1995). While it is difficult to determine whether a similar shift in the dominance of horizontal vs vertical discharge exists at other marshes through the year, there is little doubt that on an annual basis, horizontal transport is the primary route of groundwater entry into the marsh at the Ringfield study site.

High rates of groundwater discharge are typically encountered near the upland border of marshes and subject to either a linear or exponential decrease in magnitude of discharge with distance from the upland border (Harvey and Odum 1990). We acknowledge the possibility that horizontal discharge is likely maximal where we measured and perhaps the horizontal flux component does not dominate discharge throughout the marsh. However, even if, the discharge fluxes are integrated over the entire width of the marsh, the discharge per unit of upland shoreline can be large. The consequence of this approach is that fringing marshes of relatively narrow width typical of our site, the Chesapeake Bay, and its subestuaries are subject to a higher groundwater flux per meter of marsh than larger expansive marshes such as those encountered in the coastal lagoon /barrier island morphology.

Water/Salt Balance Estimates

Groundwater Discharge Estimates

While there are few estimates of groundwater inflow to tidal marshes over the seasonal timescale, our estimates of groundwater flux derived from the water/salt balance in late summer compare favorably with other mid-Atlantic marshes. Nuttle and Harvey (1995) used a statistically constrained water balance approach to derive a groundwater discharge (vertical) estimate for late August/ early September of 2.8 liters m^{-2} day^{-1} into an infrequently flooded Virginia salt marsh. Estimates from our water/salt balance during that period lie between 1.7 and 4.0 liters m^{-2} day^{-1}. This range of values however is 27-66 times the water balance derived groundwater flux for a subarctic coastal marsh whose primary freshwater input was precipitation (Price and Woo 1988). Like the Darcy estimate, the water and salt balance-derived flux is within the range of other marsh discharge estimates summarized in Harvey and Odum (1990) and 1-2 orders of magnitude less than

most reported summertime subtidal fluxes. However if high flow discharge estimates from
our model are used for comparison, our flux is within the lower 15% of most of the
reported subtidal fluxes (Harvey and Odum 1990). The seasonal pattern of discharge
agrees well with annual fluctuations in the upland hydraulic head, although the method of
data aggregation for the model precludes identifying finer scale responses in discharge to
discrete precipitation events as have been seen in some subtidal discharge systems (Staver
and Brinsfield 1996; Cable et al 1997).

The dominance of the groundwater flux in the water budget in the late winter
through spring results in a seasonal purging of solutes as is evidenced by decreased
porewater conductivities (Figure 2) encountered during high discharge. Nuttle and Harvey
(1995) suggested the importance of such a groundwater mediated flux in regulating solute
exchange with surface water. Even though high groundwater discharge may not be
occurring through the whole marsh, it is important to note three things in the context of
flushing: 1) the typical width of fringing marshes is not great; 2) conservation of mass
requires that porewater "downstream" in the marsh be pushed towards the estuary; and 3)
mixing and porewater export rates out of the subsurface are faster with closer proximity to
creeks and increased tidal inundation frequency. Consequently the seasonal flushing has
implications for export to the estuary as well as the solute balance within the marsh.

Error Estimate and Sensitivity Analysis

Confidence in the groundwater flux estimate is greater when flows are higher
(December through June) and the average flux exceeds the estimate of error as determined
by Monte Carlo analysis for a particular month. High standard deviations were
encountered between July and November when flows were low. There was no consistent
correlation between the monthly variance of any one model parameter with the high

estimate of error. Rather July and August (months with a high standard deviation of the groundwater flux estimate) were periods when several terms in the model had nearly equitable magnitudes. Therefore it is assumed that the increased error was cumulative from the individual variances of the terms. Larger total errors relative to the mean encountered in September through November, however, may reflect individually larger monthly variances associated with the more dominant model inputs at this time (tidal infiltration flux and porewater salinity). These are the terms whose uncertainty also has the greatest effect on the model output as determined by the sensitivity analysis. A full description of the determining factors driving the sources of error in the model is beyond the scope of the current study, but would prove useful in determining whether there are seasonal periods when various groundwater estimation methods warranted greater confidence based upon their estimates of error.

One of the primary assumptions in using the water and salt balance approach is that the system is well-mixed (Morris 1995). From July through December the average difference in salinity between the 0.5 and 1 meter depth piezometers was approximately 20% greater than during high discharge periods. This suggests that the system deviates more from the well-mixed condition during the summer through autumn and the estimated variance of the salinity in the sampled wells may not adequately characterize the heterogeneity of the salt distribution. Further evidence of this is seen in the differences in salinity encountered in purged vs unpurged wells, and the subsequent sensitivity of the model to changes in porewater salinity. Consequently, there must be an additional, although currently unaddressed, source of error during this period.

Composition of the Water Balance

Inputs -Groundwater and Tidal Infiltration (Q_{GW}, Q_T)

Groundwater and tidal infiltration fluxes dominate the water inflows to the subsurface during different times of the year. The groundwater flux dominates the input of water into the subsurface during late winter through the spring and early summer at the study site, while tidal fluxes represent the major input from August through December. Tidal infiltration fluxes during the late summer and early fall are slightly less than one-half of the magnitude of infiltration fluxes reported for the Carter Creek marsh (Harvey and Odum 1990), a Virginia coastal marsh (Harvey et al. 1995), and for a regularly flooded South Carolina salt marsh (Morris 1995). Tidal infiltration was the dominant source of water input to the marsh in the Fall when the size of the unsaturated zone was largest (i.e. "Z_{SED}-h_{MIN}" is large), but was a significantly less important component of the water balance in the Spring when marsh sediment was already saturated due to the greater flow of groundwater. The higher water table in the Spring effectively decreased the size of the unsaturated zone available to receive tidal water (i.e. "Z_{SED} - h_{MIN}" approaches zero). Price and Woo (1988) found tidal inputs to intertidal marshes to be insignificant to the water balance of a subarctic coastal marsh under similar periods of sediment saturation. Tidal infiltration typically dominates the water inputs to marshes, however comparison of the August water budget with that of the regularly-flooded Carter Creek marsh indicates that our groundwater flux estimate is approximately a ten-fold greater percentage of the total water input even at minimum monthly flow (Harvey and Odum 1990). Although both marshes had nearly identical groundwater inflows in the late summer, the tidal infiltration at the Carter Creek marsh composed the largest term in the water balance due to a higher frequency of tidal inundation resulting from the lower site elevation within the mean tidal range . If the rate of tidal inundation was increased in our model to a semi-diurnal

frequency, Q_T would increase by approximately 2-4 fold. These larger calculated values of Q_T would approximate infiltration fluxes observed in other regularly-flooded marshes (8.6-12 liter m^{-2} day^{-1} (Harvey and Odum 1990, Morris 1995, Harvey et al. 1995) and be equal to or greater than the groundwater flux estimates for all months except February through April. From February through April, the magnitude of Q_T is controlled primarily by the degree of saturation of the sediment when groundwater discharge is at a maximum and the Z_{SED}-h_{MIN} term is lowest. Consequently increasing the frequency of innundation would bring the infiltration flux to near parity with the groundwater flux but would likely not exceed it. For infrequently flooded high marsh zones, the higher percentage of groundwater to the total inputs is consistent with the findings of Hemond and Fifield (1982) and Nuttle and Harvey (1995) who showed that in the absence of a strong tidal signature, groundwater contributes significantly to the water and solute balance of the subsurface.

While I have suggested that groundwater discharge is likely to be of greater importance in narrow marshes that have a greater percentage of their total area closer to the upland border, marsh elevation seems to similarly influence the relative importance of groundwater flux in the overall water balance by limiting tidal infiltration. Marshes with elevations above the mean tidal range would be subject to small infiltration fluxes. Provided that the marsh elevation does not exceed the maximum upland water table elevation, narrow "elevated" marshes would be expected to derive most of their water inputs from groundwater or precipitation relative to tidal infiltration.

Precipitation (Q_P)

The importance of precipitation to the wetland water balance is dependent on both the timing and magnitude of individual precipitation events (Gehrels and Mulamoottil

1990). Monthly precipitation values for the Virginia coastal plain are nearly equal through

the year (National Climatic Data Center 1997) . Precipitation affected the water balance

only when the input was large and occurred during a period when the marsh was not

flooded. Two large precipitation events occurred in July 1997 and February 1998

respectively. The July event occurred during a period when the marsh was not flooded and

consequently was the largest water input term for that month. The rainfall that occurred in

February was of larger magnitude than the July event, but occurred over a period when the

marsh was inundated by tidal water for several days due to elevated tides caused by strong

onshore northeast winds. Consequently, Q_p in February comprised a relatively small

component of total water input.

Changes in Storage and Salt (dV/∂t, dS/∂t)

Water storage in wetlands is composed of saturation storage (derived from specific

yield) and dilation storage (derived from sediment expansion during innundation) (Nuttle et

al. 1990). Estimates of dilation storage in wetlands range from 20 - 86% of the total

change in storage (Nuttle et al. 1990) Even if these estimates of dilation storage are

combined with measured changes in saturation storage, the total monthly storage change at

our site remained small. The sensitivity analysis indicated that storage changes could have

been assumed to be at steady state on a monthly basis with little bearing on the model

results. However, the model becomes increasingly dependent on Q_{ET} when steady state

assumptions are made for salt and yields a seasonal pattern of discharge nearly opposite to

that predicted by hydraulic gradients. For most months, the rate of change in salt is related

to the rate of change in groundwater discharge, but since the system cannot be considered

to be in steady state it must be flushed relatively slowly with respect to salt. This is

evidenced in part by some tracer retention in the breakthrough curves of the March tracer

study. However, because the storage changes are small enough that one can assume steady

state without significantly effecting the model suggests that the same mechanisms that control the drainage of water from the system do not flush salt. This is difficult to reconcile, but a decoupling between porewater and salt transport has been observed, and plants have been implicated as possible mediators of preferential salt transport (Nuttle and Hemond 1988). Evapotranspiration may wick salt into hydraulically less active pore spaces, or there may be some salt storage periodically in the unsaturated zone when hydraulic conductivity and specific yield change during periods of unsaturation (Nuttle and Hemond 1988).

Outputs - Evapotranspiration and Drainage (Q_{ET}, Q_D)

Evapotranspiration is the major mechanism for water loss (55 %) from the sediment only in August and nearly balances infiltration for June, July and August (Table 2). At all other times, drainage (calculated as the residual in the model) dominated water loss from the sediments. Q_{ET} is often the major loss and most uncertain term in wetland water balances (Winter 1981; Carter 1986). Reduced error in water and isotope balances has been achieved by redefining it in terms of parameters with less variance (Hunt et al. 1996). Errors in Q_{ET} can be as high as 15% with reliable site specific radiation and temperature data (Winter 1981, Abtew and Obeysekera 1995). Equating Q_{ET} with potential evapotranspiration may yield an overestimate of evapotranspiration when non-saturated soil conditions are encountered and may be of particular importance when the water table is low and the duration between flooding events is long. In contrast, potential evapotranspiration may underestimate true evapotranspiration during periods of high transpiration (Gehrels and Mulamoottil 1990). In our experiment, estimates of Q_{ET} were derived solely from temperature data and had a mean monthly coefficient of variation of 40%. Despite this uncertainty, the model showed only moderate sensitivity to variations in Q_{ET} and even a doubling of evapotranspiration fluxes would not make it the dominant water loss term in

the budget except during July and August. When inputs of water exceeded evapotranspiration demands (all months except August), drainage was the major loss of water from the subsurface. Drainage rates of porewater have been correlated with the slope of the water table (approximated by the slope of the marsh surface) and proximity to geomorphological relief such as creekbanks and hillslopes (Hemond and Fifield 1982; , Harvey et al. 1987). Because drainage is calculated as the residual in the model, its magnitude can be determined by any of the input fluxes. For example, high drainage rates resulted from a large groundwater flux in the Spring while Autumn drainage rates reflected high infiltration rates, and the July drainage flux was primarily a function of precipitation input. Unlike evapotranspiration which removes only water, drainage removes water and salt from the system. Thus, the dominance of drainage as opposed to water removal by evapotranspiration may explain why hypersaline porewater salinities were never encountered even during periods characterized by little or no fresh groundwater inputs. Confidence in the estimate of the drainage flux is low for months where its magnitude is less than the total estimate of error for the model (July and August).

Implications for Marsh-Estuary Exchange

Because the flux of water governs the exchange of materials in and out of wetlands, Lent et al. (1997) suggested that the dominance of different components of water balances encountered in nontidal wetlands defines the degree of wetland interaction within the landscape. If this premise is applied to tidal marshes, the system has a high degree of interaction within the landscape when the water budget is controlled primarily by fluxes which connect the wetland with adjacent ecosystems (infiltration, groundwater, or drainage). Conversely, when precipitation and evapotranspiration (which exchange water with the atmosphere and not adjacent systems) are dominant in the water budget, the wetland is more hydrologically isolated within the landscape. During July and August,

precipitation and evapotranspiration comprised a larger fractional contribution to the overall water balance at the Ringfield site. Consequently, the exchange of porewater with the estuary probably decreased during this time. For all other months the marsh estuary exchange was greater because the water balance is controlled primarily by groundwater and tidal inputs, and drainage. The largest overall water fluxes through the subsurface were encountered in spring and resulted from elevated groundwater input. The groundwater induced porewater flushing in the spring must be accompanied by increased export of marsh-derived constituents towards the estuary, and any significant marsh processing of groundwater derived nutrient loads would similarly occur during this period.

Tracer Derived Estimates

In general, tracers have been used in wetlands to estimate drainage and porewater turnover, and not directly applied to deriving groundwater inputs to the system (Nestler 1977; Harvey et al. 1995). However, in this study, the addition of a conservative tracer provided validation of the alternate methods for estimating the groundwater flux under high flow conditions. The groundwater discharge rate for the Ringfield study site reconstructed from the bromide breakthrough curve indicated rapid horizontal flow in the upper 50 cm of marsh and significant lateral dispersion relative to advection during March (Fig.6). In addition to providing a measure of groundwater flux, the long "tails" encountered on the breakthrough curve (Fig. 7) suggest temporary solute storage in stagnant pore spaces.

Comparison of Estimates

One of the primary goals of this study was to compare the estimates of groundwater flux obtained using the Darcy approach with the water and salt balance and the estimates

derived from the bromide experiments. However, any comparison of the data must acknowledge the fact that, regardless of attempts to constrain the approaches so they would measure similar processes, the methods inherently measure different things. The Darcy calculations describe flow of not entirely fresh water. In this respect, this technique for calculating groundwater flow is similar to the tracer estimates. In contrast, the salt and water balance is constrained to estimating the influx of freshwater only.

Although the seasonal pattern of discharge is similar for the Darcy and the water/salt balance methods (Fig. 8), the comparison can be broken into the following three periods: June through August when the groundwater discharge estimates were nearly equal, September through December when the model estimates exceeded Darcy estimates, and February through May when Darcy estimates exceeded model predictions. During high flow conditions from late winter through spring, Darcy fluxes were approximately two times higher than the mass balance estimates at peak discharge. Implicit in the comparison is the assumption that because the tracer estimate is an empirically observed quantity with low error, it probably is a better representation of the true groundwater flux. The tracer estimate is similar in both the magnitude and pattern of discharge described by the water and salt balance in March. Therefore the Darcy fluxes most likely overestimate groundwater fluxes during the Spring. By definition, the magnitude of freshwater discharge (model estimate) must be less than the magnitude of total discharge (Darcy estimate) if the discharge is composed of a mixture of groundwater and porewater. Consequently, the Darcy measured flux includes some water of estuarine origin and represents an overestimate of true groundwater input. The salinity of water discharging at the upland border was observed to range between 0 and 4 ppt. Increasing the salinity of the C_{GW} term in the model within this range increased the output of groundwater to values close to the range of Darcy estimates during periods of high flow suggesting this as a

reasonable explanation for some of the Darcy overestimates.

During low flow conditions in the late summer and autumn the water/salt balance approach predicts groundwater discharge into the marsh of a magnitude three times higher than the Darcy predicted flux (which is out of the marsh). This mass balance predicted flux however, would be opposite to the measured hydraulic gradient. We acknowledge that it is unlikely to encounter any substantial fresh groundwater flux into the marsh during periods when the hydraulic gradient predicts net flow out of the system. The Darcy-predicted flux out of the marsh during this period is supported by the observed salt intrusion into aquifer underlying the wetland (Fig. 2) The increased estimate of error encountered in the model during low flow is further evidence of the weakness of the model at low flows. In contrast, the estimate of error for the Darcy fluxes is proportional to the discharge magnitude. Consequently at low flows the Darcy estimate may provide a more accurate and less variable estimate of groundwater flux than the water/salt balance. The elevated discharge fluxes predicted by the mass balance model at low flow may well be a model artifact which needs to be reconciled in the future.

SUMMARY AND CONCLUSIONS

We have observed large seasonal pulses of groundwater into a fringing mesohaline saltmarsh using three independent methods of quantifying groundwater flux. We suggest that water/salt mass balances provides a more reasonable estimate of groundwater flux at high flows and Darcy techniques are better estimates of flow at lower flux magnitudes. When groundwater inputs are large, flow is dominated by the horizontal transport and the groundwater flux is the major component of water inputs to the subsurface. Groundwater inputs constitute a larger portion of total water input to the subsurface in more elevated areas of the marsh which are near the upper limit of tidal infiltration. Previous studies may have missed these large contributions of freshwater to these ecosystems because of their seasonal timing.

The Ringfield marsh is hydrologically more isolated within the landscape in July and August during peak evapotranspiration, and more interactive with the adjacent estuary when groundwater, tidal infiltration, and drainage fluxes are large. The large reduction in subsurface conductivity and high percentage of groundwater flux to the total water budget from February to May suggests both a seasonal purging of porewater and solutes from the marsh to the estuary, and that any marsh processing of groundwater derived solute loads are likely to occur only during this period.

LITERATURE CITED

Abtew,W., J. Obeysekera. 1995. Lysimeter study of evapotranspiration of cattails and comparison of three estimation methods. Trans. ASAE 38:,1, 121-129.

Anderson, I.C., C.R. Tobias, B.B. Neikirk, and R.L. Wetzel. 1997. Development of a process-based nitrogen mass balance model for a Virginia Spartina alterniflora saltmarsh: Implications for net DIN flux. Marine Ecology Progress Series. 159: 13-27.

Bohlke, J.K., and J.M. Denver. 1995. Combined analysis of groundwater dating, chemical, and isotopic analyses to resolve the history and fate of nitrate contamination in two agricultural watersheds, Atlantic coastal plain, Maryland. Wat. Res. Res. 31: 9, 2319-2339.

Bokuniewicz, H. J. 1992. Analytical descriptions of subaqueous groundwater seepage. Estuaries. 15: 458-464.

Bosen, J.F. 1960. A formula for approximation of saturation vapor pressure over water. Monthly Weather Reviews. 88:8, 275-276.

Bradley, P.M., and J.T. Morris. 1991. Relative importance of ion exclusion, secretion, and accumulation in Spartina alterniflora Loisel. Journal of Experimental Botany. 42: 1525-1532.

Cable, J.E., W.C. Burnett, and J.P. Chanton. 1997. Magnitude and variations of groundwater seepage along a Florida marine shoreline. Biogeochemistry. 38: 189-205.

Carter,V. 1986. An overview of the hydrologic concerns related to wetlands in the United States. Can. J. Bot. 64: 364-374.

Chambers, R., J.W. Harvey, and W.E. Odum. Ammonium and phosphate dynamics in a Virginia salt marsh. Estuaries. 15: 349-359.

Dacey, J.W.H., and B.L. Howes. 1984. Water uptake by roots controls water table movement and sediment oxidation in short Spartina alterniflora marsh. Science. 224: 487-489.

Fetter, C.W. 1993. Contaminant Hydrogeology. Macmillan Publishing.

Finkelstein, K., and C.S. Hardaway. 1988. Late Holocene sedimentation and erosion of estuarine fringing marshes, York River, Virginia. J. Coast. Res. 4: 3, 447-456.

Focazio, M.J. 1997. Springs and seeps of Colonial National Historical Park. U.S. Geological Survey. Interagency Agreement #4000-6-9003: 1-22.

Gehrels, J., and G. Mulamoottil. 1990. Hydrologic processes in a southern Ontario wetland. Hydrobiologia 208: 221-234.

Hackney, C.T., S. Brady, L. Stemmy, M. Boris, C. Dennis. T. Hancock, M. O'Bryon, C. Tilton, and E. Barbee. 1996. Does intertidal vegetation indicate specific soil and hydrological conditions. Wetlands. **16**: 1, 89-94.

Hamon, W.R. 1961. Estimating potential evapotranspiration. Proceedings of ASCE, Journal of Hydraulics Division. **87**: HY3, 107-120.

Harvey, J.W., and W.E. Odum. 1990. The influence of tidal marshes on upland groundwter discharge to estuaries. Biogeochemistry. **10**: 217-236.

Harvey, J.W., P.F. Germann, and W.E. Odum. 1987. Geomorphological control of subsurface hydrology in the creekbank zone of tidal marshes. Estuarine Coastal Shelf Sci. **25**: 677-691.

Harvey, J.W., R.M. Chambers, and J.R. Hoelscher. 1995. Preferential flow and segregation of porewater solutes in wetland sediment. Estuaries. **18**: 4, 568-578.

Hemond, H.F., and J.L. Fifield. 1982. Subsurface flow in a salt marsh peat: A model and field study. Limnol. Oceanogr. **27**: 126-136

Hobbs, C.H. 1979. Summary of shoreline situation reports of Virginia's Tidewater localities. Special Report: Appl. Mar. Sci and Ocean Eng. 209

Hunt, R.J., D.P. Krabbenhoft, M.P. Anderson. 1996. Groundwater inflow measurements in wetland systems. Wat. Res. Res. **32**: 3, 495-507.

Hvorslev, M.J. 1951. Time lag and soil permeability in groundwater observations. Bull 36. U.S. Army Corps of Eng. Waterw. Exp. Stn., Vicksburg Miss.

Jordan, T.E., D.L. Correll, and D.F. Whigham. 1983. Nutrient flux in the Rhode River and tidal exchange by brackish marshes. Estuarine, Coastal, and Shelf Science. **17**: 6, 651-667.

LaBaugh, J.W. 1986. Wetland ecosystem studies from a hydrologic perspective. Water Resources Bulletin. **22**: 1, 1-9.

Lent, R.M., P.K. Weiskel, F.P. Lyford, and D.S. Armstrong. 1997. Hydrologic indices for nontidal wetlands. Wetlands. **17**: 1, 19-30.

Libelo, E.L., W.G. MacIntyre, and G.H. Johnson. 1990. Groundwater nutrient discharge to the Chesapeake Bay: Effects of near-shore land use practices. New perspectives in the Chesapeake System: A research and management partnership. 613-622.

Morris, J.T. 1995. The mass balance of salt and water in intertidal sediments: Results from North Inlet, South Carolina. Estuaries. **18**: 4, 556-567.

National Climatic Data Center. 1997. Climatological Data Annual Summary, Virginia. **107**, 13.

Nestler, J.A. 1997. A preliminary study of the sediment hydrology of a Georgia salt marsh using Rhodamine WT as a tracer. Southeast. Geol. 18:265-271.

Nuttle, W.K., and H.F. Hemond. 1988. Salt marsh hydrology: Implications for biogeochemical fluxes to the atmosphere and estuaries. Glob. Biogeo. Cyc. 2: 2, 91-114.

Nuttle, W.K., H.F. Hemond and K.D. Stolzenbach. 1990. Mechanisms of water storage in salt marsh sediments: The importance of dilation. Hydrol. Proc. 4: 1-13.

Nuttle, W.K., and J.W. Harvey. 1995. Fluxes of water and solute in a coastal wetland sediment. 1. The contribution of regional groundwater discharge. J. Hydrol. 164: 89-107.

Portnoy, J.W., B.L. Nowicki, C.T. Roman, and D.W. Urish. 1998. The discharge of nitrate-contaminated groundwater from a developed shoreline to a marsh-fringed estuary. Wat. Res. Res. 34: 11, 3095-3104.

Price, J.S., and M.K. Woo. 1988. Studies of a subarctic coastal marsh. 1. Hydrology. J. Hydrol. 103: 275-292.

Reilly, T.E., and A.S. Goodman. 1985. Quantitative analysis of saltwater-freshwater relationships in groundwater systems--A historical perspective. J. Hydrol. 80: 125-160.

Staver, K.W., and R.B. Brinsfield. 1996. Seepage of groundwater nitrate from a riparian agroecosystem into the Wye River estuary. Estuaries. 19: 2B, 359-370.

Wiegert, R.G., A.G. Chalmers, and P. Randerson. 1983. Productivity gradients in saltmarshes: The response of *Spartina alterniflora* to experimentally manipulated soil water movements. Oikos. 41: 1-6.

Whiting, G.J., and D.L. Childers. 1989. Subtidal advective water flux as a potentially important nutrient input to Southeastern U.S.A. estuaries. Estuarine,Coastal and Shelf Sci. 28: 417-431.

Winter, T.C. 1981. Uncertainties in estimating the water balance of lakes. Water Resources Bulletin. 17: 1, 82-115.

Yelverton, F.G., and C.T. Hackney. 1986. Flux of dissolved organic carbon and porewater through the substrate of a *Spartina alterniflora* marsh in North Carolina. Estuarine,Coastal and Shelf Sci. 22: 255-267.

SECTION II

Nitrogen Cycling Through an Aquifer - Fringing Marsh Transition Zone†

ABSTRACT

Fringing wetlands are critical components of estuarine systems, and their maintenance within the landscape is contingent upon the tight cycling and conservation of nitrogen. To determine their capacity to buffer groundwater-derived nitrogen loads, and the effects of groundwater discharge on internal nitrogen cycling, we measured several N-cycling processes in the sediment from a fringing mesohaline marsh in Virginia. Rates of mineralization, nitrification, potential denitrification (DNF), and potential dissimilatory nitrate reduction to ammonium (DNRA) were estimated along with porewater concentrations of oxygen, sulfide, and conductivity during periods of high (May 1997) and low (October 1997) groundwater discharge. All N cycling processes were confined to the upper 1-1.5 meters of marsh where organic matter and ammonium were most abundant. Depth integrated rates for mineralization, nitrification, DNRA, and DNF ranged between 0.97 -11.20, 0.00 -2.16, 0.88 -6.13, and 1.84 -17.62 mmoles N m^{-2} hr^{-1} respectively. Mineralization, measured in cores using the isotope dilution technique, was the dominant process, exceeding nitrification by 3 - 20 fold. Natural abundance $\delta^{15}N$ measurements of the ammonium, particulate organic nitrogen, nitrate, and molecular nitrogen pools suggested that in situ nitrification rates were of similar magnitude as determined by core experiments, and that coupled nitrification - denitrification was a sizeable sink for mineralized N. During Spring discharge (May) marsh porewater conductivity, and dissolved sulfide decreased by approximately 50 %, and a groundwater driven O_2 flux of 27 μmoles m^{-2} hr^{-1} into the marsh subsurface was estimated. During the Spring high discharge period, mineralization, nitrification, and DNRA rates were up to 12x, 6x, and 7.5x greater, respectively, than rates observed during low discharge in the Fall. The maximum difference in seasonal rates was observed in the marsh nearest the upland border

where groundwater discharge had the greatest effect on sediment geochemistry. DNF rates, however were 10x higher during low discharge. The higher groundwater O_2 flux in May was not sufficient to account for much of the observed increase in mineralization. The enhanced mineralization during Spring may have been due to groundwater import of alternate electron acceptors (CO_2, Fe^{3+}), or an increased mixing of porewater metabolites. The groundwater O_2 flux, however, was able to support up to 50% of the increased nitrification in the Spring below the rhizosphere. Decreases in sulfide and salinity at high discharge were sufficiently large to help explain the increased nitrification rates. Despite accelerated mineralization and nitrification during Spring discharge, the potential DNF : DNRA ratio was 0.4, indicating that more than twice as much of the N cycled through nitrification was retained as NH_4^+ rather than exported immediately as N_2 through coupled nitrification - denitrification.

INTRODUCTION

The rapid cycling of nitrogen in marsh sediments is required for the maintenance of the high primary production characteristic of these ecosystems, and is a critical element in any marsh-mediated regulation of estuarine water quality (Anderson et al. 1997, Hopkinson and Schubauer 1984). The growth of dominant marsh macrophytes (*Spartina spp.*) can be directly or indirectly limited by nitrogen (Valiela and Teal 1974; Dai and Weigert 1996; Morris 1980), and much of the study of N cycling in fresh and salt water marshes has been restricted to the rhizosphere where processes have direct relevance to macrophyte production or decomposition (Bowden 1986; Anderson et al. 1997; DeLaune et al. 1983). Similarly, methods used to determine the function of marshes (either as sources or sinks of materials) within the estuarine landscape have concentrated on processes in shallow sediments, and fluxes between the sediment surface and tidal water or the atmosphere (Anderson et al. 1997; Scudlark and Church 1989; Childers and Day 1988; Childers 1993). The sediment surface represents an interface between a reducing sediment environment and an oxidizing water column or atmosphere and is an active zone of nitrogen transformations. Of the multiple factors (Eh, pH, salinity, dissolved oxygen, dissolved inorganic nitrogen, and sulfide) controlling the pathways and magnitudes of different N transformations, organic carbon, oxygen, nitrate and sulfate have been considered primary regulators of mineralization (MIN), nitrification, (NIT) denitrification (DNF), and the dissimilatory reduction of nitrate to ammonium (DNRA). Oxygen flux into sediment enhances nitrification, and controls the ratio of aerobic to anaerobic organic matter respiration (Thompson et al. 1995; Howes et al. 1984). Denitrification rates are amplified directly by the allochthonous input of NO_3^-, indirectly by oxygen inputs through coupled nitrification/denitrification, and inhibited by large fluxes of oxygen directly to the sediment from the atmosphere at low tide. High rates of sulfate reduction occur when delivery of

sulfate to sediments is large, thus elevating rates of anaerobic N mineralization through

sulfate reduction, and inhibiting both nitrification and denitrification when H_2S accumulates

(Joye and Hollibaugh 1995; Portnoy and Giblin 1997; Sorenson 1987). Further, high free

sulfide concentrations as well as low NO_3^- : DOC ratios favor the retention of nitrogen in

the system by proportionally increasing nitrate reduction to ammonium rather than

denitrification to N_2 (King and Nedwell 1985; Brunet and Garcia-Gil 1996; Tiedje 1988).

With few exceptions, exchanges of these redox active compounds between tidal water or

the atmosphere across the sediment surface have been considered as the sole external

forcings relevant to N cycling.

There exists however a second redoxcline between the marsh strata and the

underlying aquifer which has been primarily overlooked. While not directly relevant to

macrophyte production or diffusive fluxes to the estuary, N cycling at this boundary may

be important in attenuating allochthonous groundwater N loads prior to discharge to the

adjacent water body, thereby impacting longer term N retention in the ecosystem.

Aside from localized zones of low redox potential, shallow coastal aquifers are

typically oxic, contain NO_3^- as the dominant DIN species, and are sulfate-free with respect

to mesohaline estuarine water (Fetter 1993). Consequently, discharging groundwater may

represent a source of additional N to the marsh, and additional electron acceptor (e.g., O_2)

available for respiration or nitrification, while concurrently flushing porewaters of

accumulated salt and sulfide. The effectiveness of marshes in buffering the adjacent

estuary against groundwater derived N loads is not clear (Howes et al. 1996; Portnoy et al.

1998), but groundwater derived nitrate loads have been considered important sources of N

in some marsh nitrogen budgets where anthropogenic loading of N is high (Valiela and

Teal 1979, Howes et al. 1996). A critical element in defining the nature and extent of

groundwater N processing by the marsh requires a better understanding of N cycling below the rhizosphere and specifically at the aquifer-marsh interface.

Not all shallow aquifers, however, are enriched in nitrogen, and it is the potential flux of groundwater derived oxygen that may have more wide-reaching implications for nitrogen processing in marshes subject to groundwater discharge. Mineralization of organic N to ammonium can be accelerated in anaerobic sediments by the introduction of oxygen (Hansen and Blackburn, 1991), and nitrification is often oxygen limited and tightly coupled to denitrification in ammonium-rich marsh sediments (Seitzinger 1994). Strong correlations between denitrification and oxygen consumption rates in riparian wetlands suggest that the rate of N export from the system via coupled nitrification/denitrification may be accelerated by an influx of allochthonous dissolved oxygen (Seitzinger 1994). Although the groundwater oxygen concentrations are typically lower than those encountered in tidal water and in the atmosphere, the advective flux of groundwater in some marshes can be seasonally strong and dominate the sediment water balance (over tidal infiltration) when discharge is high (Tobias et al. 2000).

We have chosen to examine several nitrogen cycling processes in a fringing mesohaline marsh that receives seasonal inputs of fresh groundwater of up to $18 \, 1 \, m^{-2} \, day^{-1}$. We present a characterization of mineralization, nitrification, denitrification potential and potential dissimilatory nitrate reduction to ammonium from the marsh surface into the underlying aquifer, during a high and a low groundwater discharge period through the use of ^{15}N tracer and natural abundance techniques.

SITE DESCRIPTION AND METHODS

The study site is located in the Colonial National Historical Park (37° 16' 42" N , 76° 35' 16" W) bordering the York River in southeastern Virginia (Fig. 1). It consists of an upland slope of approximately 1:1 which grades through a mixed community of *Spartina cynosuroides* and *Spartina alterniflora* short form into a monotypic *S. alterniflora* (short form) fringing marsh approximately 25 meters in width. The study area borders the mesohaline portion of the York River (salinity range 12-21 ppt). Upland geology and marsh evolution near the site are discussed in Libelo et al. (1990) and Finkelstein and Hardaway (1988), respectively. The small scale marsh stratigraphy consists of an upper 30 -80 cm of sandy marsh peat underlain by a semi-continous layer of lower permeability glauconitic silty sand with a 10-20 cm thickness. Below 150-200 cm, the glauconitic deposits grade into cleaner oxidized iron rich sands and shell hash of pre-Holocene origin. The site receives maximal groundwater discharge from January through July when the upland water table elevation exceeds the elevation of the glauconite unit, and receives little to no discharge from August through December (Tobias et al. 2000a).

Methods

The cycling of nitrogen from 0-2 meters depth during periods of high and low groundwater discharge was investigated using ^{15}N isotope dilution, acetylene (C_2H_2) block, and natural abundance techniques. N cycling processes were determined directly in sediment cores or slurries, and porewaters were analyzed for constituents generally relevant to N cycling (Table 1).

Figure 1. Site location and cross section. Letters denote location of cores taken in August 1996.
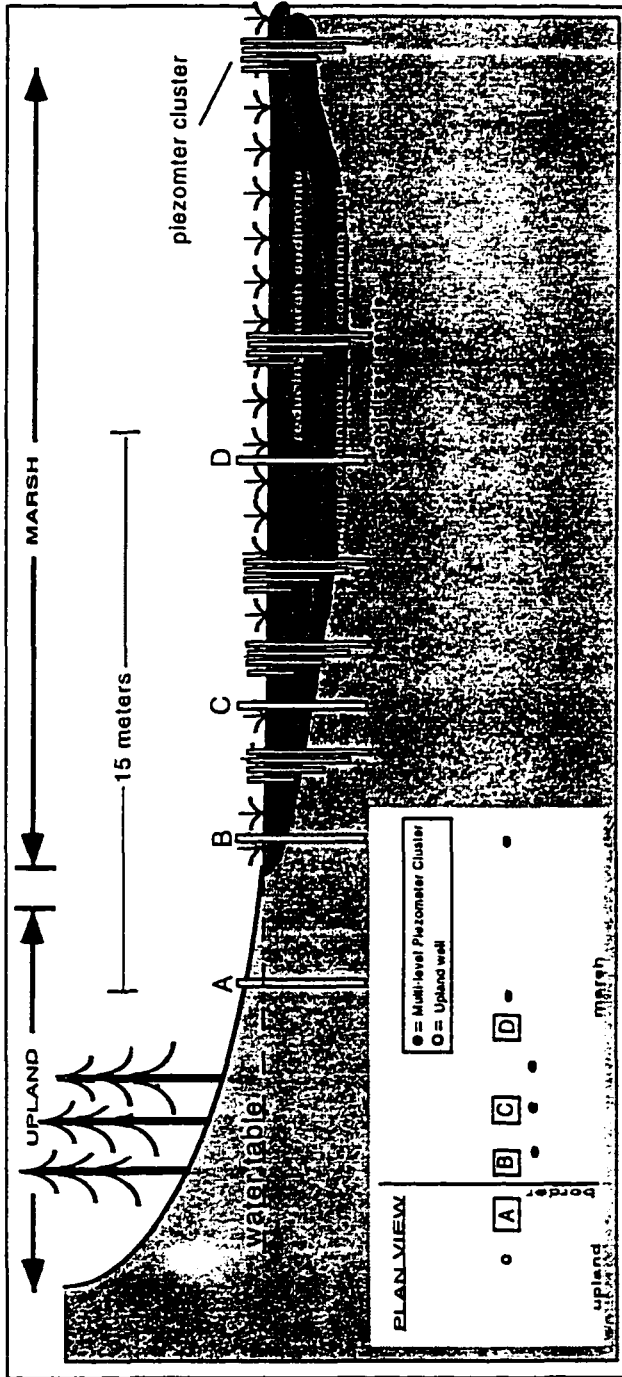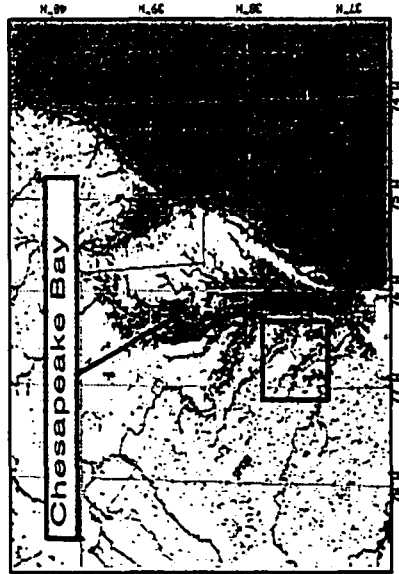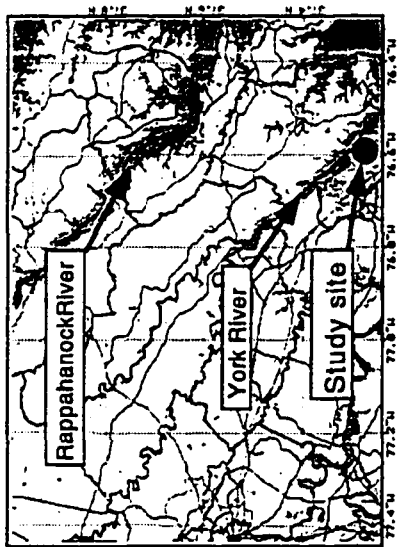
Table 1. Summary of analyses of sediments and porewaters. With the exception of $\delta^{15}N_2$, $\delta^{15}N$-PON and $\delta^{15}N$-DIN, all parameters were quantified during periods of high and low groundwater discharge. Sediments were characterized to a depth of 2 meters at 10 - 20 cm intervals. Porewaters were characterized to a depth of 2 meters in 50 cm intervals.

	Aug 96	Sep 96	Dec 96	May 97	Oct 97	Mar 97
Groundwater Flow	low	low	low	high	low	high
SEDIMENT						
Bulk Sediment Properties	X					
Eh	X					
DIN	X	X		X	X	
C:N	X					
$\delta^{15}N$-PON	X					
Mineralization				X	X	
Nitrification				X	X	
Denitrification Potential				X	X	
DNRA Potential				X	X	
POREWATER						
Conductivity				X	X	
Temp				X	X	
pH				X	X	
D.O.				X	X	
H_2S				X	X	
$\delta^{15}N$-DIN			X			
$\delta^{15}N$-N_2						X

Porewater Characterization

<u>Field Sampling</u>

Porewaters were collected from a multi-level piezometer transect extending from the upland marsh border to 15 meters into the marsh (Fig. 1). The transect contained 5 piezometer clusters with each cluster composed of 4-5 piezometers spanning sediment depths from 2.5 meters to 5 cm below the sediment surface at increments of 50 cm. The piezometers were constructed of polyvinylchloride (PVC) pipe (2.54 cm diameter) mated with 50 cm of 0.0254 cm PVC slot screen. Piezometers were installed into 7.62 cm diameter hand-augered holes, surrounded with a fine sandpack over the length of the screen, capped with a bentonite plug and backfilled with auger cuttings. All piezometers were sealed to the atmosphere and sampled through gas tight stopcocks connected to internal sampling tubes. Atmospheric contamination was excluded from the piezometer during purging and sampling by attaching an ultra high purity helium headspace reservoir to the piezometer, and a water trap during post purging recharge. A detailed description of the piezometer design, and sampling protocol is presented in Tobias et al. (2000). All piezometers were purged periodically over several months following installation to facilitate equilibration with the surrounding strata, and purged immediately prior to sampling to minimize storage artifacts in the geochemical analyses. Water withdrawal was accomplished with either a peristaltic pump or syringe.

<u>Physical, Chemical, and Isotopic Analyses</u>

Temperature, pH, conductivity, dissolved oxygen (DO), sulfide (H_2S), dissolved organic carbon (DOC), and natural abundance $\delta^{15}N$- NH_4^+, $\delta^{15}N$- NO_3^- and dissolved $\delta^{15}N$- N_2 were determined on porewaters collected from the site.

Temperature and pH : Temperature and pH were determined on water drawn from each piezometer depth in the field using an Fisher Scientific AP-10 pH meter immediately following sample collection.

Dissolved Oxygen: D.O. was determined by the azide modification of the Winkler titration method (Benson and Krause 1984). Water samples were fixed in the field with manganous sulfate and alkali-iodide-azide solution in BOD bottles, and stored in the dark. Acidification and the thiosulfate titration used to quantify D.O. was performed within 24-48 hours of collection.

Sulfide: Samples for sulfide (H_2S) analysis were collected according to Hines et al. (1989). Water samples were filtered at the time of collection through a 0.2 μm polyether sulfone (Gelman -Supor) syringe filter into an equal volume of 6% zinc acetate solution. Preserved samples and standards were stored under refrigeration for less than one week and sulfide quantified spectrophotometrically following reaction with diamine colorometric reagent according to Cline (1969).

Soluble Iron . Analysis of Fe^{2+} was performed using the ferrozine assay as described by Stookey, (1970). Water samples were filtered (0.2 μm) at the time of collection and immediately reacted with ferrozine. Fe^{2+} was determined colorometrically by absorbance at a wavelength of 562 nm.

Dissolved Organic Carbon: Porewater for DOC determination was collected with new dedicated polypropylene syringes and field filtered through 0.7 μm glass fiber filters into teflon capped glass scintillation vials and immediately stored on ice. Both filters and scintillation vials had been precombusted at 500 °C for 4-5 hours prior to sample collection.

Samples were frozen for up to two months, and analysis was performed using a Shimadzu TOC 5000 Total Organic Carbon Analyzer.

^{15}N Isotopic Analysis: Porewater samples for the determination of the isotopic composition of $\delta^{15}N$-NH_4^+, $\delta^{15}N$-NO_3^-, and $\delta^{15}N$-N_2 were collected in December 1996 (DIN), and March 1997 (N_2). Water samples for $\delta^{15}NH_4^+$ and $\delta^{15}NO_3^-$ analyses were filtered through a 0.7 μm ashed glass fiber filter and frozen. Isolation of NH_4^+ and NO_3^- for natural abundance $\delta^{15}N$ characterization was performed sequentially on the same sample fraction according to the steam distillation technique described by Velinsky et al. (1989). Sample pH was increased above 12 with NaOH and the NH_3 steam distilled into a weak HCl solution using a Rapid Still II steam distillation system. Ammonium in the acid trap was bound to 100 mg zeolite molecular sieve (Union Carbide Ionsiv W-85), dried at 50 °C, and scraped into quartz combustion tubes. Cupric oxide, and copper metal were added to the tube to catalyze the conversion of NH_4^+ to N_2 following atmosphere evacuation from the tube, sealing, and combustion at 800°C. Following the combustion, tubes were cracked in a vacuum line, CO_2 separated cryogenically, and $\delta^{15}N$ determined on the N_2 fraction using a dual inlet Prism isotope ratio mass spectrometer (IRMS) at the University of Virginia (UVA). NO_3^- in the remaining sample was converted to NH_4^+ using 0.4 g Devarda's Alloy, and the distillation, zeolite binding, was repeated. Water samples for the determination of $\delta^{15}N_2$ were collected from piezometers with a peristaltic pump into 13 ml Hungate tubes containing 150 mg $ZnCl_2$ as a preservative. Tubes were stoppered and capped without headspace or bubbles and stored upside down under water and refrigerated prior to analysis. Three days prior to isotopic analysis, a 4 ml ultra high purity helium headspace was introduced into the tubes while venting an equal volume of

sample. Tubes were vortexed for five minutes to promote headspace equilibration and returned to storage. For isotope analysis, 1.5 ml of headspace was withdrawn with a gas tight syringe and injected into a vacuum line. CO_2 was cryogenically removed and the N_2 fraction analyzed for $\delta^{15}N$ as described above.

Sediment Characterization and Determination of N Cycling Rates

Field Sampling

Core tubes were constructed from a 3 meter length of 5.08 cm diameter schedule 40 pvc pipe which had 1 mm diameter holes drilled at 2 cm intervals along the length of the tube offset by 90 degrees (Fig. 2). All holes were sealed with silicone prior to sampling. Cores were driven to a depth of 2 meters below the marsh surface using a jack hammer and scaffolding. Compaction of 5 - 30% among the cores was observed, and resulting depth profiles were corrected accordingly. Following driving, cores were capped and cranked out of the ground using either a winch or "come along" attached to the scaffolding. Upon extraction from the ground, core bottoms were immediately capped and cores transported to the laboratory at the Virginia Institute of Marine Science. The resulting holes in the marsh were back-filled with bentonite.

Four cores (Fig 1) were collected in August 1996 along a transect from the upland to approximately 8 meters into the marsh for characterization of sediment Eh, extractable dissolved inorganic nitrogen (DIN), % organic, C:N ratio, %N, $\delta^{15}N$-particulate organic nitrogen (PON) , and selected bulk sediment properties (density, % water, porosity). Four replicate 1 meter cores were collected in Sep 1996 for extractable DIN only. Measurement of gross nitrification, gross mineralization, and potential DNRA were performed on

Figure 2. Methods flow chart for the N-cycling rate measurements.

Silicone-filled
Injection Ports

$^{15}NH_4^+$
or
$^{15}NO_3^-$

2 meter

10 - 20 cm sections

Mineralization, Nitrification, DNRA Potential

DIN Analysis

Diffusion

Mass
Spectrometry

Incubate Intact Core

Subsection

KCl Extraction

2 meter

10 - 20 cm sections

Denitrification Potential

aqueous port

headspace port

N_2O Analysis

Collect Core

Subsection

Incubate
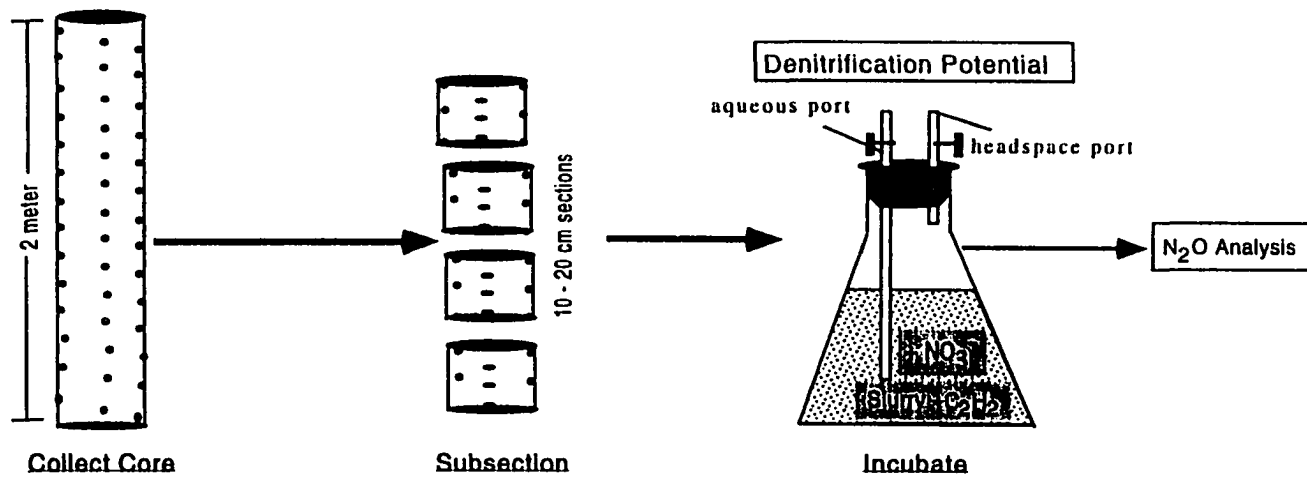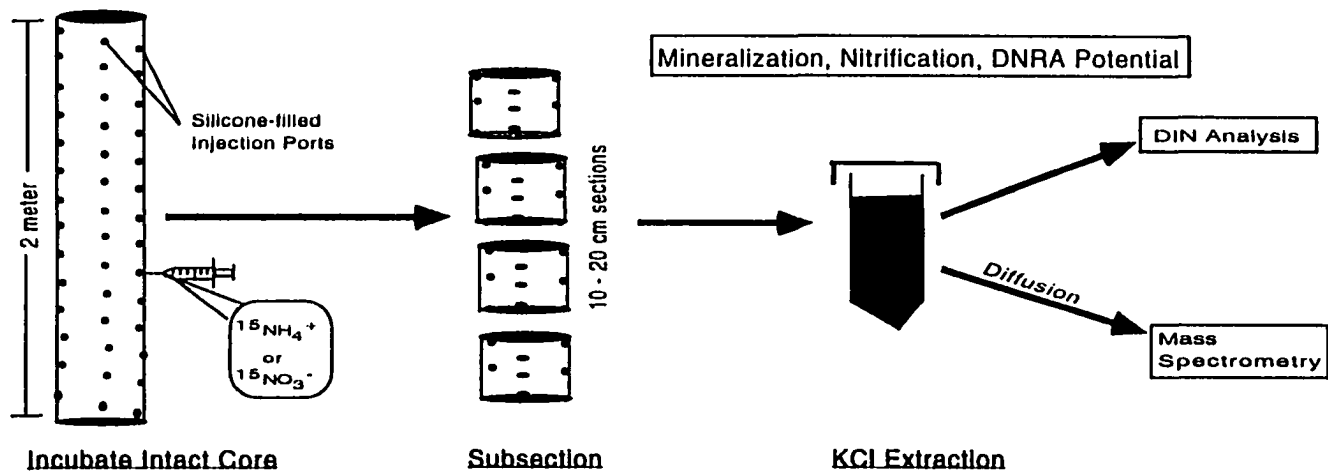
duplicate cores collected in May and October 1997 at sites located 2 meters and 6 meters into the marsh from the upland border.

Redox Potential: Eh profiles were determined in intact cores collected in August 1996 by using a pH meter fitted with fine gauge platinum Eh electrode and a calomel reference electrode. The reference electrode was placed in approximately 10 cm of estuarine water, added to the top of the core, and the platinum electrode was inserted into each of the silicone-plugged holes along the axis of the core. Eh was defined as the potential difference (millivolts) between the two probes and a 240 millivolt correction factor was added to the observed electrical potential to account for the potential of the reference electrode.

Bulk Sediment Properties: Cores collected in August 1996 were sectioned into 10 or 20 cm depth intervals and sub-sectioned into thirds longitudinally. Each subsection was weighed wet and allowed to dry to a constant weight at $60\,^\circ$ C. Wet bulk density, % water, and porosity, were determined from subsection volumes and wet and dry weights. Percent organic content of the subsection was defined as the mass lost (as a percent of dry weight) from the subsection following combustion at $500\,^\circ$C overnight.

Carbon to Nitrogen Ratios and $\delta^{15}N$-PON : C:N Ratios and δ^{15}N-PON were determined simultaneously on a homogenized sediment subsection. DIN was extracted from wet sediment through a series of KCl extractions (2x) and DI water rinses (2x). Each extraction consisted of shaking wet sediment with an equal volume of 2N KCl for 1 hour, centrifugation, decanting the extract, and rinsing the remaining sediment with DI water 2x. Sediment was then dried to a constant weight, ground with a mortar and pestle, acidified

with 30% HCl to remove inorganic carbon, oven dried again and stored in a desiccator

prior to analysis. C:N and $\delta^{15}N$ -PON was determined simultaneously on an Optima IRMS

fitted with an elemental analyzer (C,H,N) located at UVA.

Dissolved Inorganic Nitrogen: Extractable DIN was determined in order to generate

DIN depth profiles from the August and September 1996 cores, and as part of the

quantification of N cycling rates in cores collected in May and October 1997. DIN was

extracted from wet sediments by addition of an equal volume of 2N KCl and shaking for 2

hours on a rotary shaker table. The extract was filtered through a 0.2 μm Gelman-Supor

filter into sterile whirlpak bags, and frozen until analysis. Ammonium was determined by

the phenol hypochlorite method of Solorzano (1969). Nitrate was determined

spectrophotometrically using an Alpkem autoanalyzer following cadmium reduction to

nitrite and diazotization (Perstorp 1992).

N Cycling Rates: Gross mineralization, gross nitrification, and potential DNRA

rates were estimated in intact cores collected in May and October 1997. Denitrification

potential was assessed in slurried sediments from cores collected during the same period.

Cores for mineralization, nitrification and DNRA determination were collected at two

locations within the marsh : 1) within 2 meters of the upland border (border cores), and 2)

approximately 4-6 meters into the marsh from the upland border (marsh cores). Cores for

DNF experiments were collected midway between the border and marsh core sampling

locations.

Gross mineralization rates were determined following the $^{15}NH_4^+$ isotope dilution

technique outlined by Davidson et al. (1990). The rate of gross mineralization derived

from the isotope dilution technique includes a contribution from DNRA and should technically be considered an ammonification estimate. However, because allochthonous inputs of nitrate were low and nitrification rate estimates were small relative to the ammonification estimates, we are confident that the technique provides an estimate primarily of mineralization. For each experiment (May and October 1997) a solution of argon sparged $^{15}(NH_4)_2SO_4$ was injected into each siliconed injection port along the length of the core to achieve a final porewater concentration of 300 μM and 30 atom% ^{15}N enrichment in the porewater. Cores (n=4) were incubated intact in the horizontal position at 23 °C, and sacrificed at T= 0 and 24 hours for the May experiment and T=0 and 72 hours for the October experiment. Cores were sectioned into 10 or 20 cm sections, extruded from the core tube, and the ammonium extracted with KCl as outlined above (Fig.2). Extracts were filtered (0.2 μm) and split into a fraction for NH_4^+ analysis and a fraction for $^{15}NH_4^+$ determination. Both fractions were stored frozen in sterile whirlpak bags prior to analysis. Isolation of the NH_4^+ for ^{15}N isotopic analysis followed the diffusion procedure described by Brooks et al. (1989) requiring the volatilization of ammonium to ammonia under basic conditions and subsequent trapping of NH_3 on an acidified filter disk. Filter disks were dried in a desiccator over concentrated sulfuric acid, wrapped in tin capsules, and analyzed at the University of California Davis, Stable Isotope Facility using an isotope ratio mass spectrometer linked to an elemental analyzer (C,H,N). Mineralization rates were calculated according to the model of Wessel and Tietema (1992) which assumes that rates are constant during the duration of the incubation,

$$\text{Rate} = \left[\frac{(C_{fin} - C_{init})}{time} \right] \times \left\{ \frac{\ln\left[\frac{(At\% _{fin} - 0.37)}{(At\% _{init} - 0.37)} \right]}{\ln\left(\frac{C_{init}}{C_{fin}} \right)} \right\} \qquad (1)$$

which includes changes in atom % enrichment of the labelled pool (At%), changes in concentration of that pool (C), and a correction for natural abundance ^{15}N (0.37).

Nitrification and DNRA: Similarly, nitrification rates were determined by ^{15}NO$_3^-$ isotope dilution. Intact cores were injected with an argon sparged solution of K^{15}NO$_3$ solution to achieve a final porewater concentration of 300 µM NO$_3^-$ and 30 at% ^{15}N enrichment (Fig. 2). Cores (n=4 per experiment) were incubated horizontally and sacrificed at T=0, T=16 hours (top 40 cm), and T=67 hours (lower 160 cm) for the May experiment, and T=0, 12 hours (top 40 cm), and 66 hours (lower 160 cm) for the October experiment. Incubation of the top 40 cm was limited to 16 and 12 hours because of high nitrate reduction rates encountered in those strata. NO$_3^-$ extraction followed the procedure outlined for mineralization. NO$_3^-$ was isolated for isotopic analysis by adding 0.4g Devardas Alloy to the extract fraction that had previously been subject to NH$_4^+$ removal as described by Brooks et al. (1989). The NH$_4^+$ generated from the Devardas reaction was volatilized under basic conditions, trapped on KH$_2$SO$_4$-treated filters, which were dried, wrapped in tin capsules, and sent to the University of California Stable Isotope Facility (UCD) for IRMS analysis. Calculation of nitrification rates also followed the Wessel and Tietema (1992) model where NO$_3^-$ concentration and enrichments were substituted into equation [1].

Ammonium concentrations and ^{15}N enrichments were concurrently measured in the sediment extracts and used to estimate potential DNRA rates. Rates were calculated from modified isotope tracer equations presented in Glibert and Capone (1993):

$$DNRA\ Rate = V \cdot (NH_4^+)_{final} \qquad (2)$$

where $(NH_4^+)_{final}$ is the concentration of ammonium at the end of the incubation, and V is the specific tracer uptake rate as defined by:

$$V = \frac{\left(At\% \ NH_4^+ \ _{final} \right)}{\left[\left(At\% \ NO_3^- \ _{init} \right) \bullet (t) \right]}$$

(3)

where At% denotes the ^{15}N enrichment of either the ammonium pool at the end of the incubation or the nitrate pool at the start of the incubation, and t is the incubation time.

Denitrification potential was determined in argon sparged slurries using the acetylene block technique (Knowles 1990). Cores collected in May and October 1997 were sectioned into 10 or 20 cm intervals, split into thirds and each third mixed with DI water in a ratio of 1:3 by volume. Slurries (n=3 per depth) was transferred to 1000 ml erlenmeyer flasks sealed with a stopper fitted with two gastight stopcocks (headspace and aqueous ports), and an internal sampling tube (Fig.2). Slurries were sparged with argon, and an acetylene sparged KNO_3 solution was injected into the slurry through the internal aqueous sampling tube to achieve a final concentration of 300 μM NO_3^-. Acetylene was generated by adding CaC_2 to water and collecting the gas in 60 ml syringes. An additional 120 ml of C_2H_2 was added to the headspace through the headspace sampling port to achieve a final dissolved C_2H_2 concentration of 10-15% assuming 100% solubility of C_2H_2. Flasks were immediately shaken, and positive pressure vented to the atmosphere, then sealed. Headspace samples were withdrawn with a gas tight syringe at T= 0, 5, and 22 hours for the May sampling and T= 0 and 24 hours for the October sampling. Headspace samples were analyzed for N_2O using a Shimadzu Model 8A gas chromatograph fitted with a poropak Q column and an electron capture detector, with a soda lime trap to minimize CO_2 interference with the N_2O peak. Total dissolved N_2O concentrations were calculated from headspace values using the Ostwald coefficient (Weiss and Price 1980). Potential rates of

denitrification were derived from best fit lines of the resulting N_2O vs. time plots for the May experiment, and by dividing total N_2O production by the incubation time for the October experiment which had only t_0 and t_{final} measurements.

RESULTS

Porewater Analysis

The horizontal and vertical extent of freshwater intrusion expanded in May and contracted in October when some salt encroachment into the shallow upland aquifer was observed (Fig. 3). At both periods, the conductivity encountered in the subsurface was lower than that of tidal water infiltrating the site by 30-70%.

Concurrent with the decrease in porewater conductivity resulting from groundwater discharge, there was an increase in the subsurface concentration and spatial extent of dissolved oxygen (DO) (Fig. 4). DO concentrations increased with increasing sediment depth and distance into the upland to maximal values of 65 and 40 uM for May and October, respectively. Nearly all of the marsh subsurface to a depth of 2.25 meters was anoxic (< 5 μM) in October while only approximately one half of the subsurface sampled had D.O concentrations less than 5 μM in May. DO concentrations above 10μM at depths greater than 1 meter in May were encountered to a distance of 15 meters from the upland border. Multiplying the maximal upland groundwater DO concentrations by estimates of groundwater discharge in May and October of 10, and 0 1 m^{-2} d^{-1} respectively (Tobias et al. 2000) yielded a total groundwater derived flux of DO to the upper 1 meter of marsh in May of 650 μM m^{-2} d^{-1}.

Fe $^{2+}$ concentrations were maximal nearest the upland border and at 1 meter depth in the marsh (> 200 μM; Fig. 5). Fe $^{2+}$ was undetectable in upland wells or below 1.5 meters depth in the marsh. Consequently, Fe $^{2+}$ was restricted to a zone extending from the upland border to 5 meters into the marsh. Subsurface Fe $^{2+}$ concentrations did not differ seasonally.

Figure 3. Contour plots of subsurface porewater conductivity in May and October 1997. Salinity is approximately equal to conductivity / 1.65. The average conductivity of tidal flooding water in May and October was 23 and 34 mS cm^{-1}. Squares indicate sampling locations. The border between the marsh and upland is located at shore normal distance = 0. The surface of the water table is equal to the elevation of the marsh surface in May and 10 cm below the marsh surface in October.
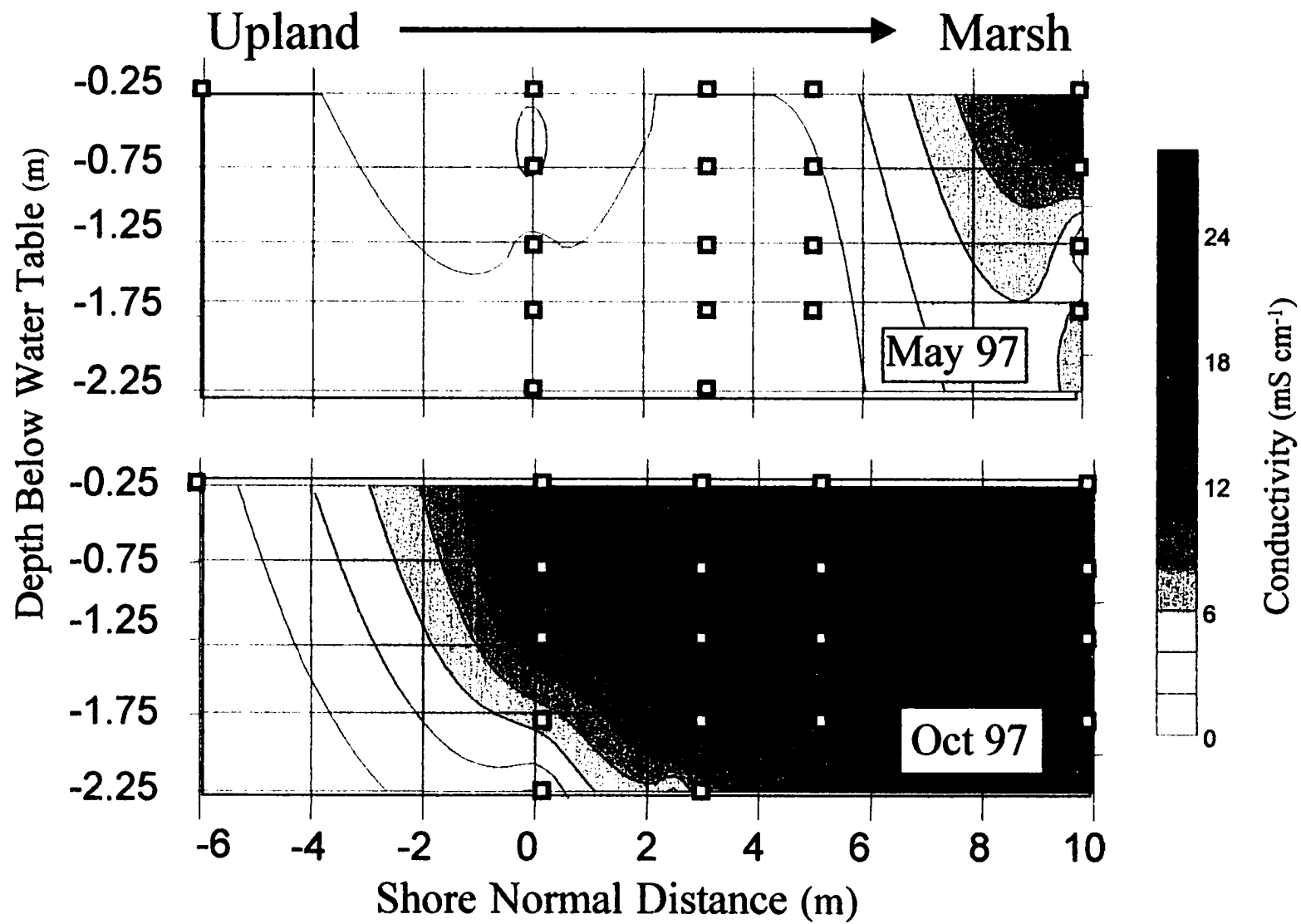
Figure 4. Contour plots of subsurface porewater dissolved oxygen concentrations. Scale

and sampling locations are identical to Figure 3. Detection limit of the D.O. titration was 1

μM. See Figure 3 legend for orientation of the plot.
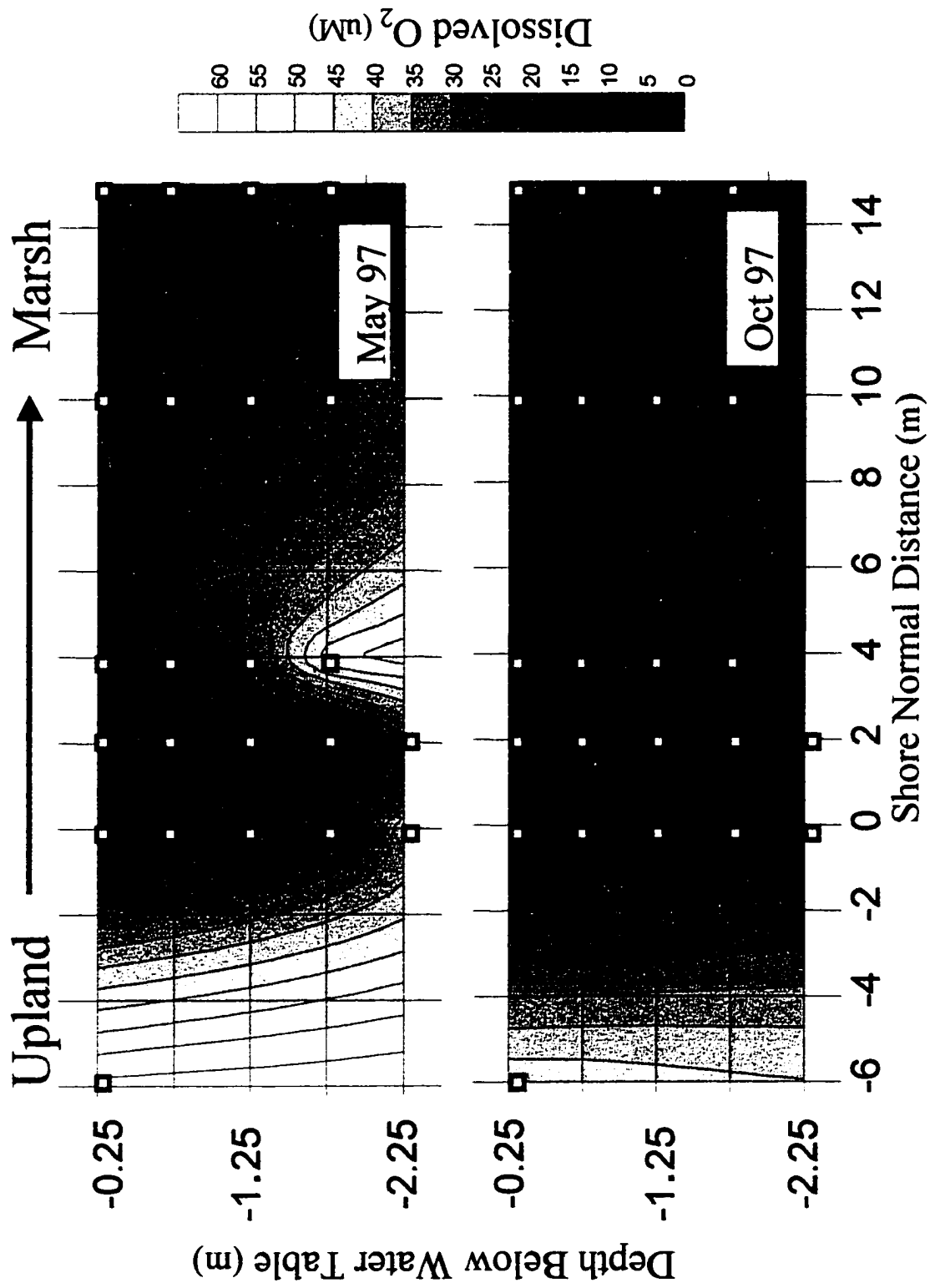
Figure 5. Porewater dissolved iron concentrations (Fe^{2+}) for October and May of 1997. See Figure 3 legend for orientation of the plot.
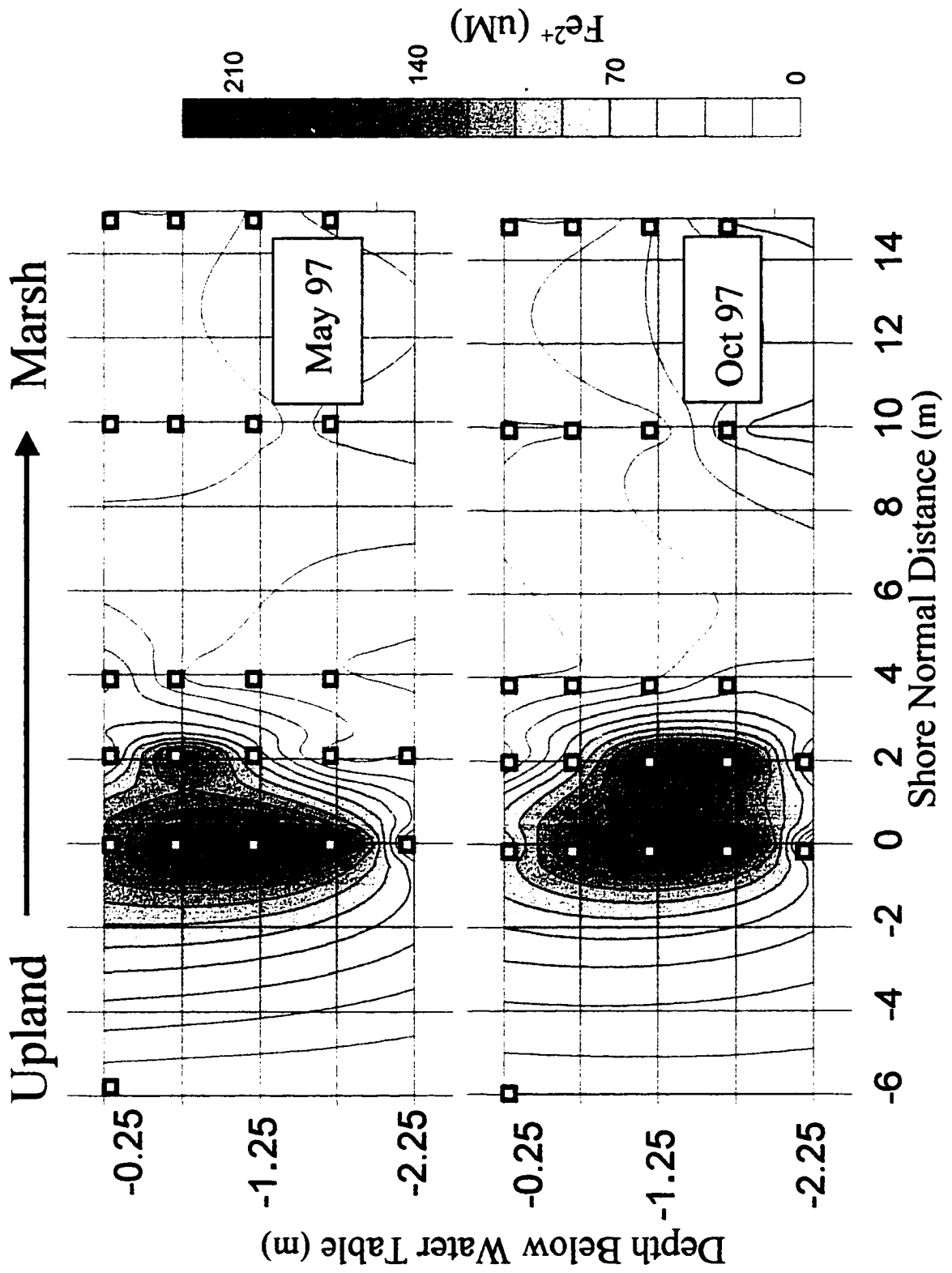
Average H_2S concentrations in the upper 2 meters of marsh (Fig. 6) were

approximately 2-4 times higher during October than in May. Generally, H_2S concentrations

decreased with sediment depth and increased with distance into the marsh where tidal

infiltration contributed a greater proportion of the sediment water budget (Tobias et al.

2000). Maximal H_2S concentrations of nearly 250 and 500 µM were detected in the upper

25 cm of sediment and 15 meters into the marsh from the upland during May and October

respectively. In May when discharge was high, the zone of marsh 5 meters nearest the

upland was nearly sulfide free, while during October, H_2S encroached landward in shallow

sediments to within 1 meter of the upland border.

Porewater measurements of dissolved organic carbon were made from piezometer

clusters during each of the discharge periods (Fig. 7). Maximal DOC concentrations of

1400 and 400 µM were found during October and May, respectively. The highest

concentrations were encountered in the shallow rhizosphere at both sample periods, and

decreased exponentially to 50 µM at approximately 2 meters depth during both seasons.

DOC was elevated in October relative to May at all depths and by a factor of 3.5 in the

upper 50 cm. The DOC concentration in the upland aquifer was between 50 and 168 µM

throughout the year (unpublished data).

Background natural abundance ^{15}N isotope values for NH_4^+, NO_3^-, and N_2 were

determined during a moderate discharge period in December 1996 (DIN) and in March

1997 (N_2). $\delta^{15}N$-PON (measured in August 1996) became isotopically enriched by up to

7 per mil (3 - 10 per mil) as sediment depth increased from the surface to 2 meters (Fig

8A). With the exception of the 80 cm depth, all$\delta^{15}N$-NH_4^+ values were 3-8 per mil

enriched relative to the PON fraction ranging from 7 per mil at 80 cm to 14.8 per mil at

Figure 6. Contour plots of subsurface porewater hydrogen sulfide concentrations. See

Figure 3 legend for orientation of the plot.
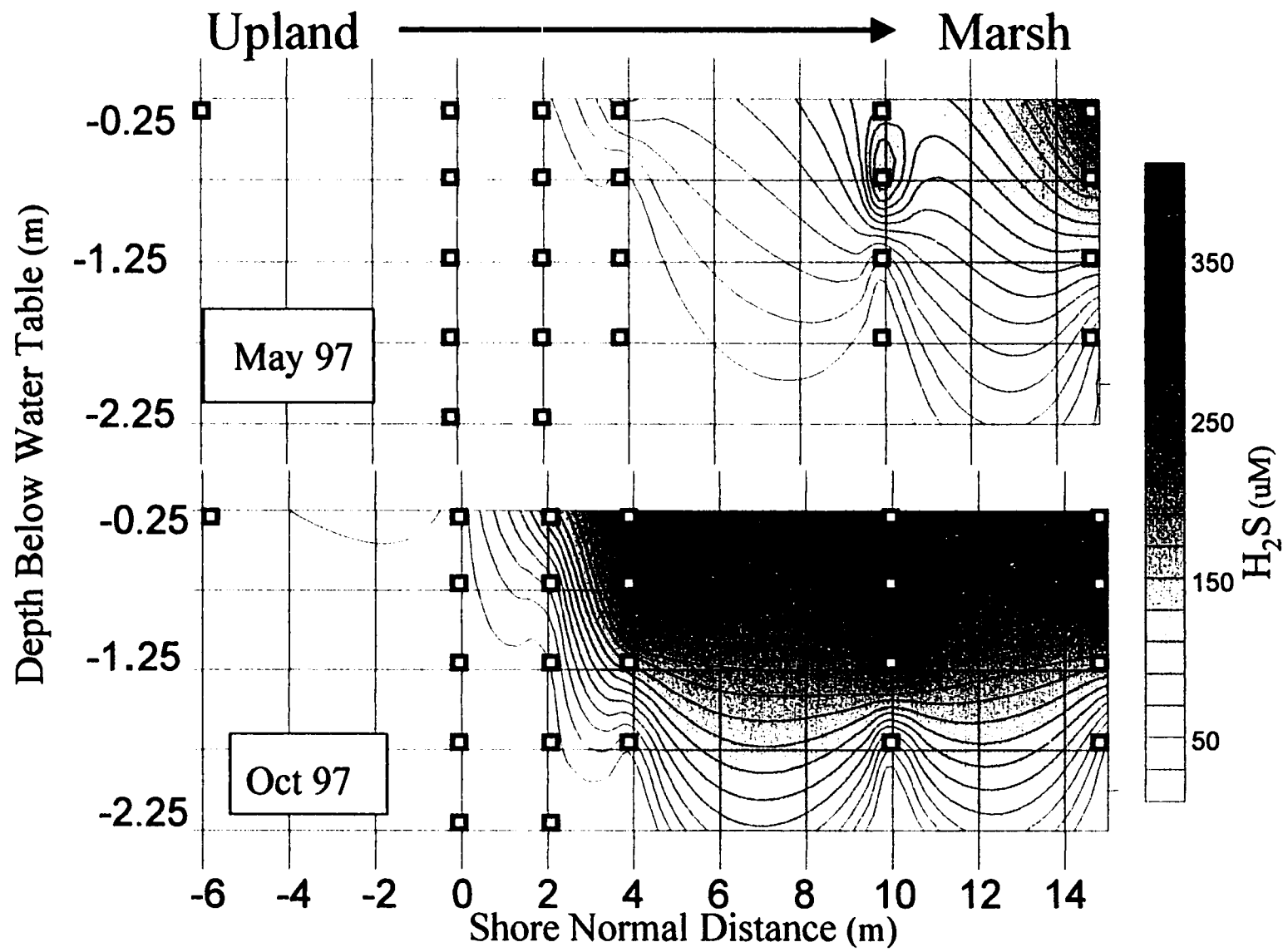
Figure 7. Porewater dissolved organic carbon concentrations in May and October 1997. Values are located in the middle of 50 cm screens denoted by the vertical error bars. Data is averaged by depth from the three piezometer clusters nearest the upland border (i.e., composite from the border to 6 meters marshward). Error bars denote standard error between the clusters.
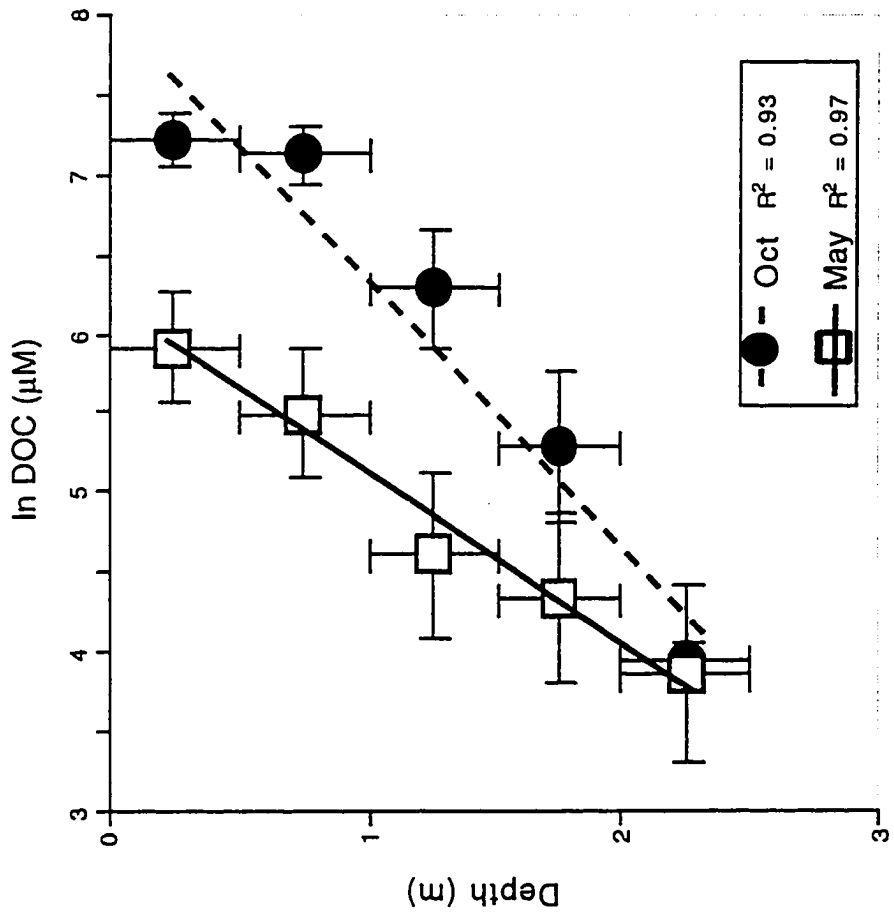
Figure 8. (A) Natural abundance $\delta^{15}N$ isotope values for DIN (NO_3^- and NH_4^+), PON,

and N_2. All data in Figure 8 were taken within 2 meters of the upland border. In panel A,

vertical error bars represent the depth interval over which the measurement was derived.

Horizontal errors bars for DIN samples represent the standard deviation of replicate

distillations of standard solutions. Horizontal error bars for N_2 samples are the range for

selected duplicates. Horizontal error bars for PON samples represents the poorest analytical

precision observed. Panel B shows the change in $\delta^{15}N$- PON as a function of decreasing

%N in sediments. The x axis is defined as the natural log of % N in sediments deeper than

10 cm ($N\text{-}PON_{,z}$) divided by .21 times the %N in sediment less than 10 cm deep (N-

$PON_{,0}$). The proportion of mineralizable N to the total N-PON in the upper 10 cm was

estimated at 21% by minimizing the absolute value of the intercept of the model. The y

axis is defined as the ratio of the observed $\delta^{15}N$-PON in deeper sediments ($\delta^{15}N\text{-}PON_{,z}$)

relative to $\delta^{15}N$-PON in 0-10 cm sediment ($\delta^{15}N\text{-}PON_{,0}$) The slope of the linear model fit

to the data is the enrichment factor (ε) which describes the difference in isotope values for

the product of a unidirectional single step reaction relative to the substrate. Applied to

mineralization, ε expresses the enrichment NH_4^+ relative to PON. ε is equal to the

fractionation factor [(α) -1] x 1000 (Marriotti et al. 1982).

B

$$y = -4.8438x - 0.0336$$
$$R^2 = 0.9461$$

$\varepsilon = -4.8\ o/oo$

Ln f N-PON

$$10^3\ Ln\left[\frac{10^{-3}\ \delta^{15}N - PON,z}{10^{-3}\ \delta^{15}N - PON,0}\right]$$

A

$\delta^{15}N\ (o/oo)$

Sediment Depth (m)

15 PON
$^{15}NH_4^+$
$^{15}N_2$
$^{15}NO_3^-$
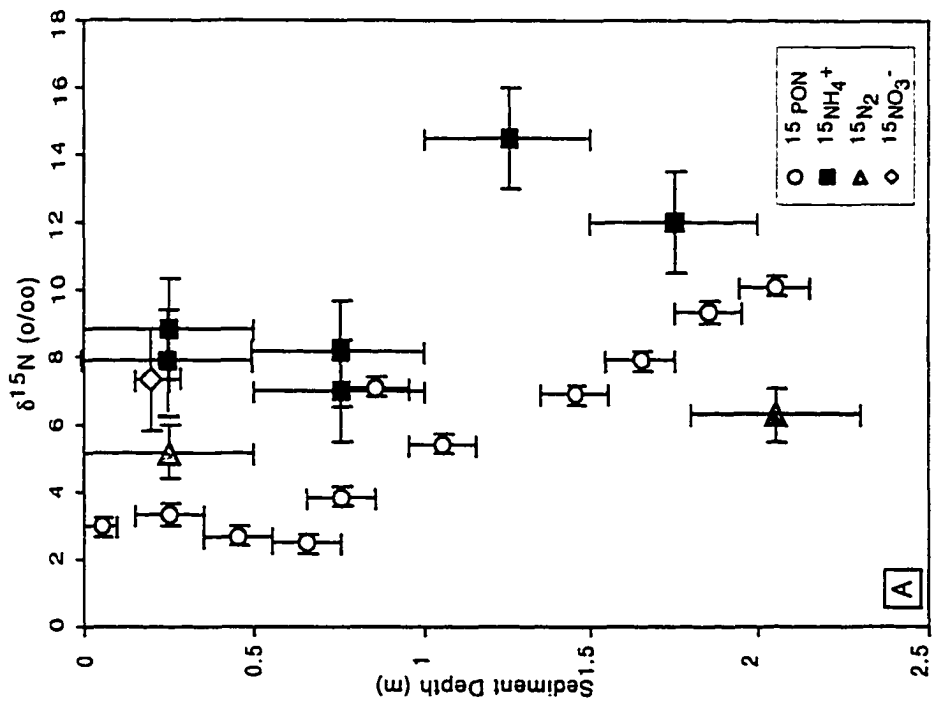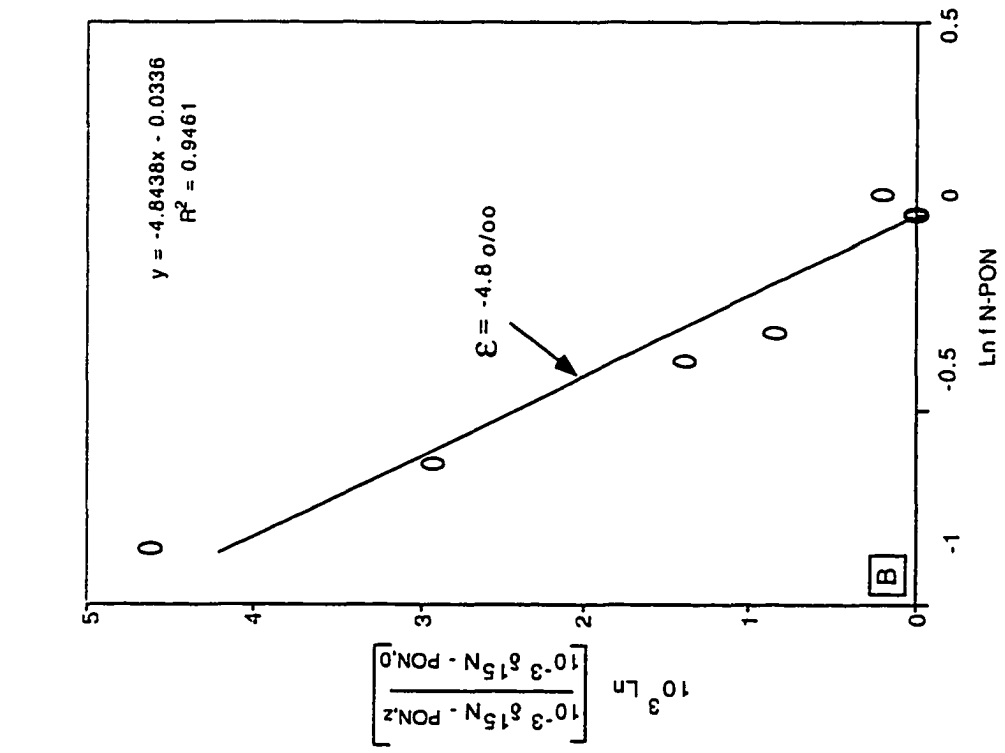
1.25 meters. Nitrate was rarely detected in the piezometers and consequently a single isotopic value of 7.6 per mil was determined from a sample collected at the 20 cm depth. The nitrate value was only slightly isotopically depleted (0.5 - 2 per mil) relative to the $\delta^{15}N\text{-}NH_4^+$ values at similar depths. $\delta^{15}N_2$ ranged between 5.0 and 5.9 per mil. The isotopic signal of N_2 was approximately 4 - 6 per mil depleted relative to ammonium collected from the same stratum, and enriched 5 - 6 per mil relative to tidal flooding water (- 0.5 per mil). The $\delta^{15}N_2$ signal was within 2 per mil of the measured $\delta^{15}N\text{-}NO_3^-$. Figure 8B is a plot of the $\delta^{15}N\text{-}PON$ data presented in a format modified from Mariotti et al. (1982; 1988). Natural abundance ^{15}N increased with a decrease in the % N of the sediment PON pool. This is shown as a linear decrease in the isotopic composition of the ratio of PON (> 10 cm deep) : PON (<10 cm deep) with an increase in the natural log of the fraction of unmineralized N-PON remaining relative to the estimated amount of initial mineralizable N-PON in the sediment. See the figure legend for a more detailed description of the plot. The slope of a least squares linear fit to the data in this plot yields an enrichment factor (ε) for the diagenesis of PON of 4.8 per mil.

Sediment Analysis

Shallower sediments in the marsh were more porous, held more water and had a lower bulk density. The organic composition of the surface sediments (C:N ratio, %PN, and total % organic) was higher than that found in the deeper sediments which were more characteristic of aquifer material (Table 2). Most of the changes in the measured parameters occurred below the 30 or 50 cm depths which denote the base of the rhizosphere. The lowest C:N ratios were encountered below 50 cm where peat and macroorganic matter concentrations were low.

Table 2. Bulk sediment properties by sediment depth interval from cores collected in August 1996. Averages of n=2 cores shown from cores collected within 4 meters of the upland border. ( ) denotes range of measurements.

Sediment Interval (cm)	% Porewater	Bulk Density (gdw cm^{-3})	Porosity	% Organic	C:N	%N
0-10	58.7 (12.2)	0.8	.79	18.5 (7.0)	17.2 (1.5)	.158 (.096)
20-30	32.6 (7.2)	1.1 (.04)	.56 (.20)	4.9 (1.10)	16.3 (5.6)	.042 (.039)
40-50	20.9 (.05)	1.6 (.09)	.43 (.02)	1.9 (.02)	20.3 (1.5)	.025 (.006)
70-80	18.3 (2.9)	1.7 (.15)	.39 (.04)	1.7 (.30)	12.8 (2.4)	.021 (.002)
80-90	19.3 (3.4)	1.7 (.20)	.39 (.04)	1.9 (1.1)	12.9 (2.1)	.016 (.004)
100-110	17.0 (1.4)	1.8 (.20)	.36 (.01)	1.3 (.5)	9.6 (3.9)	.010 (.003)
120-130	17.5	1.8 (.12)	.38 (.03)	1.1 (.20)	8.3 (1.3)	.010 (0)
140-150	17.3 (.49)	1.5 (.08)	.32 (.03)	1.0 (.20)	8.6 (0.8)	.008 (.001)
160-170	17.8 (.93)	1.9 (.31)	.41 (.04)	0.9	10.6 (1.1)	.008 (.002)
180-190	18.3 (.63)	1.9 (.29)	.43 (.04)	0.9 (.40)	8.4	.010
200-210	17.5	1.9	.40	0.6	8.9	.009

Increasing bulk density, % porewater, porosity, and % organic matter with sediment depth could be described by logarithmic decay equations with R^2 values of 0.88, 0.87, 0.81, and 0.84 respectively (data not presented).

The DIN profiles (Fig. 9A) were derived from data pooled from all cores in which DIN was extracted (Table 1). Highest extractable ammonium concentrations (up to 900 ng N gdw sed^{-1}) were detected in the upper 5 cm of sediment. NH_4^+ decreased exponentially with depth to less than 5 ngN gdw^{-1} in the deepest sediments (> 2 m) which constituted the shallow aquifer. Nitrate concentrations were undetectable through most of the cores with the exception of the upper 5 cm where concentrations ranged from 20 - 100 ngN gdw sed^{-1}.

Redox potential profiles (Figure 9B) were generated from four cores taken along a transect from the upland (core A) to approximately 8 meters into the marsh (core D). Eh values in the upland core decreased when the water table was encountered at 80 cm and again at 120 cm but remained positive through the length of the core. For all other cores the Eh of the overlying water in the core was positive but values dropped sharply within the first 2 cm of sediment. The initial drop was followed by a rebound in the Eh starting at 20 -30 cm depth. For all cores the Eh recovery reached positive values by 2 meters depth. The lowest Eh values, as well as the largest shifts in Eh with sediment depth, were observed in cores collected furthest into the marsh from the upland. In general, most of the marsh sediment from 0-1 meter had an average Eh between -200 and 0 while most of the upland sediments ranged between -100 and 200 mv.

N Cycling Rates

N cycling rates in all cores were maximal within the upper 30 cm of sediment, and decayed exponentially with sediment depth (Figs. 10, 11, 12). The exponential decline is evidenced by high linear regression coefficients ($0.76 < R^2 < 0.96$) of the fitted least

Figure 9. KCl extractable DIN pooled from multiple locations and times, and redox

profiles on single cores collected in August 1996. In the left panel, vertical error bars

denote standard error of the sediment subsection, and horizontal error bars indicate the

standard error from like depth from multiple cores ($2 < n < 9$). In the right panel, A-->D

represents a transect from the upland into the marsh (see Figure 1). Eh measurements were

taken at 10 cm intervals and smoothed to create the profiles.
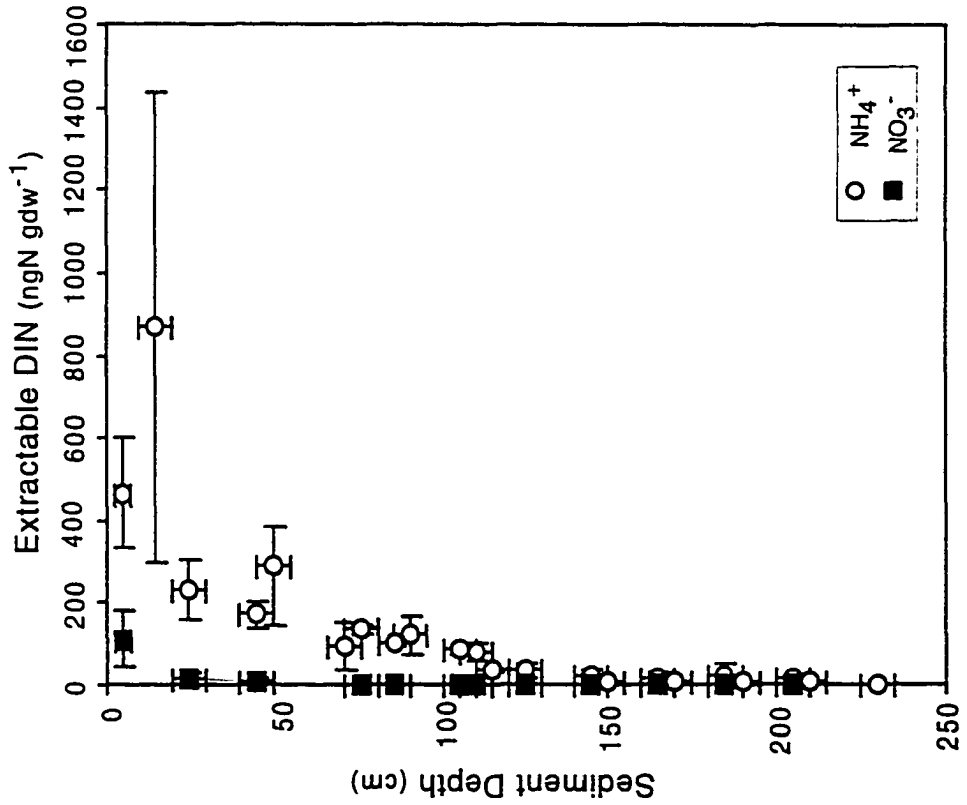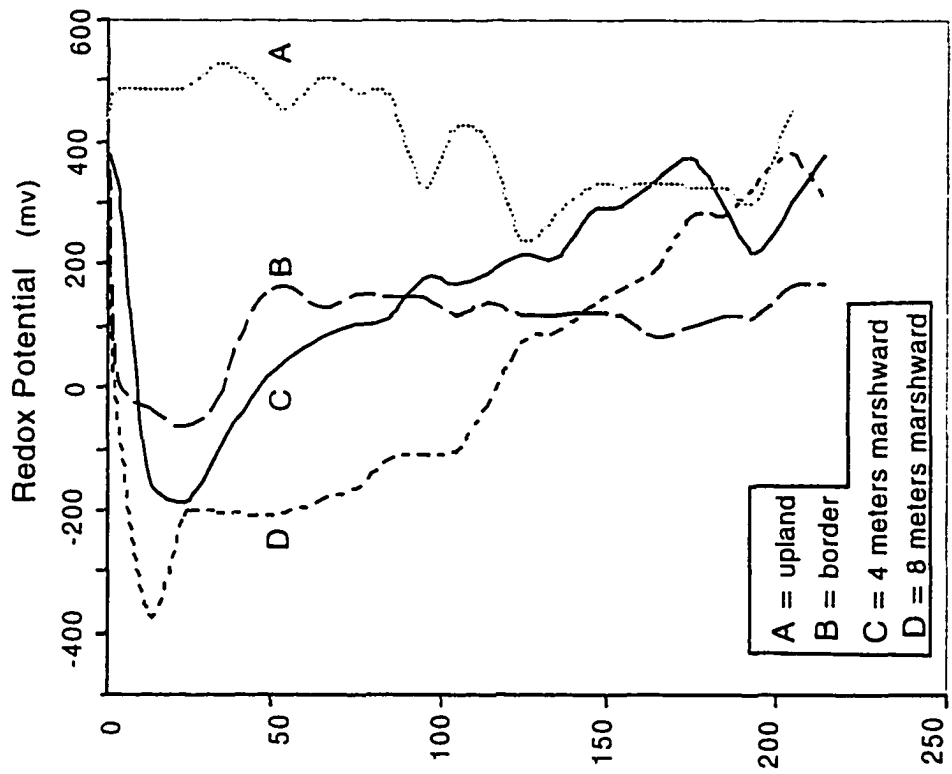
Figure 10. Summary of gross N cycling rates and potential rates. All cores all times (4

cores x 2 seasons) for each process were pooled by depth. Means and standard errors are

reported.

Nitrification (ngN gdw sed^{-1} hr^{-1})

$y = -2.4156 \ln(x) + 12.201$
$R^2 = 0.8919$

Mineralization (ngN gdw sed^{-1} hr^{-1})

$y = -51.874 \ln(x) + 253.35$
$R^2 = 0.8678$

DNRA Potential (ngN gdw sed^{-1} hr^{-1})

$y = -36.364 \ln(x) + 174.79$
$R^2 = 0.8007$

DNF Potential (ngN gdw sed^{-1} hr^{-1})

$y = -101.1 \ln(x) + 469.33$
$R^2 = 0.8083$
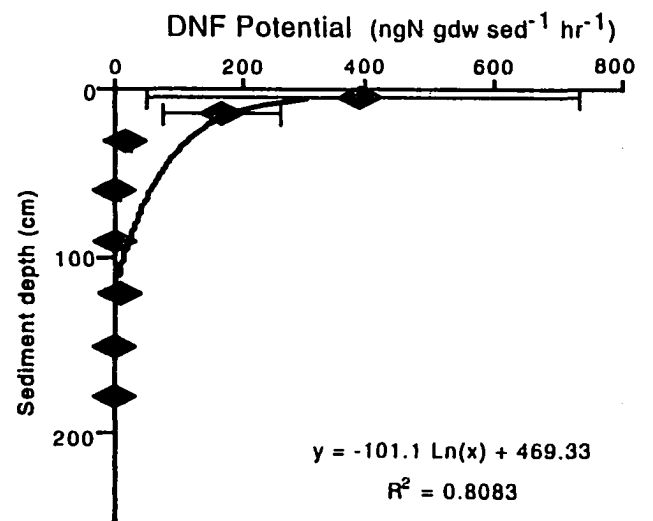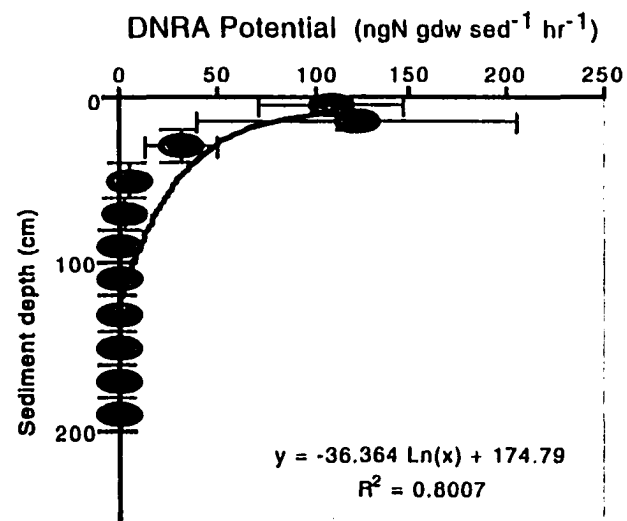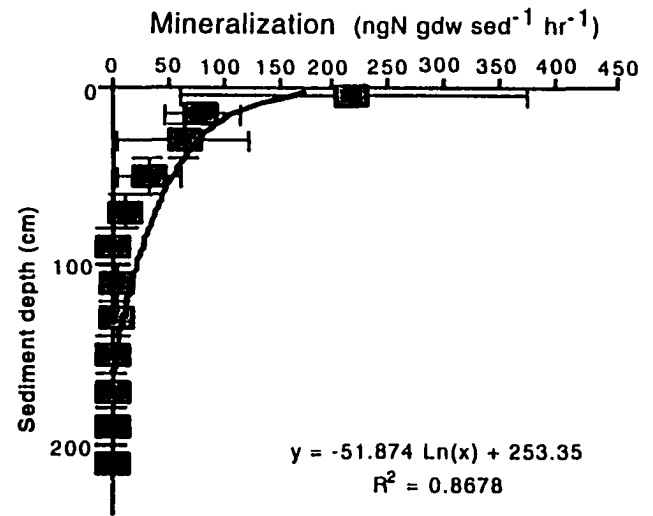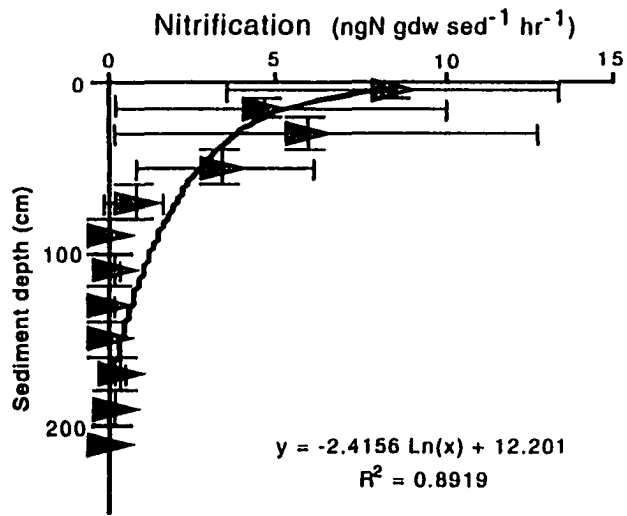
Figure 11. Mineralization (MIN) and nitrification (NIT) rates (ln x ln transformed) as a function of depth for border and marsh cores at both seasons.

Ln Rate (ng N gdw^{-1} hr^{-1})

Ln Depth (cm)

B. MIN May

D. NIT May

A. MIN Oct

C. NIT Oct

Border Core
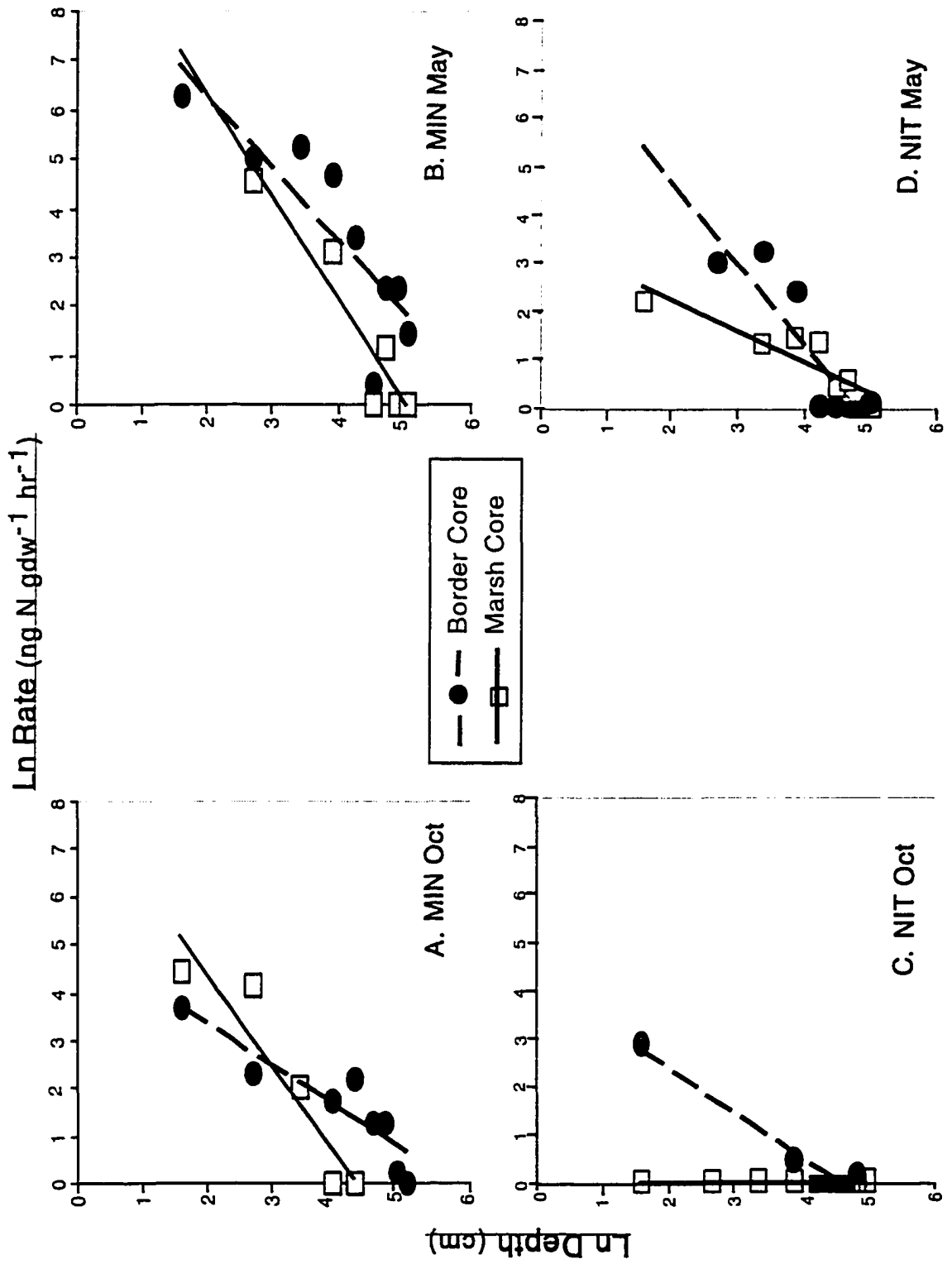
Marsh Core

Figure 12. Potential denitrification (DNF) and dissimilatory nitrate reduction to ammonium

(DNRA) rates (ln x ln transformed) as a function of depth for border and marsh cores

(DNRA) at both seasons.

Ln Potential Rate (ng N gdw^{-1} hr^{-1})

Ln Depth (cm)

B. DNRA May

D. DNF May

A. DNRA Oct

C. DNF Oct

Border Core
Marsh Core
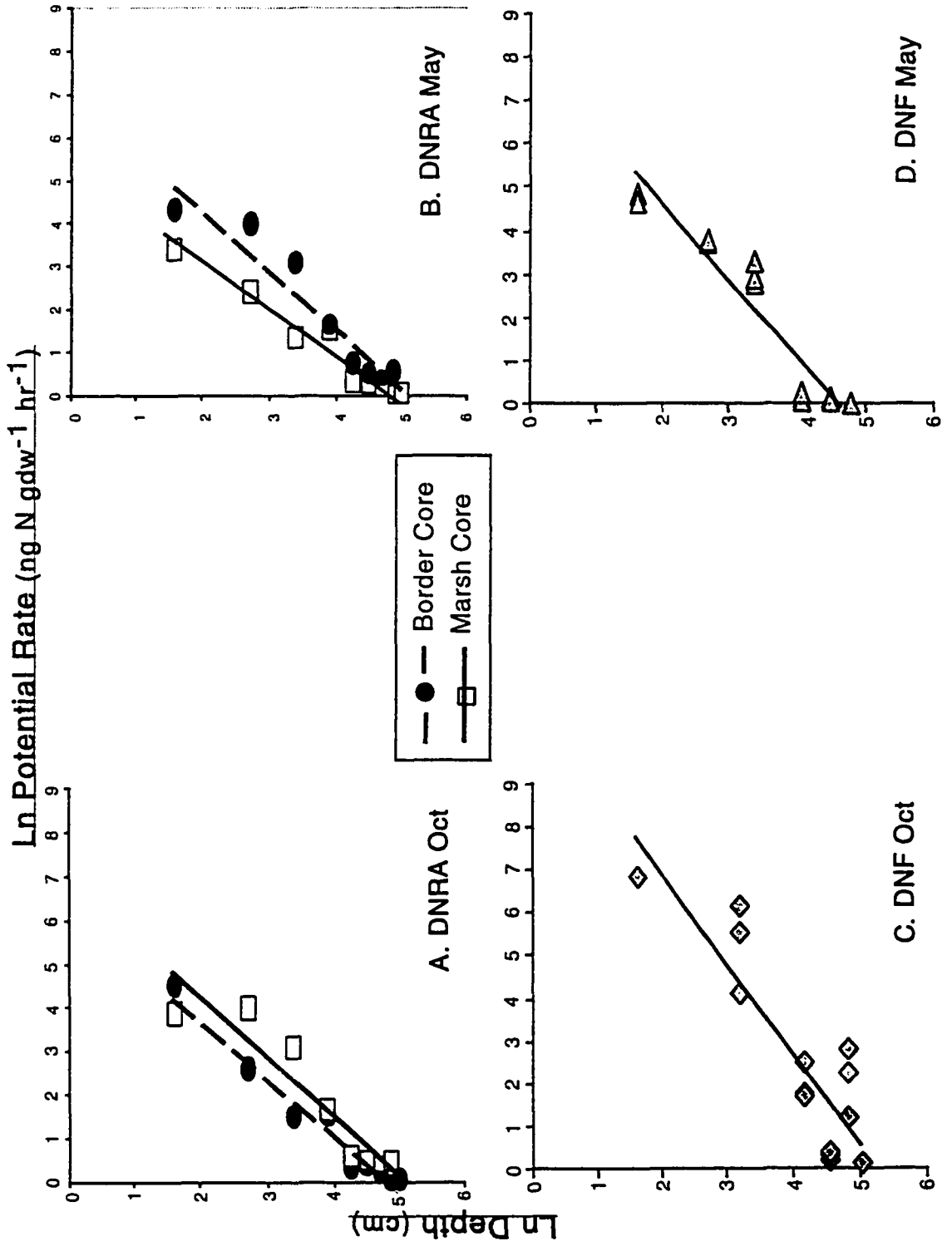
squares function following log x log transformation of the data (Table 3). No detectable rates for any of the measured processes were observed below 150 cm, and depth integrated rates from 5 - 150 cm were estimated (Table 3) based on the regression lines shown in Figs. 11 and 12.

Of the gross rate measurements, mineralization was 3 -20 times larger than nitrification. The maximum observed mineralization (530 ng N gdw^{-1} hr^{-1}), and nitrification (24 ng N gdw^{-1} hr^{-1}) rates, as well as the depth integrated rates (11.20 and 2.16 mmoles N m^{-2} hr^{-1}), were encountered in the border cores during Spring discharge (Fig. 11; Table 3). The largest change in depth integrated rates between discharge periods was also observed in the border cores such that during Spring, mineralization was higher by a factor 12, and nitrification by a factor of 7 over rates observed in the Fall. Depth integrated rates of nitrification in border cores were higher than marsh cores regardless of discharge period, and nitrification was nondetectable in the marsh core during low discharge in the Fall. The depth integrated rate of mineralization was higher in the marsh core (by a factor of 1.4) in the Fall, and in the border core (by a factor of 1.12) in the Spring.

Of the potential rate measurements, the maximum observed (330 ng N gdw^{-1} hr^{-1}), and depth integrated (6.13 mmoles N m^{-2} hr^{-1}) DNRA rate occurred in the border core in the Spring (Fig. 12; Table 3). In contrast, DNF potential was 10 fold higher during low discharge in the Fall when the observed maximal rate was 944 ng N gdw^{-1} hr^{-1}, and the depth integrated rate was 17.62 mmoles N m^{-2} hr^{-1}. The depth integrated DNF rate was 12 - 20 times larger than that of DNRA during low discharge in the Fall, but the ratio of DNF : DNRA decreased to approximately 0.33 - 0.77 in the Spring.

Table 3. Summary of regressions and depth integrated rates for all core experiments. Data were fit with a power function in the form of y = [exp (b)] • (x^m), where y is the rate of the selected N cycling process (ng N gdw^{-1} hr^{-1}), x is sediment depth (cm), b is the natural log of the maximal rate at 1 cm depth as determined from the model, and m is the slope of the least squares linear fit of ln depth vs. ln rate plots (Figs. 11,12). Depth integrated rates (mmoles N m^{-2} hr^{-1})were calculated by: 1) converting sediment depth to mass (gdw^{-1}) using bulk densities in Table 2, and assuming an area of one m^2; followed by 2) the integration of the rate (ng N gdw^{-1} hr^{-1}) vs. sediment mass (gdw) with respect to sediment mass from 5 cm to 150 cm depth.

	Slope (m)	Intercept (b)	R^2	Depth Integrated Rate
MINERALIZATION				
Oct-Border	-0.90	5.13	0.82	0.97
Oct-Marsh	-1.91	8.18	0.87	1.43
May-Border	-1.49	9.26	0.74	11.20
May-Marsh	-2.12	10.56	0.88	9.94
NITRIFICATION				
Oct-Border	-0.92	4.25	0.95	0.37
Oct-Marsh	----	---	----	0.00
May-Border	-1.68	8.07	0.80	2.16
May-Marsh	-0.64	3.53	0.80	0.47
POTENTIAL DNRA				
Oct-Border	-1.29	6.21	0.96	0.88
Oct-Marsh	-1.37	6.98	0.87	1.56
May-Border	-1.84	9.48	0.88	6.13
May-Marsh	-1.58	7.96	0.91	2.41
POTENTIAL DNF				
Oct	-2.10	11.1	0.76	17.62
May	-1.72	8.02	0.90	1.84

DISCUSSION

N Cycling Profiles

The cycling of nitrogen through mineralization, nitrification, denitrification, and dissimilatory nitrate reduction to ammonium was confined to the upper 1-1.5 meters of sediment where extractable ammonium, and particulate and dissolved organic matter concentrations were high (Fig. 10).

Mineralization

The average gross mineralization rate of 216 ± 156 ng N gdw^{-1} hr^{-1} observed in shallow sediments is within the range of reported values for other estuarine and coastal marshes as is the depth integrated rate of 0.97 -11.2 mmoles N m^{-2} hr^{-1}. Anderson et al. (1997) reported mineralization rates in 0 - 10 cm-deep saltmarsh sediments of 81 - 382 ng N gdw^{-1} hr^{-1} with maximum rates encountered in the Fall. Bowden (1984) estimated an average annual mineralization rate of 11.6 mmoles N m^{-2} hr^{-1} in a freshwater marsh and noted highest rates in November and an exponential decrease in rates with depth to 50 cm. Despite the greater depth used to calculate depth integrated rates in this study, these results compare favorably to previously reported values. Total % organic matter, %N of the sediment organic matter, and DOC concentrations, all decreased exponentially with depth, but decayed more slowly with depth than the observed mineralization rates. These measures of potentially mineralizable organic matter do not however, characterize lability of the substrate. Specifically, the disparity between the mineralization rate profile and the DOC profile (Fig. 7) may have resulted from decreasing lability of the DOC pool with depth. Freshly deposited detritus near the sediment surface, as well as carbohydrate rich macrophyte exudates released into the rhizosphere (Burney et al. 1981) are more likely to be labile and support higher mineralization rates than older more recalcitrant peats, or older dissolved organics found in deeper sediments. The DOC concentration (50 μM) at 2

meters below the marsh surface (in the aquifer) was constant between seasons. This concentration is nearly equivalent to upland groundwater concentrations. Natural abundance ^{14}C-DOC analysis of upland groundwater indicates that the carbon was fixed approximately 1000 years ago, and suggests that it is probably refractory with respect to mineralization (Raymond and Tobias unpublished data). Given that all the DOC is not labile within the marsh sediments, the source of new DOC is constrained to the upper sediments, and the deeper DOC is likely to be refractory, the labile organic matter available for mineralization probably decreases more rapidly with depth than the concentration decrease in DOC implies. Consequently, the depth profile of mineralization probably more accurately reflects the distribution of labile organic matter in the subsurface.

The importance of organic matter labilility on long term mineralization is supported by Fig 8B. Mariotti et al. (1982) showed that the isotopic fractionation between substrate and product of a single step unidirectional fractionating reaction (mineralization of PON ----> NH_4^+) could be described from the slope of plots similar to Fig 8B provided that a straight line could be fit to the data with the intercept passing through the origin. This was acheived with in Fig. 8B by assuming that only 21% of the more recently deposited PON (shallower than 10 cm) was labile. The isotopic fractionation factor (α) of 1.0048 estimated from the plot was nearly equivalent to previously reported α's for mineralization (Velinsky et al. 1991; Benner et al. 1991), and reinforces the assumption that only 1/5 of the "fresh" PON is mineralizable.

An additional factor contributing to the mineralization profile may be that of terminal electron acceptor limitation. Rates of mineralization in many organic-rich anaerobic sediments are accelerated by an enhanced flux of oxygen (Hansen and Blackburn 1991;

Holmer 1999). Aerobic respiration supports between 8-50% (Howarth and Teal 1979; Howes et al. 1984) of the total respiration in these systems either directly, or indirectly through the re-oxidation of alternate electron acceptors (Roden and Wetzel 1996). Although all of the oxygen flux in subtidal sediments is limited to the transport of dissolved oxygen from the overlying water or sediment microalgae, much of the oxygen flux to intertidal marshes occurs directly from the atmosphere at low tide, or enters the rhizospere through roots (Nuttle and Hemond 1988; Howes and Goehringer 1984; Armstrong et al. 1985).

Another source of electron acceptor which fluxes directly to the surface of the sediment is sulfate. Highest observed sulfide concentrations in this study were 420 μM are small relative to salt marshes flooded by higher salinity water (Hines et al. 1989). These low concentrations may suggest that total sulfate reduction (and, therefore, the flux of sulfate to the sediment) was unimportant in regulating the magnitude and distribution of the mineralization rate. However, H_2S concentrations are likely to underestimate the total reduced sulfur potentially produced from sulfate reduction in this system. Fe^{2+} concentrations exceed 200 μM in the shallow subsurface (Fig. 5) indicating both that iron reduction is a potentially important contribution to anaerobic mineralization, and that much of the reduced sulfur is likely to be bound as FeS or FeS_2 and not measurable as free H_2S. Roden and Wetzel (1996) determined that in freshwater marshes, the high contribution of iron reduction to the overall mineralization is maintained ultimately by re-oxidation of Fe^{2+} to Fe^{3+} by oxygen via root channels. Regardless, the higher rates of mineralization encountered in surface sediments and in the rhizosphere, may be in part due to a more direct supply of terminal electron acceptors (O_2, SO_4^{-2}, Fe^{3+}) either from the atmosphere at low tide, overlying water at high tide, or through macrophyte roots. However, because little mineralization is observed below 1.5 meters amidst dissolved oxygen concentrations

up to 100 µM, mineralization in these deeper strata is almost certainly limited by the supply of labile organic matter from above.

Nitrification

Exchangeable sediment NH_4^+ provided a good indicator of the spatial distribution of mineralization rates, indicating that there is little NH_4^+ removal from the sediment pool (i.e., nitrification rates were small relative mineralization rates). Average depth integrated nitrification rates were 3-20 fold lower than the mineralization rates (Table 3). Maximal observed nitrification rates of 2 - 24 ng N gdw^{-1} hr^{-1} and depth integrated rates of 0.37 - 2.16 mmoles N m^{-2} hr^{-1} during the low and high discharge periods respectively, were consistent with previously reported values for fresh and salt marshes. Bowden (1986) observed nitrification rates less than 1 nmole N cm^{-3} hr^{-1} using a combination of N-serve and isotope dilution techniques in a New England freshwater marsh. Rates for the Ringfield marsh were approximately equal to the annually averaged nitrification rates (23.5 ng N gdw^{-1} hr^{-1}) in a Virginia coastal saltmarsh (Anderson et al. 1997). Conversely, Thompson et al. (1995) measured nitrification rates of 0-0.5 mmoles N m^{-2} day^{-1} (one order of magnitude lower than rates observed in this study) in both a restored and natural saltmarsh in North Carolina.

Nitrification can be either oxygen or ammonium limited in subtidal and wetland sediments (Henriksen and Kemp 1988) and is typically confined to shallow sediments (less than 2 cm) where oxygen penetration is constrained (Jensen et al. 1994). In our study, highest nitrification rates were observed in the sediment closest to the surface within the zone of highest NH_4^+, and nearest the primary source of oxygen (the atmosphere), but measurable rates were also observed to greater depths (30-100 cm) than previously reported. Despite lower rates of nitrification in sediments deeper than 10 cm, the

integration of these rates through the sediment profile accounted for nearly 34 -77 % of the total depth integrated rate and suggest that a depth integration of only the top few centimeters directly affected by "top down" O_2 flux may underestimate the total nitrification in the system. At depths below 10 cm, extractable ammonium concentrations still exceeded 100 ngN gdw^{-1} but dissolved oxygen was undetectable, suggesting that ammonium was in excess and O_2 was limiting. It is possible that the sites of nitrification may have been concentrated around roots and rhizomes which had been actively pumping O_2 into the sediments prior to core collection (Howes et al. 1981), but the O_2 was consumed either by nitrification or mineralization fast enough to prevent any measurable accumulation in the dissolved pool. This mechanism could support nitrification, however, only through the rhizosphere (maximum depth 30-50 cm). Consequently it is not entirely clear what source of oxygen supports nitrification from 50 - 100 cm. Below 1.5 meters, DO concentrations and redox potential were sufficiently high to support nitrification, yet none was observed indicating that deeper sediments received inadequate transport of NH_4^+ from upper sediments. As seen in other studies (Jensen et al. 1994), nitrification appears to be spatially coupled to mineralization and rates were maximal when diffusional distance between the source of ammonium and oxygen was small.

The depth integrated nitrification rate relative to mineralization rate derived from the sediment core experiments is supported by the natural abundance stable isotopic data from the marsh near the upland border, which shows an isotopic enrichment of the ammonium pool relative to the PON fraction. A small ^{15}N isotopic fractionation has been shown for mineralization resulting in a 3 - 5 per mil depletion in the NH_4^+ pool relative to the particulate organic nitrogen substrate (Velinsky et al. 1991; Benner et al. 1991). Assuming that the sediment PON was the ultimate source of N which was mineralized to NH_4^+, and no fractionation took place, the $^{15}N-NH_4^+$ should be equal to that of PON. However, if

fractionation during mineralization occurred, NH_4^+ should be isotopically lighter than PON. The plot in Fig.8B provides evidence that fractionation during mineralization does occur in this system. An isotopic enrichment factor of 4.8 per mil was estimated based on the slope of the plot. Therefore, NH_4^+ would be expected to be considerably (up to 4.8 per mil) lighter than PON. However, because the NH_4^+ pool is from 3 - 8 per mil heavier than its source PON, either an import of heavy NH_4^+ enriched the pool or there was a process removing N from the marsh NH_4^+ pool that had a large fractionation associated with it. Neither tidal water nor upland groundwater have sufficiently high NH_4^+ concentrations to significantly alter the isotopic signal of the large marsh ammonium pool, but nitrification can fractionate NH_4^+ by up to 30-40 per mil (Heaton 1986; Mariotti et al. 1981). Alternate explanations for the observed enrichment of NH_4^+ relative to PON include: immobilization, and an inability to determine $\delta^{15}N$ of the labile PON idependently of bulk $\delta^{15}N$ - PON. Immobilization rates of NH_4^+ in marshes are high (Anderson et al. 1997) and immobilization (microbial uptake of NH_4^+) can fractionate NH_4^+ up to 13 per mil (Macko et al. 1987; Hoch et al. 1992) leading to a heavier residual $\delta^{15}NH_4^+$.

Additionally, our measurements of $\delta^{15}N$ - PON aggregate both labile and refractory N pools. Given the 4.8 per mil fractionation during mineralization, it is possible that the labile PON pool is significantly more enriched (perhaps equivalent to $\delta^{15}NH_4^+$) than the bulk $\delta^{15}N$ - PON would suggest. Despite these alternatives, additional support for the importance of nitrification in determining the observed isotope values was seen in the N_2 pool. The natural abundance values of $\delta^{15}N_2$ are nearly equal to the $\delta^{15}NO_3^-$ value and 5.5 per mil more enriched than flooding tidal water (-0.5 per mil). NO_3^- is rarely detected in this marsh and is likely to be denitrified immediately. Clearly the isotopic signal of the

large N_2 pool (approximately 600 μM) is derived from marsh nitrogen and not atmospheric N_2. Consequently, nitrification is the only process that removes NH_4^+ with a fractionation large enough to enrich the NH_4^+ pool by up to 4-10 per mil relative to PON, and isotopically enrich the N_2 pool through coupled denitrification. Assuming a fractionation of 30 per mil, this isotopic shift in NH_4^+ requires that the rate of nitrification is approximately 30% of the mineralization rate. At the upland border, this rate is supported (depth integrated nitrification is 20 -30% of mineralization), but is not maintained further into the marsh away from the source of discharge (nitrification is only 5% of mineralization). Both the sediment core and isotopic evidence suggest that in zones of fringing marshes nearest the upland border, nitrification may be a more important fate for NH_4^+, and when coupled to denitrification, represents a greater N export term than previously believed.

Potential Nitrate Reduction Rates

Compared with literature values for high nitrate or nitrate-amended marsh environments the observed depth-integrated potential DNF rates of 1.7 - 10.5 mmoles N m^{-2} hr^{-1} are higher than denitrification rates typically reported for freshwater and salt marshes (.71 - 7.85 mmoles N m^{-2} hr^{-1}) and are close to the median of rates reported for estuarine and coastal sediments (Koike and Sorenson 1988; Hee et al. 1994; Seitzinger 1988; Howes et al. 1996). Depth integrated potential DNRA rates of 1.37 - 4.23 mmoles m^{-2} hr^{-1} were consistent with the range (0.8 -50 mmoles N m^{-2} hr^{-1}) of observed rates in estuarine sediments (Koike and Sorenson 1988).

In general, potential nitrate reduction in marshes is believed to be NO_3^- limited. Although reduced iron and reduced sulfur compounds can act as electron donors for both denitrification and DNRA, DOC is thought to be the primary source of electrons fueling

NO_3^- reduction in organic rich sediments. The peak potential DNF and DNRA rates measured in the shallow sediments are consistent with the occurrence of high DOC concentrations near the surface, and less consistent with Fe^{2+} profiles which peak at 1 meter depth and fall to nondetectable concentrations by 2 meters (Fig. 5). As with mineralization, potential rates of both DNF and DNRA decreased more rapidly with depth than DOC concentrations, reinforcing the importance of organic matter lability in controlling the reduction of nitrate as well as in mineralization. Oxygen inhibition of denitrification has been encountered in marshes (Currin et al. 1996) and, although the incubation conditions of the DNF experiment (argon sparged slurries) effectively removed oxygen as a potentially limiting factor, in situ dissolved oxygen concentrations and redox potential was sufficiently high below 1.5- 2 meters to inhibit DNF and DNRA regardless of labile DOC availability. The restriction of nitrate reduction to the upper 1 meter of marsh implies that the effectiveness of the marsh in reducing groundwater nitrate loads is contingent upon groundwater discharging through these shallow sediments. Nitrate removal from groundwater flowing below 1.5 meters would be negligible on all but time scales of several hundred years.

Variation in N Cycling with Seasonal Discharge

A number of factors including temperature, pH, salinity, sulfide, DOM and oxygen availability can be expected to affect rates of the N cycling processes studied. Between study periods, it is likely that fluctuations in groundwater discharge affected all of these except pH and temperature either by direct flux (oxygen, and oxidized species), or by increased porewater flushing via advection. In situ temperature, as well as core incubation temperature, were constant (October and May porewater temperatures were 14.7 - 16.2 °C and 14.5 - 16.8 °C respectively) between experiments and should not have contributed to the observed seasonal differences in process rate measurements. Jones and Hood (1980)

describes sensitivity of nitrification to pH changes, but porewater pHs were comparable

between seasons (pH in the upper 1 meter of sediment averaged 6.77 ± 0.15 in May and

6.50 ± 0.09 in October). It is unlikely that this small difference in the observed pH

affected any of the N cycling processes significantly. Assuming a conservative estimate of

discharge of $10 \ l \ m^{-2} \ day^{-1}$ (Tobias et al. 2000) and observed upland dissolved oxygen

concentrations in May of 65 μM, groundwater contributed a flux of 27 μmoles $O_2 \ m^{-2} \ hr^{-1}$

into the upper 1 meter of marsh near the upland border in May, and had no contribution in

October. The flow of fresh groundwater reduced porewater salinity by 30 - 70% and

sulfide concentrations by approximately 50 - 300 μM respectively. While direct

determination of the causative elements controlling seasonal differences in the observed

rates for each of the processes is beyond the scope of the current study, there is a clear

difference in the depth integrated rates of gross nitrification, gross mineralization, and

potential DNRA coincidental with high and low groundwater discharge. These differences

appear greatest in the cores collected nearest the upland border where groundwater

discharge tends to concentrate (Harvey and Odum 1990). The following section will

address the possible effects of groundwater mediated flux and porewater flushing on each

of the N cycling processes studied.

Mineralization

Although few studies have examined seasonal variations in gross mineralization in

marsh sediments, peak rates tend to occur in the fall when plants scenesce and the supply

of fresh macrophyte detritus increases (Anderson et al. 1997; Bowden 1984; Neubauer et

al. 2000). In contrast, and despite higher porewater DOC concentrations, mineralization

rates in the Ringfield marsh were 10 fold lower in October than in May. Alternatively,

accelerated rates of mineralization in sediments can be catalyzed by an increased supply of

terminal electron acceptors (SO_4^{-2}, O_2). Portnoy and Giblin (1997) attributed increased

rates of mineralization in a restored salt marsh to elevated sulfate reduction rates when the ecosystem was innudated with higher salinity (higher sulfate) water. However, the decrease in salinity at our site indicated that the supply of sulfate was smaller during the Spring period of high mineralization.

Although groundwater was a source of O_2 in May, this estimated oxygen flux to the marsh subsurface could stoichiometrically account for less than 1% of the observed increase in N mineralization at that time. Although at first this may seem surprising, even large increases in the O_2 load to sediments have been shown to have little effect on mineralization rates. Moore et al. (1992) observed only a slight increase in N mineralization in lake sediments following a 2-order of magnitude increase in O_2 input and Lee (1992) found little effect of oxygen on carbon diagenesis and preservation in oxic and anoxic environments. While beyond the scope of this study, it is possible that the Springtime O_2 flux affected mineralization indirectly, in excess of what C:N:O stoichiometry predicts. Intermittent reoxidation of sediments and increased porewater mixing may result from the increased advection of water through the subsurface (Tobias et al. 2000). These processes may be analagous to the sediment reoxidation, and enhanced metabolite mixing that results from sediment resuspension, and catalyzes the high mineralization rates observed in deltaic sediments (Aller 1988). Nevertheless, it is doubtful that the increased flux of DO during high discharge is solely responsible for the higher mineralization rates observed.

Groundwater, however, may contribute electron acceptors in addition to oxygen. Groundwater at the site contained dissolved CO_2 in excess of 3000 μM, which constitutes a larger flux of oxidant that may support higher rates of methanogenesis (Capone and Kiene 1988). Similarly, iron is a potentially important regulator of mineralization in

freshwater marshes, and the shallow aquifer at this site is rich in iron oxyhydroxides.

Marsh porewater contained subsurface Fe^{2+} concentrations in excess of 200 μM and

concentrations decreased with distance from the upland border into the marsh (Fig 5).

Because discharge was highest near the upland border and similarly decreased with

distance into the marsh (Tobias unpublished data), Figure 5 suggests that groundwater may

be a source of Fe^{3+} that is subsequently reduced in the marsh during discharge. This

mechanism is contingent on Fe^{3+} transport (probably in the form of colloids) through the

aquifer and requires further investigation.

Nitrification

The 6-fold increase in the depth integrated rates of nitrification observed during the

high discharge period resulted both from an increase in the maximum rate in the top ten

centimeters and the depth to which measureable rates were encountered. Possible

mechanisms responsible for the increases in nitrification during high discharge are:

reduced porewater sulfide and salinity due to flushing; and increased O_2 delivery by

groundwater.

Free sulfide (HS^-) can inhibit nitrification by up to 75% at 60 μM concentrations,

and completely at 100 μM (Joye and Hollibaugh 1995). The higher porewater sulfide

concentrations encountered in October (Fig. 6) resulted from infiltration of higher salinity

(20 psu) tidal water accompanied by reduced porewater flushing at low discharge. The

highest H_2S concentrations were encountered further into the marsh where tidal water

becomes proportionally more important to the total sediment water balance (Tobias et al

2000). Therefore, the difference in H_2S concentrations in the upper 1 meter of marsh

sediment at the location of the marsh core and the border core was 100-320 and 0-75 μM

HS^- during low vs. high discharge periods, respectively. These concentrations may

sufficiently suppress nitrification rates to the observed levels in October and contribute to the undetectable rate of nitrification in the marsh core at low discharge. It should be noted that the sulfide inhibition of nitrification observed by Joye and Hollibaugh (1995) was determined in homogenized slurries. In situ nitrification, in contrast, probably occurs in more oxidized microenvironments where sulfide is excluded (Seitzinger et al. 1991), and the porewater H_2S concentrations reported in this study represent a composite of porewaters over a 50 cm piezometer screen that do not reflect any spatial heterogeneity in H_2S distribution in the subsurface. If the concentrations of sulfide that inhibit nitrification reported by Joye and Hollibaugh (1995) were taken at face value, it would be difficult to account for the observed nitrification in any marine sediment or salt marsh where sulfide concentrations in excess of 100 μM are common (Hines et al. 1989). Nevertheless, the accumulation of H_2S observed at low discharge may contribute to the decreased rates of nitrification observed in October, particularly in the marsh cores where H_2S concentrations were highest.

Salinity effects on nitrification rates through either direct physiological constraints, or by mediating exchangeable ammonium have been documented in freshwater and saline systems (Jones and Hood 1980; Rysgaard et al. 1999; Seitzinger et al. 1991; Seitzinger 1988). Average porewater salinity in the upper 0-1 meters of sediment ranged between 3.5 and 4.5 in May and 10-12 ppt in October. Rysgaard et al. (1999) observed a 75% drop in nitrification rates in cores taken from subtidal sediments and exposed to 10 ppt water vs. 0 ppt water, a salinity range similar to the Ringfield site (3.5 - 13 ppt). This depression in rates was nearly equivalent to the decrease in nitrification rates that we observed at higher vs. lower porewater salinities. Salinities, however, at Ringfield never fell below 3.5 ppt and Jones and Hood (1980) reported little change in the nitrification rate of estuarine isolates between 5 and 12 ppt. This suggests that the salinity change observed between

seasons (4 - 12 ppt) may not have had a large influence on the overall nitrification rate in the Ringfield marsh. Seitzinger et al. (1991) and Gardner et al. (1991) suggested that reduced salinity increases the fraction of sediment-bound ammonium available for nitrification, thereby increasing rates. The increased flux of ammonium from sediments (10 - 25 μmoles NH_4^+ m^{-2} hr^{-1}) incubated with 9 ppt water vs. freshwater, observed by Gardner et al. (1991), would only be sufficient to account for 2-4% of the observed increase in nitrification between seasons at the Ringfield marsh. Additionally, most of the literature examining changes in NH_4^+ adsorption with changes in salinity compare elevated salinity incubations with freshwater. Because adsorption and cation exchange kinetics are nonlinear, it is plausible that much of the NH_4^+ desorption with increasing salinity may occur over very small increases in salinity at relatively low salt concentrations (e.g. 0-3 ppt). Zimmerman and Benner (1994) observed no significant correlation of coupled nitrification / denitrification or NH_4^+ efflux from Galveston Bay sediments with salinity, although rates were maximal below 5-6 ppt, suggesting a salinity limit above which cation exchange has little effect on NH_4^+ sorption kinetics. Because the lower salinity limit of the Ringfield site is 3.5 ppt, sediments may release little of the bound NH_4^+ with the increased salinity encountered in October. Consequently, the increase in supply of bound NH_4^+ to nitrifiers during low porewater salinity in the Spring may likewise be small. Salinity reduction therefore does not seem to be solely responsible for elevated nitrification rates during Spring discharge.

Although the influx of O_2 co-regulates nitrification in sediments (Henriksen and Kemp 1988), the calculated groundwater derived O_2 flux at high discharge (assuming a O_2:N stoichiometry of 2) could support a nitrification rate of 27 μmoles N m^{-2} hr^{-1} or only 6% of the observed inter-season rate difference. If more liberal estimates of discharge at the site (derived from Darcy's Law) are used in the calculation (Tobias et al. 2000) the O_2

flux into the subsurface could account for 24% of the observed increase in nitrification rate between discharge periods. These estimates, however, require that all of the new oxygen be consumed by nitrification, which is unlikely given the high rates of organic matter respiration (Jensen et al. 1994). Despite the seemingly small effect of groundwater derived O_2 flux directly on nitrification there exists some mechanism at high discharge operating to increase the size of the nitrifying zone as well as increase the maximal rates. One possibility is the pumping of oxygen into the subsurface via macrophyte roots (Howes et al. 1981). The oxidizing potential of the sediment is affected by the rate of O_2 pumping where larger volumes of sediment are oxidized near plants with higher rates of primary production (Howes et al. 1981). Although macrophyte production rates are typically higher in May than in October by 3-fold (Neubauer et al. 2000), the effects of oxygen pumping would be limited to the rhizosphere (upper 30 to 50 cm). We observed elevated nitrification rates below 1 meter during high discharge. While the groundwater derived flux of O_2 is small relative to the total O_2 flux from the atmosphere flux to the surface sediments, it is proportionally more important to sediments below the rhizosphere (50 cm). The between-season difference in depth-integrated nitrification rates between 50 - 120 cm is 0.14 mmoles N m^{-2} hr^{-1} and the estimated groundwater derived O_2 flux could therefore support 12-47% of this rate. The rates below 50 cm account for an average of 30% of the total depth integrated nitrification rates at both low and high discharge periods. Thus, the groundwater O_2 flux is potentially important to zones of nitrification which lack a direct atmospheric flux of O_2 like deeper marsh sediments or subtidal environments, but cannot account for all of the elevated nitrification at high discharge at Ringfield.

Regardless of the mechanisms controlling mineralization and nitrification, the enhanced rates of both of these processes during Spring discharge is consistent with studies in riparian wetlands which demonstrate a tight coupling between the supply of

NH_4^+ from mineralization and coupled nitrification/ denitrification rates. (Seitzinger 1994).

Therefore, the increases in mineralization and nitrification during Spring high groundwater

flow periods may concurrently accelerate N loss from the ecosystem via denitrification.

Potential Nitrate Reduction

Because both DNF and DNRA are reductive processes, it was expected that any

seasonal effect on their rates would be similar. Maximal rates of both processes should

have been observed when DOC concentrations were highest. This was evidenced by a

nearly 10-fold increase in depth integrated potential DNF rates in October when DOC

concentrations were highest. However the DNRA rates were 2 - 3.5 fold higher in May

vs. October when DOC concentrations were lowest. The hypothesis that denitrification

tends to be favored by high NO_3^- : DOC ratios and DNRA by low NO_3^-:DOC (Tiedje

1988; King and Nedwell 1985), was not supported by the results of this study. Initial

NO_3^- concentrations were similar (300 μM) in the core and slurry experiments used to

determine DNRA and DNF potentials during both seasons. Consequently, the NO_3^-:DOC

ratio in each seasonal experiment was solely dependent on DOC concentration which was

4-fold higher in the Fall than in the Spring. The ratio of DNF:DNRA, however, increased

from 0.6 to 16 from May to October. Both the higher H_2S and DOC concentrations

encountered during periods of low discharge should have favored nitrate reduction via

DNRA but did not. Based upon our current understanding of the factors regulating DNF

vs. DNRA rates, it is difficult to identify any environmental difference measured at our site

during the two seasons that would simultaneously increase DNRA and decrease DNF

during high discharge. We suggest that the observed seasonal changes in DNF and DNRA

result from seasonal shifts in microbial populations or changes in the source and lability of

the DOC substrate. Microbial populations capable of DNF and DNRA are widely

distributed, but with the exception of a few genera (*Wolinella, Bacillus, and Pseudomas*),

are not capable of performing both processes. The fermentative organisms that perform DNRA may have different carbon requirements than denitrifiers and their growth could be supported by exudates from actively growing macrophytes in May which then scenesce in the Fall. Alternately, the fermenters may require an organic carbon source that is produced as an intermediate during mineralization which is at its peak rate during high discharge. This latter hypothesis is consistent with the observed similarity between mineralization and potential DNRA rates at low discharge, (Table 3) when overall rates were smaller, and the processes likely to be more tightly coupled. Perhaps bulk DOC measurements are not reflective of changes in the DOC compounds supporting DNF and DNRA. Therefore, characterization of DOC quality would enhance our understanding of controls on DNRA and DNF, and should therefore be a focus of future work.

Regardless of the mechanisms regulating the proportion of DNF:DNRA, the increased DNRA rates that accompanied the higher mineralization and nitrification rates at high discharge would result in the retention of a higher proportion of the nitrified N in the system as NH_4^+ (Aziz and Nedwell 1986). During Spring, the nitrification rate increased 6-fold but the DNF:DNRA was 0.4. The net result was that N exported out of the marsh was only 2.4 times greater than during low discharge in the Fall. The retention of the remaining N indicates that the more rapid cycling of N encountered during Spring discharge is not concurrent with equivalently large exports of N out of the marsh.

SUMMARY AND CONCLUSIONS

Because the cycling of N in this fringing marsh is restricted to the upper 1 - 1.5 meters, its effect on attenuating groundwater derived N loads is likely to be small. However, the effect of groundwater discharge (despite the absence of allochthonous N loads) on the marsh is potentially large. N cycling was most affected by groundwater discharge in regions of the marsh where discharge was greatest (near the upland border). Mineralization, nitrification and potential DNRA rates were greater during Spring discharge by a factor of 3-12, and DNF was higher during low discharge in the Fall by a factor of 10. Nitrate removal from groundwater flowing below 1.5 meters would be negligible on all but time scales of several hundred years. The restriction of nitrate reduction to the upper 1 meter of marsh implies that the effectiveness of the marsh in reducing groundwater nitrate loads is contingent upon groundwater discharging through these shallow sediments. Both the sediment core and isotopic evidence suggest that in zones of fringing marshes nearest the upland border, nitrification may be a more important fate for NH_4^+, and when coupled to denitrification, represents a greater N export term than previously believed. Therefore, the increases in mineralization and nitrification during Spring high groundwater flow periods may concurrently accelerate N loss from the ecosystem via denitrification. However, the accompanied increase in DNRA at that time indicates a greater retention of N and suggests that the more rapid cycling of N encountered during Spring discharge is not concurrent with equivalently large exports of N out of the marsh.

Therefore, internal N cycling was higher during high discharge, while the relative proportion of N exported from the marsh (DNF) to the total N turnover was greater during low discharge. No single discharge related factor could account for the observed changes in N cycling rates. Instead it is likely that a synergy between an increased flux of electron

acceptors, and porewater mixing and flushing of salt and sulfide, was responsible for the changes in rates. Groundwater discharge at the coastal margin is not restricted to fringing wetlands, and seasonal shifts in N cycling coincident with Spring discharge may likewise occur in subtidal sediments receiving fresh groundwater discharge. Based on the results of this study, and given a sufficient areal extent of discharge, we suggest that groundwater flow may be an important seasonal regulator of N cycling, and N retention, in intertidal and nearshore subtidal estuarine habitats.

LITERATURE CITED

Aller, C. 1988. Mobile deltaic and continental shelf muds as suboxic, fluidized bed reactors. Marine Chemistry. **61**: 143-155.

Anderson, I.C., C.R. Tobias, B.B. Neikirk, and R.L. Wetzel. 1997. Development of a process-based nitrogen mass balance model for a Virginia Spartina alterniflora saltmarsh: Implications for net DIN flux. Marine Ecology Progress Series. **159**: 13-27.

Armstrong, W. E.J. Wright, S. Lythe, and T.J. Gaynard. 1985. Plant zonation and the effects of the spring-neap tidal cycle on soil aeration in a Humber salt marsh. Journal of Ecology. **73**:1, 323-229.

Aziz, S., and D.B. Nedwell. 1986. The nitrogen cycle of an East Coast, U.K. saltmarsh: II. Nitrogen fixation, nitrification, denitrification, tidal exchange. Estuar. Coast Shelf Sci. **22**: 689-704.

Benner, R., M.L. Fogel, and E.K. Sprague. 1991. Diagenesis of belowground biomass of *Spartina alterniflora* in salt-marsh sediments. Limnol Oceanogr. **36**: 1358-1374.

Benson, B.B., and D. Krause. 1984. The concentration and isotopic fractionation of oxygen dissolved in freshwater and seawater in equilibrium with the atmosphere. Limnol. Oceanogr. **29**: 620-.

Bowden, W.B. 1986. Nitrification, nitrate reduction, and nitrogen immobilization in a tidal freshwater wetland. Ecology. **67**: 88-99.

Bowden, W.B. 1984. A nitrogen-15 isotope dilution study of ammonium production and consumption in a marsh sediment. Limnol. Oceanogr. **29**:1004-1015.

Brooks, P.D., J.M. Stark, B.B. McInteer, and T. Preston. 1989. Diffusion method to prepare soil extracts from automated nitrogen-15 analysis. Soil Sci. Soc. Am. Proc. **53**:1707-1711.

Brunet, R.C., and L.J. Garcia-Gil. 1996. Sulfide-induced dissimilatory nitrate reduction to ammonia in anaerobic freshwater sediments. FEMS Microbio. Ecol. **21**: 131-138.

Burney, C.M., K.M. Johnson, and J.M. Sieburth. 1981. Diel flux of dissolved carbohydrate in a salt marsh and a simulated estuarine ecosystem. Mar. Biol. **63**: 175-187.

Capone, D.G., and R.P. Kiene. 1988. Comparison of microbial dynamics in marine and freshwater sediments: Contrasts in anaerobic carbon catabolism. Limnol. and Oceanogr. **33**: 725-749.

Childers, D.L. 1993. Fifteen years of marsh flumes-a review of marsh-water column interaction in Southeastern USA estuaries. In: INTECOL Fourth International Wetlands Conf. (ed) Elsevier Press.

Childers, D.L., and J.W. Day. 1988. Direct quantification of nutrient and material fluxes between microtidal gulf coast wetlands and the estuarine water column. Estuar Coast Shelf Sci. **36**: 105-131.

Cline, J.D. 1969. Spectrophotometric determination of hydrogen sulfide in natural waters. Limnol. Oceanogr. **14**: 454-458.

Currin, C.A., S.B. Joye, and H.W. Paerl. 1996. Diel rates of N_2-fixation and denitrification in a transplanted *Spartina alterniflora* marsh: Implications for N-flux dynamics. Estuar. Coast. Shelf Sci. **42**: 597-616.

Dai, T., and R.G. Wiegert. 1997. A field study of photosynthetic capacity and its response to nitrogen fertilization in *Spartina alterniflora*. Estuar., Coast Shelf Sci. **45**: 273-283.

Davidson, E.A., J.M. Stark, and M.K. Firestone. 1990. Microbial production and consumption of nitrate in an annual grassland. Ecology. **71**: 1968-1975.

DeLaune, R.D., C.J. Smith, and W.H. Patrick. 1983. Nitrogen losses from a Louisiana Gulf Coast salt marsh. Estuar. Coast Shelf Sci. **17**: 133-141.

Fetter, C.W. 1993. Contaminant Hydrogeology. Macmillan Publishing.

Finkelstein, K., and C.S. Hardaway. 1988. Late Holocene sedimentation and erosion of estuarine fringing marshes, York River, Virginia. Journal of Coastal Research. 4:3, 447-456.

Gardner, W.S., S.P. Seitzinger, and J.M. Malczyk. 1991. The effects of sea salts on the forms of nitrogen released from estuarine and freshwater sediments: Does ion pairing affect ammonium flux? Estuaries. **14**: 157-166.

Glibert, P.M., and D.G. Capone. 1993. Mineralization and assimilation in aquatic, sediment, and wetland systems. In: R. Knowles and T.H. Blackburn [eds.], Nitrogen Isotope Techniques. Academic Press. 243-272.

Hansen, L.S., and T.H. Blackburn. 1991. Aerobic and anaerobic mineralization of organic material in marine sediment microcosms. Mar. Ecol. Prog. Ser. **75**: 283-291.

Harvey, J.W., and W.E. Odum. 1990. The influence of tidal marshes on upland groundwater discharge to estuaries. Biogeochemistry. **10**: 217-236.

Heaton, T.H.E. 1986. Isotopic studies of nitrogen pollution in the hydrosphere and atmosphere: a review. Chemical Geology. **59**: 87-102.

Hee, C., B.L. Howes, and P.K Weiskel. 1995. The potential of denitrification for intercepting groundwater nitrate in a sal marsh ecosystem. *In* J.P. Grassle, A. Kelsey, E. Oates, and P.V. Snelgrove [eds.] Twenty Third Benthic Ecology Meeting Conference Proceedings.

Henriksen, K., and M. Kemp. 1988. Nitrification in estuarine and coastal marine sediments. In: T.H. Blackburn and J Sorensen [eds.], Nitrogen Cycling in Coastal Marine Environments. John Wiley and Sons. 207-249.

Hines, M.E., S.L. Knollmeyer, and J.B. Tugel. 1989. Sulfate reduction and other sedimentary biogeochemistry in a northern New England salt marsh. Limnol. Oceanogr. 34: 578-590.

Hoch, M.P., D.L. Kirchman, and M.L. Fogel. 1992. The nitrogen isotope fractionation uptake by Vibrio harvey. Limnol. Oceanogr. 37: 1447-1459.

Holmer, M. 1999. The effect of oxygen depletion on aerobic orgnic matter degradation in marine sediments. Estuarine, Coastal, and Shelf Science. 48: 383-390.

Hopkinson, C.S., and J.P. Schubauer. 1984. Static and Dynamic aspects of nitrogen cycling in the salt marsh gramminoid Spartina alterniflora. Ecology. 65: 961-969.

Howes, B.L., R.W. Howarth, J.M. Teal, and I. Valiela. 1981. Oxidation-reduction potentials in a salt marsh: Spatial patterns and interactions with primary production. Limnol. Oceanogr. 26:2, 350-360.

Howes, B.L., and D.D. Goehringer. 1994. Porewater drainage and dissolved organic carbon and nutrient losses through the intertidal creekbanks of a New England salt marsh. Mar. Ecol. Prog. Ser. 114:3, 289-301.

Howes, B.L., J.W.H. Dacey, and G.M. King. 1984. Carbon flow through oxygen and sulfate reduction pathways in salt marsh sediments. Limnol. and Ocanogr. 29: 1037-1051.

Howes, B.L., J.W.H. Dacey, and J.M. Teal. 1985. Annual carbon mineralization and belowground production of Spartina alterniflora in a New England salt marsh. Ecology. 66:2, 595-605.

Howes, B.L., P.K.Weiskel,D.D. Goehringer, and J.M. Teal. 1996. Interception of freshwater and nitrogen transport from uplands to coastal waters: the role of saltmarshes. p. 287-310. In K.F. Nordstrom and C.T. Roman [eds.] Estuarine shores: evolution, environments and human alterations. John Wiley and Sons.

Howarth, R.W., and J.M. Teal. 1979. Sulfate reduction in a New England salt marsh. Limnol. Oceanogr. 24: 999-1013.

Jensen, K., N.P. Sloth, N. Risgaard-Peterson, S. Rysgaard, and N.P. Revsbech. 1994. Applied and Environmental Microbiology. 60:6, 2094-2100.

Jones, R.D., and M.A. Hood. 1980. Effects of temperature, pH, salinity, and inorganic nitrogen on the rate of ammonium oxidation by nitrifiers isolated from wetland environments. Microb. Ecol. 6: 39-347.

Joye, S.B., and J.T. Hollibaugh. 1995. Influence of sulfide inhibition of nitrification on nitrogen regeneration in sediments. Science. 270: 623-625.

King, D., and Nedwell. 1985. The influence of nitrate concentration upon the end-products of nitrate dissimilation by bacteria in anaerobic salt marsh sediment. FEMS Microbial Ecol. **31**: 23-28.

Knowles, R. 1990. Acetylene inhibition technique: development, advantages, and potential problems, p. 151-166. *In* N.P Revsbech and J. Sorenson [eds,], Denitrification in soil and sediment. Plenum Press.

Koike, I., and J. Sorenson. 1988. Nitrate reduction and denitrification in marine sediments, p. 251-270. *In* T. Blackburn and J. Sorenson [eds.], Nitrogen cycling in the coastal marine environments. John Wiley and Sons.

Lee, C. 1992. Controls on organic carbon preservation: the use of stratified water bodies to compare intrinsic rates of decomposition in oxic and anoxic systems. Geochemica et Cosmochimica Acta. **56**: 3323-3335

Libelo, E.L., W.G. MacIntyre, and G.H. Johnson. 1990. Groundwater nutrient discharge to the Chesapeake Bay: Effects of near-shore land use preactices. New perspectives in the Chesapeake System: A research and management partnership. 613-622.

Macko, S.A., M.L. Fogel, P.E. Hare, and T.C. Hoering. 1987. Isotopic fractionation of nitrogen and carbon in the synthesis of amino acids by microorganisms. Chem. Geol. **65**: 79-92.

Mariotti, A., J.C. Germon, and A. Leclerc. 1982. Nitrogen isotope fractionation associated with the NO_2^- ---> N_2O step of denitrification in soils. Can. J. Soil Sci. **62**: 227-241.

Mariotti, A., A. Landreau, and B. Simon. 1988. [15]N isotope biogeochemistry and natural denitrification process in groundwater: application to the chalk aquifer of northern France. Geochimica et Cosmochimica Acta. **52**: 1869-1878.

Mariotti, A., J.C. Germon, P. Hubert, P. Kaiser, R. Letolle, A. Tardieux, and P. Tardieux. 1981. Experimental determination of nitrogen kinetic isotope fractionation: some principles, illustration for the denitrification and nitrification processes. Plant and Soil Sci. **62**: 413-430.

Morris, J.T. 1980. The nitrogen uptake kinetics of *Spartina alterniflora* in culture. Ecology. **61**: 1114-1121.

Moore, P.A., K.R. Reddy, and D.A. Graetz. 1992. Nutrient transformations in sediments as influenced by oxygen supply. J. Env. Qual. **21**: 387-393.

Neubaur, S.C., Miller. W.D., and I.C. Anderson. 2000. Carbon cycling in a tidal freshwater marsh ecosystem: a carbon gas flux study. Submitted to Mar. Ecol. Prog. Ser.

Nuttle, W.K., and H.F. Hemond. 1988. Salt marsh hydrology: Implications for biogeochemical fluxes to the atmosphere and estuaries. Glob. Biogeo. Cyc. **2**: 2, 91-114.

Perstorp. 1992. Nitrate/nitrite flow solution methodology. Document no. 00630. Perstorp Analytical Inc.

Portnoy J.W., and A.E. Giblin. 1997. Biogeochemical effects of seawater restoration to diked salt marshes. Ecological Applications. 7:3, 1054-1063.

Portnoy, J.W., and I. Valiela. 1997. Short-term effects of salinity reduction and drainage on salt-marsh biogeochemical cycling and Spartina (cordgrass) production. Estuaries. 20:3, 569-578.

Portnoy, J.W., B.L. Nowicki, C.T. Roman, and D.W. Urish. 1998. The discharge of nitrate-contaminated groundwater from a developed shoreline to a marsh-fringed estuary. Wat. Res. Res. 34: 3095-3104.

Roden, E.E., and R.G. Wetzel. 1996. Organic carbon oxidation and suppression of methane production by microbial Fe(III) oxide reduction in vegetated and unvegetated freshwater wetland sediments. Limnol Oceanogr. 41: 1733-1748.

Rysgaard, S., P. Thastum, T. Dalsgaard, P.B. Christensen, and N.P. Sloth. 1999. Effects of salinity on NH_4^+ adsorption capacity, nitrification , and denitrification in Danish estuarine sediments. Estuaries. 22:1, 21-30.

Scudlark, J.R., and T.M. Church. 1989. The sedimentary flux of nutrients at a Delaware salt marsh site: a geochemical perspective. Biogeochemistry. 7: 55-75.

Seitzinger, S.P. 1988. Denitrification in freshwater and coastal marine ecosystems: Ecological and geochemical significance. Limnol. and Oceanogr. 33: 702-724.

Seitzinger, S.P. 1994. Linkages between organic matter mineralization and denitrification in eight riparian wetlands. Biogeochemistry. 25: 19-39.

Seitzinger, S.P., W.S. Gardner, and A.K. Spratt. 1991. The effect of salinity on ammonium sorption in aquatic sediments: Implications for benthic nutrient recycling. Estuaries. 14: 167-174.

Solorzano, L. 1969. Determination of ammonia in natural waters by the phenylhypochlorite method. Limnol.Oceanogr. 14: 799-801.

Sorenson, J. 1987. Nitrate reduction in marine sediment: pathways and interactions with iron and sulfur cycling. Geomicrobiology Journal. 5: 401-422.

Stookey, L. 1970. Ferrozine - a new spectrophotometric reagent for iron. Analytical Chemistry. 42: 779-781.

Thompson, S.P., H.W. Paerl, and M.C. Go. 1995. Seasonal patterns of nitrification and denitrification in a natural and a restored salt marsh. Estuaries. 18: 399-408.

Tiedje, J.M. 1988. Ecology of denitrification and dissimilatory nitrate reduction to ammonium. . In A. Zehnder [ed.] Biology of anaerobic organisms. John Wiley and Sons. pp. 179-224

Tobias, C.R., J.W. Harvey, and I.C. Anderson. 2000. Estimating groundwater discharge into a mesohaline saltmarsh: A comparison of methods and implications for marsh function. In prep.

Valiela, I. and J.M. Teal. 1974. Nutrient limitation in salt marsh vegetation. In : Reimod, R.J. and W.H. Queen [eds.]. Ecology of halophytes. Academic Press.

Valiela, I., and J.M. Teal. 1979. Nitrogen budget for a salt marsh ecosystem. Nature. **280**: 652-655.

Velinsky, D.J., J.R. Pennock, J.H. Sharp, L.A. Cifuentes, and M.L. Fogel. 1989. Determination of the isotopic composition of ammonium-nitrogen at the natural abundance level from estuarine waters. Mar. Chem. **26**: 351-361.

Velinsky, D.J., D.J. Burdige, and M.L. Fogel. 1991. Nitrogen diagenesis in anoxic marine sediments: Isotope effects. Carnegie Inst. Washington Annu. Rep. Director. 151-162.

Weiss, R.F., and B.A. Price. 1980. Nitrous oxide solubility in water and seawater. Mar. Chem. **8**: 347-359.

Wessel, W.W., and A. Tietema. 1992. Calculating gross N transformation rates of ^{15}N pool dilution experiments with acid forest litter: analytical and numerical approaches. Soil Biol. Biochem. **24**: 931-942.

Zimmerman, A.R., and R.B. Benner. 1994. Denitrification, nutrient regeneration and carbon mineralization in sediments of Galveston Bay, Texas, USA. Mar. Ecol. Prog. Ser. **114**: 275-288.

Appendix 1a. Mineralization Rates (ng N gdw-1 hr-1)

Depth (cm)	LOW FLOW Min Border	Min Marsh	HIGH FLOW Min Border	Min Marsh
5	38.69	82.70	529.14	
15	8.89	62.91	152.41	95.59
30		6.37	184.44	0.00
50	4.71	0.00	106.95	21.58
70	7.82	0.00	29.18	0.00
90	2.51	0.00	0.51	0.00
110	2.62	0.00	9.74	2.16
130	0.23	0.00	9.51	0.00
150	0.00	0.00	3.13	0.00
170	0.08	0.00	0.00	0.00
190	0.12		0.00	0.41
210	0.12			

Appendix 1b. Nitrification Rates (ng N gdw-1 hr-1)

Depth (cm)	LOW FLOW Nit Border	Nit Marsh	HIGH FLOW Nit Border	Nit Marsh
5	17.05	0.00		8.37
15	0.00	0.00	18.79	
30	0.00	0.00	23.43	3.49
50	0.49	0.00	9.94	3.18
70	0.00	0.00	0.01	3.10
90	0.00	0.00	0.00	0.70
110	0.00	0.00	0.00	0.73
130	0.17	0.00	0.01	0.00
150	0.00	0.00	0.08	0.00
170	0.00	0.00	0.67	0.44
190	0.00	0.00	0.05	0.38
210	0.00			

Appendix 1c. Potential DNRA Rates (ng N gdw-1 hr-1)

Depth (cm)	LOW FLOW		HIGH FLOW	
	DNRA Border	DNRA Marsh	DNRA Border	DNRA Marsh
5	53.44	83.30	201.56	102.24
15	58.97	11.30	330.11	91.54
30	23.03	3.08	77.24	24.64
50	3.91	3.33	7.02	6.45
70	0.95	0.31	2.87	1.20
90	0.58	0.39	1.53	0.25
110	0.53	0.20	0.97	0.84
130	0.56		0.59	0.41
150	0.50		0.12	0.00
170	0.71		0.04	0.04
190			0.02	0.08

Appendix 1d. Potential DNF Rates (ng N gdw-1 hr-1)

Depth (cm)	LOW FLOW			Depth (cm)	HIGH FLOW		
	Rep #1	Rep #2	Rep #3		Rep #1	Rep #2	Rep #3
5	946.00			5	124.22	103.69	·
25	459.67	251.30	60.86	15	39.27	42.07	
65	11.21	4.63	4.23	30	15.42	17.86	26.60
95	0.17	0.33	0.44	60	0.15	0.05	0.26
125	2.23	8.13	15.76	90	0.12	0.09	0.10
155	0.12		0.09	120	0.02	0.01	0.02
				150	0.00		0.01
				180	0.00	0.00	

SECTION III

Tracking the Fate of a High Concentration Groundwater Nitrate Plume Through a Fringing

Marsh: A Combined Natural Gradient Tracer and In Situ Isotope Enrichment Study†

†: To be Submitted to *Limnology and Oceanography*

ABSTRACT

The effectiveness of fringing marshes as buffers against groundwater derived nitrate loads depends in part on the pathways of nitrate reduction in the marsh, and the proportion of new nitrogen exported from or retained within the ecosystem. An n $situ$ ^{15}N -NO_3^- enrichment was combined with natural gradient groundwater tracer techniques to assess the fate of groundwater- derived nitrate during discharge through a mesohaline marsh. A high concentration nitrate plume enriched in ^{15}N to 7800 ‰ flowed through the marsh and was monitored for 100 days. Nitrate loss was rapid with peak loss rates ranging from 208 - 645 μmoles liter^{-1} day^{-1}. Approximately 90% of the added NO_3^- was reduced relative to the conservative co-tracer (Br$^-$) within 67 days. Changes in concentrations and ^{15}N enrichment of the NH_4^+, PON, dissolved N_2O, and dissolved N_2, pools over a 67-day period accounted for 14 - 36% of the observed NO_3^- loss. N_2O represented the largest sink (7-23 %) for nitrogen derived from NO_3^-, followed by PON (5 - 9 %), N_2 (2 - 3 %), and finally NH_4^+ (less than 1%). These percentages were likely to be gross underestimates, and after consideration of potential losses through evasion from the gaseous N pools, and rapid turnover of the ammonium pool, we were able to indirectly account for nearly all of the N lost from the NO_3^- pool. It is suggested that denitrification followed by rapid export of N_2 to the atmosphere, and large uncertainties associated with estimating nitrogen incorporation into the PON pool can account for much of the missing nitrogen in the mass balance. The adjusted mass balance indicated that 68% of the nitrate load was denitrified, and 30% was assimilated and retained in the marsh. The use of conservative tracers in the dissolved (bromide) and gas phase (argon) were critical in the reconstruction of the mass balance. This in $situ$ ^{15}N enrichment provided the ability to quantify nitrogen incorporation into several different pools simultaneously under natural conditions.

INTRODUCTION

Groundwater enriched in nitrogen has been recognized as an important non-point nutrient source to nearshore ecosystems yet there is only cursory knowledge of the patterns of groundwater discharge into estuaries and little is understood about the behavior of nitrogen at biogeochemically reactive discharge interfaces (Johannes 1980; Capone and Bautista 1985; Giblin and Gaines 1990; Valiela et al. 1992). One such interface exists at the ecotone between the shallow aquifer and marsh fringed estuaries. Groundwater discharge is typically focussed into intertidal or nearshore subtidal zones, and fringing marshes (both tidal fresh and salt) occupy much of the intertidal shoreline of trailing continental margins (Reilly and Goodman 1985; Bokuniewicz 1992). In previous studies, the nature of the interaction between fringing marshes and groundwater derived nitrogen loads discharging to estuaries has been examined primarily from two perspectives: water quality, and marsh ecology.

Cycling of autochthonous nitrogen (N) within these ecosystems is rapid and marshes generally demonstrate high rates of allochthonous nitrogen consumption through denitrification (Anderson et al. 1997; Kaplan et al. 1979). Because of the ability of these processes to "buffer" the receiving water mass against new nitrogen inputs, much of the recent attention devoted to defining the interaction between groundwater nitrogen loads and marshes has focussed on the marsh acting as a potential nitrogen filter thus regulating the water quality of the adjacent water body (Howes et al. 1996). Central to this premise is the requirement that a significant proportion of the total groundwater discharge (and the accompanying N load) passes through the marsh. Although marsh scale estimates of discharge have been difficult to quantify due to spatially and temporally heterogenous discharge patterns, salt balances for tidal creeks draining some New England pocket

marshes have suggested substantial marsh/groundwater interaction (Tobias et al. 2000a;

Valiela and Teal 1979; Howes et al. 1996). Calculation of discharge through fringing

marshes,which lack well defined tidal conduits, however, is more difficult. In contrast,

hydraulic characterization of fringing coastal marshes in New England using thermal

imagery, seepage meter, and head measurements, and under riparian fringing wetlands on

the Delmarva Peninsula using chlorofluorocarbon dating, have indicated that much of the

groundwater flow passes underneath these marshes and subsequently discharges directly

into nearby subtidal sediments or streambeds (Portnoy et al. 1997; Bohlke and Denver

1995). These disparate discharge scenarios are compounded by uncertainties in

estimating total groundwater discharge on an estuary scale, and a limited ability to

determine whether the marshes are intercepting more recently recharged and

disproportionately NO_3^- enriched groundwater, while deeper less NO_3^- rich water bypasses

marsh systems and discharges directly to the estuary (Oberdorfer et al. 1990; Simmons

1989; Howes et al. 1996). Consequently, the role of fringing marshes as buffers has not

yet been wholly established.

The importance of groundwater derived N loads to the marsh ecosystem itself,

however, is less constrained by the hydrological uncertainties described above. Because

the marsh possesses a smaller total water volume than the adjacent estuary, relatively small

fluxes of groundwater and nitrogen (on an estuarine scale) may drastically influence the

water and nitrogen balance of the ecosystem (on a marsh scale) (Tobias et al 2000a).

Therefore the mechanism of nitrogen processing within the context of N retention or export

assumes a critical role in defining the interaction between the marsh and the groundwater

derived nitrogen load.

Aside from localized zones of low redox potential, nitrate is the dominant species of dissolved inorganic nitrogen (DIN) in most shallow, aerobic, carbon-poor aquifers characteristic of the Atlantic Coastal Plain (Fetter 1993; Kraynov et al. 1992). Consequently it is the most frequently encountered form of anthropogenically enriched DIN observed discharging both subtidally and into coastal marshes (Portnoy et al. 1997; Reay et al. 1993, Valiela and Teal 1979). Marsh sediments with high organic carbon and low redox potential typically demonstrate high rates of potential nitrate reduction. In many wetland studies, denitrification (NO_3^- -> NO_2^- -> N_2O ->N_2) has been considered to be solely responsible for observed nitrate disappearance in sediments irregardless of whether denitrification (DNF) was measured or not (Xue et al. 1999). Although DNF (based on direct measurement) has figured prominently in the N budget of some New England marshes where the primary source of new nitrate is from groundwater, most efforts to study nitrate reduction in marsh or anaerobic subtidal sediments have not considered alternate nitrate reduction pathways (Valiela and Teal 1979; Howes et. al 1996; Koike and Sorenson 1988).

Nitrate processing in the marsh may also occur through assimilatory nitrate reduction, dissimilatory nitrate reduction to ammonium (DNRA), indirect microbial assimilation of NO_3^- derived NH_4^+ or NO_2^-, and plant uptake. Microbial assimilation of NO_3^- may be expected when NO_3^- concentrations are high and labile dissolved organic N and NH_4^+ concentrations are low (Tiedje 1988). The DNRA contribution to total nitrate reduction has been shown to be small in freshwater systems but comparable to DNF rates in salt marsh and anoxic marine sediments and can be expected to comprise a greater proportion of total NO_3^- reduction in sediments containing high electron donor/ electron acceptor ratios (i.e. high DOC/NO_3^-) (Bowden 1986; Koike and Hattori 1978; Tiedje 1988; King and Nedwell 1985). Salt marsh sediments exhibit rapid immobilization of NO_2^- and

NH_4^+, products of nitrate reduction, into the sediment organic N pool (Anderson et al. 1997; Smith et al. 1982). Similarly, White and Howes (1994) and Bowden (1996) demonstrated that nitrogen assimilation into the detrital particulate organic nitrogen (PON) pool of both salt and freshwater marshes was a significant sink for new NH_4^+. Once in the PON detrital fraction, the nitrogen tends to be sequestered over longer timescales (years). The gaseous products of denitrification (N_2O and N_2) presumably equilibrate relatively quickly with the atmosphere, while the products of DNRA, and assimilation are prone to more extensive cycling within the sediments. Therefore, the specific pathway of nitrate reduction may dictate the extent of export vs. retention of allochthonuos nitrogen within the ecosystem.

Here we describe an attempt to determine the relative importance of denitrification, nitrate reduction to ammonium, and assimilation of nitrogen into the sediment PON pool to the total consumption of groundwater derived nitrate during discharge into a mesohaline fringing marsh. In this advection-dominated discharge zone characterized by strong redox and flow gradients, traditional techniques used to measure N cycling process (C_2H_2 Block, ^{15}N tracers) which required the isolation of sediment into cores or slurries were avoided (Knowles 1990; Koike and Sorenson 1988). Instead, we chose a novel approach that combined a natural gradient groundwater tracer test with an in situ ^{15}N-NO_3^- enrichment in an attempt to track *in situ* marsh processing of high concentration groundwater derived NO_3^- loads. This approach of using a ^{15}N release *in situ* within an advectively-dominated system has been used in streams and small estuaries to elucidate N assimilation and food web structure (Holmes et al. 1999 in press; Hughes et al. 1999 in press; Peterson et al. 1997; Bowden et al. 1998). To our knowledge this approach has not been used in conjunction with a natural gradient groundwater tracer study within a marsh discharge environment in order to provide a comprehensive accounting of nitrate fate and transport.

SITE DESCRIPTION AND METHODS

The study site is located in the Colonial National Historical Park (37° 16' 42" N , 76° 35' 16" W) bordering the York River in southeastern Virginia (Fig. 1). The site consists of an upland slope of approximately 1:1 which grades through a mixed community of *Spartina cynosuroides* and *Spartina alterniflora* short form into a monotypic *S. alterniflora* (short form) fringing marsh approximately 25 meters in width. The study area borders the mesohaline portion of the York River (salinity range 12-21 psu). Upland geology and marsh evolution near the site are discussed in Libelo et al. (1990) and Finkelstein and Hardaway (1988), respectively. The small scale marsh stratigraphy consists of the upper 30 -80 cm of sandy marsh peat underlain by a semicontinous layer (10-20 cm thickness) of lower permeability glauconitic silty sand. Below 150-200 cm the glauconitic deposits grade into cleaner oxidized iron rich sands and shell hash of pre-Holocene origin. The site receives maximal groundwater discharge from January through July when the upland water table elevation exceeds the elevation of the glauconite unit and receives little to no discharge from August through November (Tobias et al. 2000a).

Methods

A groundwater plume was created by introducing an injectate enriched in NO_3^-, ^{15}N, and a conservative tracer (Br⁻) at the upland-marsh border and monitored as it flowed into shallow marsh sediments. Dissolved concentrations and ^{15}N isotopic enrichment of nitrate, ammonium, nitrous oxide, and dinitrogen (N_2) in the plume were measured over a 100 day period to estimate the transfer of nitrogen from nitrate into the selected reduced nitrogen pools. Nitrogen incorporated into the sediment particulate nitrogen fraction was assessed in cores taken preceding the injection and at the end of the study.

Figure 1. Site location and site cross section. The target wells used in the mass balance calculation are identified as 2, 3, and 4 in the plan view of the study site.

The three injection wells were separated by 50 cm and located along the upland/marsh border (Fig. 1). The target wells were spaced at 50 cm intervals extending 2.5 meters into the marsh and covering a total marsh area of approximately 5 m^2. Injection and target wells were constructed of 5 cm and 2.5 cm diameter polyvinylchloride (pvc) pipe, respectively. The wells were screened from 5-45 cm below the sediment surface with 0.025 cm pvc slot screen. All wells were installed with a 7.6 cm diameter hand auger, surrounded by a fine sandpack and capped with a bentonite plug. Target wells were fitted with dual stopcocks and an internal polyethylene sampling tube to allow the maintenance of an anaerobic headspace during and between samplings (Fig. 2A).

The injectate was prepared on site by mixing water pumped from the injection wells with KNO_3 and KBr salts in He sparged 5 liter aspirator bottles modified to act as constant-drip Mariott bottles (Figure 2B). The bottles were sealed to the atmosphere and water was pumped into the bottle through a stopcock while He headspace was vented through a second stopcock via a water trap. Previous tracer tests at the site indicated an approximate 100 - 1000 fold dilution of tracer. The final target injectate concentrations for NO_3^- and Br^- were therefore 0.12 and 1.0 M, respectively, and the ^{15}N enrichment was 7800 ‰. One liter of injectate was initially introduced into each of the three injection wells by inserting a rubber-gasketed 4.4 cm diameter PVC pipe into the injection wells and the well pumped dry. An equal volume of injectate (1 liter) was added and the liner removed. This single slug was followed by a constant drip at a rate of approximately 150 ml hr^{-1}. The rate of addition was slow enough relative to the transport velocity to avoid any artificial elevation of the head and cause accelerated flow. The injectate was kept on ice and the headspace replaced with ultra high purity He from a reservoir stored in a tedlar bag attached to the injectate bottle (Fig. 2B). Because the duration of the injectate drip was small (26 hrs) relative to the duration of the study, the release was regarded as a single slug.

Figure 2. Target well diagram {A.} and injection apparatus (Mariott bottle {B.}). The wells and Mariott bottles were kept O_2 free by the attachment of the helium reservoir. The drip rate from the Mariott bottle was kept constant and regulated by the distance between the elevation of the outlet and the bottom of the vent tube (dh).

B.

Injection Bottle

He filled Tedlar bag

Injectate

He Headspace

dh

Drip into well

A.

Sampling Well

He filled Tedlar bag

O₂ free headspace

Depth (cm)

0

25

50

Sediment
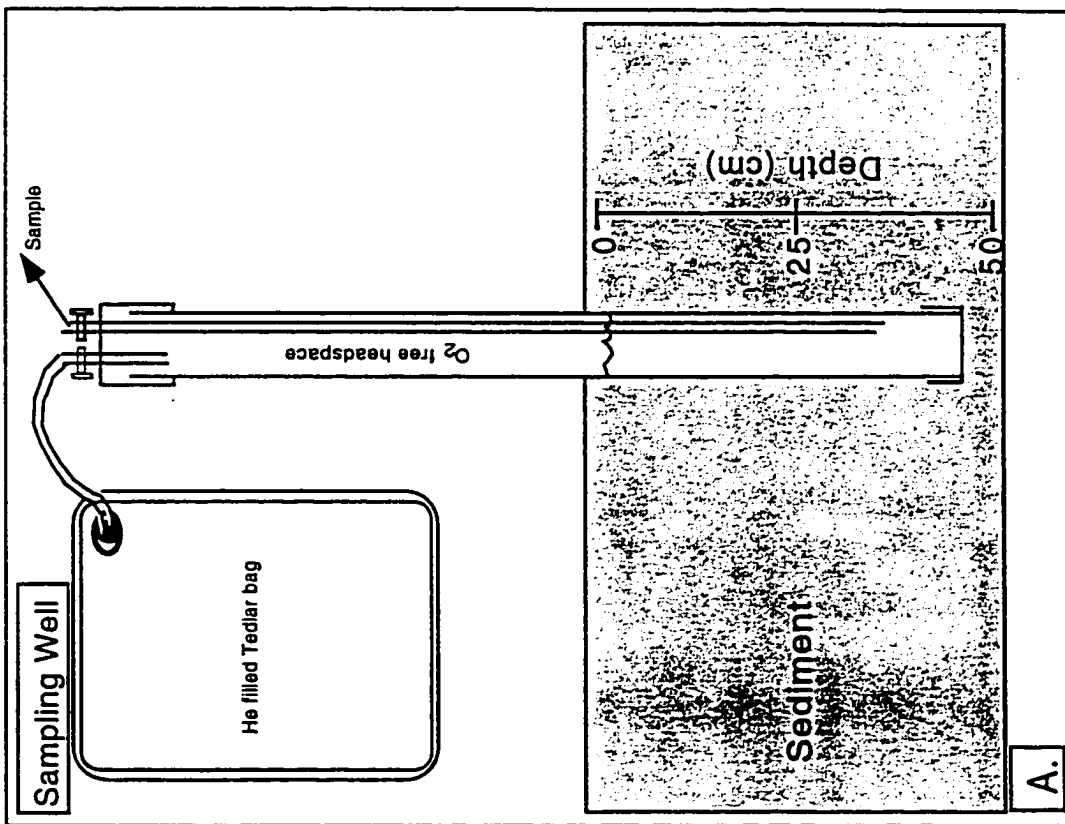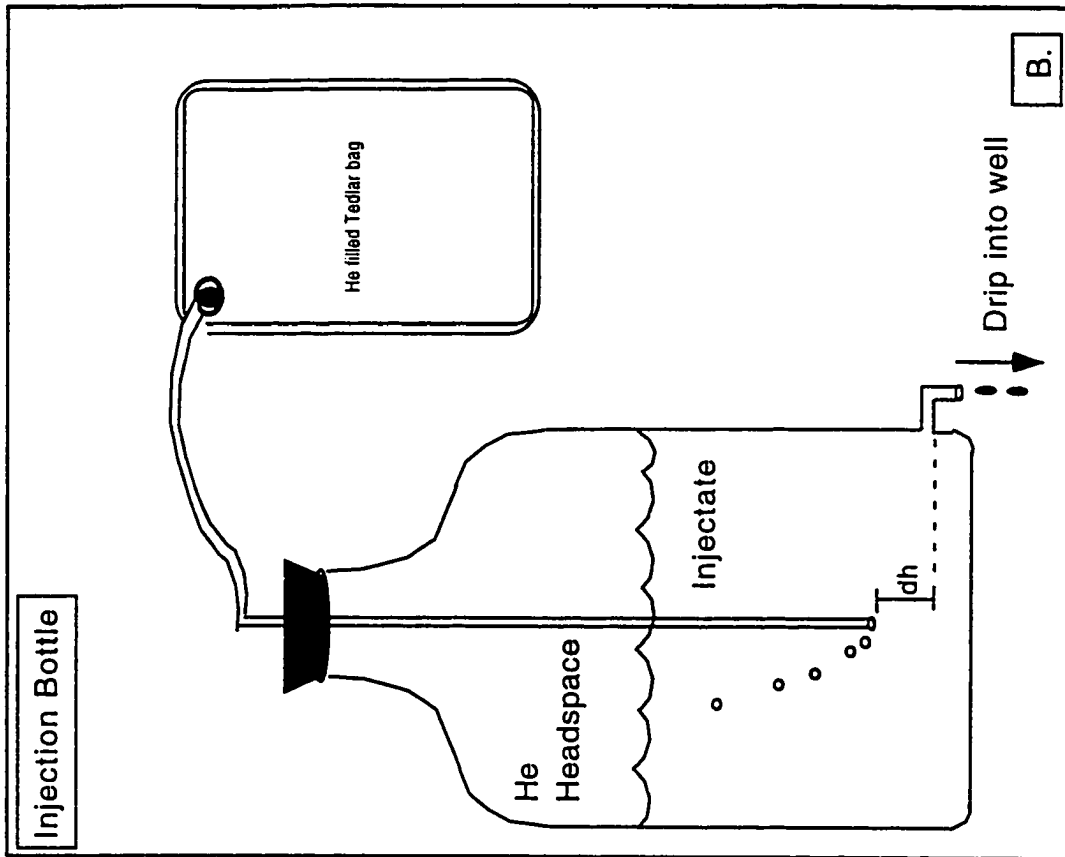
The injection and target wells were sampled at 1-3 day intervals near the start of the experiment and from 7-14 day intervals after peak Br⁻ concentrations were detected. Wells were purged of 3 well volumes or to dryness and allowed to recharge while venting the headspace through a water trap prior to sampling. Headspace was kept air-free by attaching a He filled tedlar bag during purging and sample withdrawal (Fig. 2A). Water samples were either withdrawn with a syringe or a peristaltic pump.

Characterization of N Pools

Dissolved Inorganic Nitrogen (DIN) and Br⁻

All DIN samples were filtered in the field through a 0.2 μm polyether sulfone (Supor) filter, and frozen in sterile whirlpak bags for subsequent analysis. Ammonium (NH_4^+) concentrations were determined by the phenol-hypochlorite method (Solorzano 1969). NO_3^- and NO_2^- concentrations were determined spectrophotometrically following cadmium reduction using an Alpkem autoanalyzer (Alpkem 1992). Br⁻ concentrations were measured in the laboratory using an Orion 94-35 Br⁻ specific electrode following temperature equilibration. Sensitivity of the probe was limited to 10x background Br⁻ concentrations (which were approximately 0.25mM). Isolation of NH_4^+ and NO_3^- for determination of ^{15}N isotopic enrichment followed the diffusion method outlined by Brooks et al. (1989). DIN trapping efficiency on replicate standards was better than 90%. Isotopic analysis for $^{15}N-NH_4^+$ was performed at the University of Virginia (UVA) Stable Isotope Facility on a VG Optima isotope ratio mass spectrometer (IRMS) coupled to a C:H:N elemental analyzer. Isotopic abundance was measured relative to an air standard. Isotopic measurements were expressed as "per mil (‰)" in "δ" notation where,

$$\delta^{15}N = [(R_{samp} - R_{std}) / R_{std}] \times 1000 \qquad [1]$$

and R was the ratio of $^{15}N/^{14}N$ for the sample or air standard. Analytical precision was typically better than 0.3 ‰. Because of the greater isotopic enrichment of the nitrate pool, $^{15}N-NO_3^-$ was analyzed at the University of California, Davis (UCD) Stable Isotope facility. With an analytical precision of less than .01 at% excess (approximately 28 ‰).

Nitrous Oxide (N_2O)

Water samples for N_2O analysis were collected with a syringe and equilibrated in the field with an equal volume He headspace by shaking in the sealed syringe vigorously for 1 minute. Following equilibration, headspace was transferred to a clean new syringe fitted with a stopcock. N_2O in the headspace sample was quantified on a Shimadzu GC-8 gas chromatograph equipped with a poropak Q column, electron capture detector, and a soda lime trap to remove interfering CO_2 peaks. Total dissolved N_2O was determined after correction of headspace concentrations using the Ostwald coefficient. The remaining headspace sample was transferred into pre-evacuated "exetainers" which were stored overpressured and upside down in brine prior to isotope analysis. $^{15}N-N_2O$ was determined at UCD from masses 44 and 45, following CO_2 removal in a Carbosorb trap. Precision for $^{15}N-N_2O$ ranged between 28 and 200 ‰.

Molecular Nitrogen (N_2)

Samples for dissolved N_2, Ar and $^{15}N-N_2$ determination were pumped from wells into 13 ml Hungate tubes containing approximately 150 mg of $ZnCl_2$ as a preservative. Tubes were overfilled and sealed bubble-free with stoppers and screwcaps, and stored underwater at 5 °C. Samples were analyzed for dissolved N_2 and Ar within 2 months of collection. $^{15}N-N_2$ was determined within 2 weeks of collection. NO_3^- analysis of samples stored for 90 days indicated that the $ZnCl_2$ and lower temperature prevented

continued NO_3^- reduction during storage. Post storage NO_3^- concentrations were within

10% of initial NO_3^- concentrations. Dissolved N_2 and Ar concentrations were determined

simultaneously using membrane inlet spectrometry according to Kana et al. (1994).

Sample preparation for ^{15}N-N_2 analysis followed a modification of Nielsen (1992). A 4

ml ultra high purity He headspace was introduced into the Hungate tubes containing the

water samples for ^{15}N-N_2 analysis. Tubes were vortexed for 5 minutes and stored

inverted in water under refrigeration for two - three days to allow equilibration. Following

storage, 1.5 ml of headspace gas was removed; CO_2 was cryogenically removed. The

remaining N_2 was analyzed for ^{15}N using a dual inlet Prism IRMS at UVA. Analytical

precision was typically better than 0.3 ‰ but atmospheric contamination biased some

replicate samples causing up to a 10-80% depletion in the measured values.

Particulate Organic Nitrogen (PON)

Cores (50 cm) collected prior to the injection, and on day 70 after the injection,

were sectioned at 10 cm intervals for the determination of the sediment organic nitrogen

pool. Two separate KCl (2N) extractions followed by distilled water rinses and

centrifugation were performed on each core section to remove exchangeable DIN and DON

in the porewater. Sediments were then air dried, ground, acidified with 30% HCl to

remove inorganic carbon, and oven dried at 30 °C. The %N, %C, C:N, ^{13}C, and ^{15}N of

the sediment organic pool were determined simultaneously using the elemental

analyzer/IRMS at UVA.

<u>Construction of Nitrogen Mass Balance</u>

The total amount of nitrogen lost from the NO_3^- pool and the total amount of

nitrogen incorporated into the NH_4^+, N_2O, N_2, over a 67-day period was estimated

according to:

$$\text{Total N}_{\text{lost, incorporated}} = \sum_{t=0}^{t=67} \left(N_{\text{lost, incorporated}} \right)_t \cdot \left(\frac{V_t}{t} \cdot \Delta t \right) \tag{2}$$

where $N_{\text{lost, incorporated}}$ is an estimate of either N consumed from the NO_3^- pool, or N incorporated into the individual product pools $\{NH_4^+, N_2O, \text{ or } N_2\}$ at time t (μM), V_t is the discharge volume at time t, and Δt is the time interval between samplings. Estimation of N incorporation into the PON pool is described in the following sections. Mass balance estimates were aggregated from three wells (#'s 2, 3, and 4) located along the central axis of the discharge plume 50 cm from the injection points (Fig. 1).

N Lost from the NO_3^- Pool

The total nitrogen lost from the NO_3^- pool at each sampling time for each well was calculated from Br^- and NO_3^- concentrations according to:

$$N\text{-}NO_{3\ \text{lost}}^- = (NO_{3\ \text{pred}}^- - NO_{3\ \text{obs}}^-) \tag{3}$$

such that:

$$NO_{3\ \text{pred}}^- = \left(NO_{3\ \text{init}}^- \right) \times \left(\frac{Br_t^-}{Br_{\text{init}}^-} \right) \tag{4}$$

where $(NO_{3\ \text{init}}^-)$ and (Br_{init}^-) are the nitrate and bromide concentrations (μM) of the injectate immediately after addition to the injection wells respectively, and $(NO_{3\ \text{obs}}^-)$ and (Br_t^-) are the measured nitrate and bromide concentrations at time (t), respectively.

$NO_{3\ pred}^{-}$ was the expected nitrate concentration (μM) if transport was conservative (i.e. allowing for dilution of the nitrate by physical processes only). It assumes a negligible *in situ* concentration of nitrate relative to the plume, and similarity in adsorption characteristics of bromide and nitrate. ($NO_{3\ obs}^{-}$) is a net measurement which includes dilution through mixing, biogeochemical loss of NO_3^{-}, and any *in situ* nitrate production (i.e. nitrification).

N Incorporation into NH_4^+, N_2O, or N_2

The total nitrogen incorporated (N gained in μmoles N l^{-1}) into each of the N product pools (NH_4^+, N_2O, or N_2) was determined for each well at each time from:

$$N_{incorporated} = \frac{\left[\left(R_{prod} - 0.00365\right) \cdot C_{prod}\right]}{R_{sub}} \tag{5}$$

where (R_{prod}) and (R_{sub}) are the $^{15}N/^{14}N$ ratios for the product and substrate pools respectively, and (C_{prod}) is the dissolved concentration of either NH_4^+, N_2O, or N_2 (μM). NO_3^{-} was considered the substrate for NH_4^+, N_2O and PON, and N_2O was considered the substrate for the N_2, and 0.00365 is natural ^{15}N abundance. Because the isotopic enrichment of the substrate pools was nearly constant through the study, the calculation of N gained using average substrate $\delta^{15}N$ yielded estimates equivalent to [5]. Each sampling time was converted to an estimate of discharge volume (V) according to:

$$V_t = v_t \cdot A \cdot n \cdot t \tag{6}$$

where v_t is the linear velocity (cm day^{-1}) calculated as a function of time; A is the effective

area normal to discharge (cm^3); n is the porosity of the sediment 0.79, and t is time (days). Linear velocity at the start of the injection was determined by dividing the elapsed time until the peak in the bromide breakthrough curve was achieved at each well by the distance between the well and the injection point (50 cm). This initial velocity was calibrated to discharge fluxes derived from Darcy's Law for adjacent shallow piezometer clusters. A linear equation was fit to the monthly average decrease in Darcy discharge vs. time and the slope of that line applied to the linear velocity determined by the Br$^-$tracer at time zero. This equation was then used to determine (v) for each sampling time. The effective area (A) for each well (500 cm^2) was assumed to consist of a shore parallel linear dimension which was equal to the well plus one-half the distance between wells (i.e. 25 cm on each side of the well = 50 cm), and a depth of 10 cm. Ten cm is the estimated plume thickness and justification for its selection is discussed in the following sections.

The estimates of N lost and N gained (μmoles N l^{-1}) were plotted against discharge volume (liters) and the area under each curve integrated to yield the total mass (μMoles) of N lost or gained for the entire 67 day period.

N Incorporation into PON

The estimate of N incorporation into PON was determined for the total duration of the study as:

$$\text{New N}_{PON} = \frac{\left[(\rho) \cdot (V_{sed}) \cdot \left(\frac{\%N}{100}\right) \cdot (.071) \cdot (R_{PON\,fin} - R_{PON\,init}) \right]}{R_{NO_3^-}} \qquad [7]$$

where (ρ) is the bulk sediment density (gdw cm^{-3}), V_{sed} is the effective sediment volume

(cm^3), %N is the percent nitrogen of the sediment, (0.071) converts grams N to moles N, R_{PON} is the $^{15}N/^{14}N$ ratio of PON before the injection or at 67 days post injection, and R_{NO3-} is the average $^{15}N/^{14}N$ ratio of NO_3^- over the entire study). The effective sediment volume was assigned the same shore parallel and depth dimensions as described above, and a shore normal dimension equal to the distance from the injection point to the target well (50 cm). Total sediment volume assigned to each well was therefore 25000 cm^3. Because no time series samples from the PON pool were collected for fear of disrupting the flow pattern, N incorporation into the PON fraction was determined from sets of cores collected prior to the injection and at the experiment's conclusion.

RESULTS

Plume Transport

Plume characteristics were monitored for a period of 100 days and an isotope-based mass balance constructed for the first 67 days of the study. Contour plots of the Br⁻ plume for days 6, 24, and 60 are shown in Figure 3. Day 6 was prior to the arrival of peak Br⁻ concentrations at any well and day 24 occurred after peak Br⁻ concentrations were achieved at wells 2 and 4 and concurrent with the arrival of peak Br⁻ concentrations at well 3. The plume did not migrate as a uniform solute from the injection wells, but rather followed preferential flowpaths centered about wells 2 and 4 (Fig. 3A). At day 6 the majority of the mass in the plume was located within the sediment volume between the injection points and the first well fence. By day 24, the two plume centers had merged into one center of mass located near well 3 (approximately 50 cm from the injection wells) and by day 60 the plume showed pronounced dispersion and dilution. As defined by the 10 mM bromopleth, the plume dispersed to an area of approximately 5 m² from the injection points while the area-averaged plume concentration decreased by approximately 100-fold within the 60 day period. Figure 4 shows the Br⁻ breakthrough curves for the wells used in the mass balance (wells 2, 3 and 4). Peak Br⁻ concentrations (expressed as C/C_o where C_o is the concentration in the injection wells at time = 0) were achieved for wells 2, 3 and 4 on days 11, 17 and 24 respectively. These peaks translated into linear plume velocities near the start of the study (t_o) of approximately 4.5, 3, and 2.1 cm day⁻¹. The equations used to describe the decrease in linear velocities over the duration of the study were derived from head measurements in adjacent wells. The adjusted velocities at 30 day intervals are shown in Table 1. The faster velocities encountered in wells 2 and 4 are manifested in the asymmetrical shape of the plume seen in Figure 3. The highest maximum concentration of Br⁻ was encountered in well 4 and indicated that much of plume flowed through the vicinity of well 4. However, the low concentrations of Br⁻ on day 6 in wells on either side of well

Figure 3. Bromide contour plot of the plume on days 6 (A), 24 (B), and 60 (C).
Concentrations were determined in wells screened from 5 - 45 cm depth. Ovals indicate
sampling wells. Open symbols identify wells 2,3, and 4 from left to right. Triangles
represent the injection points. The upland border is located at a shore normal distance equal
to zero.

Distance Shore Normal (cm)

Distance Longshore (cm)

Bromide (mM)
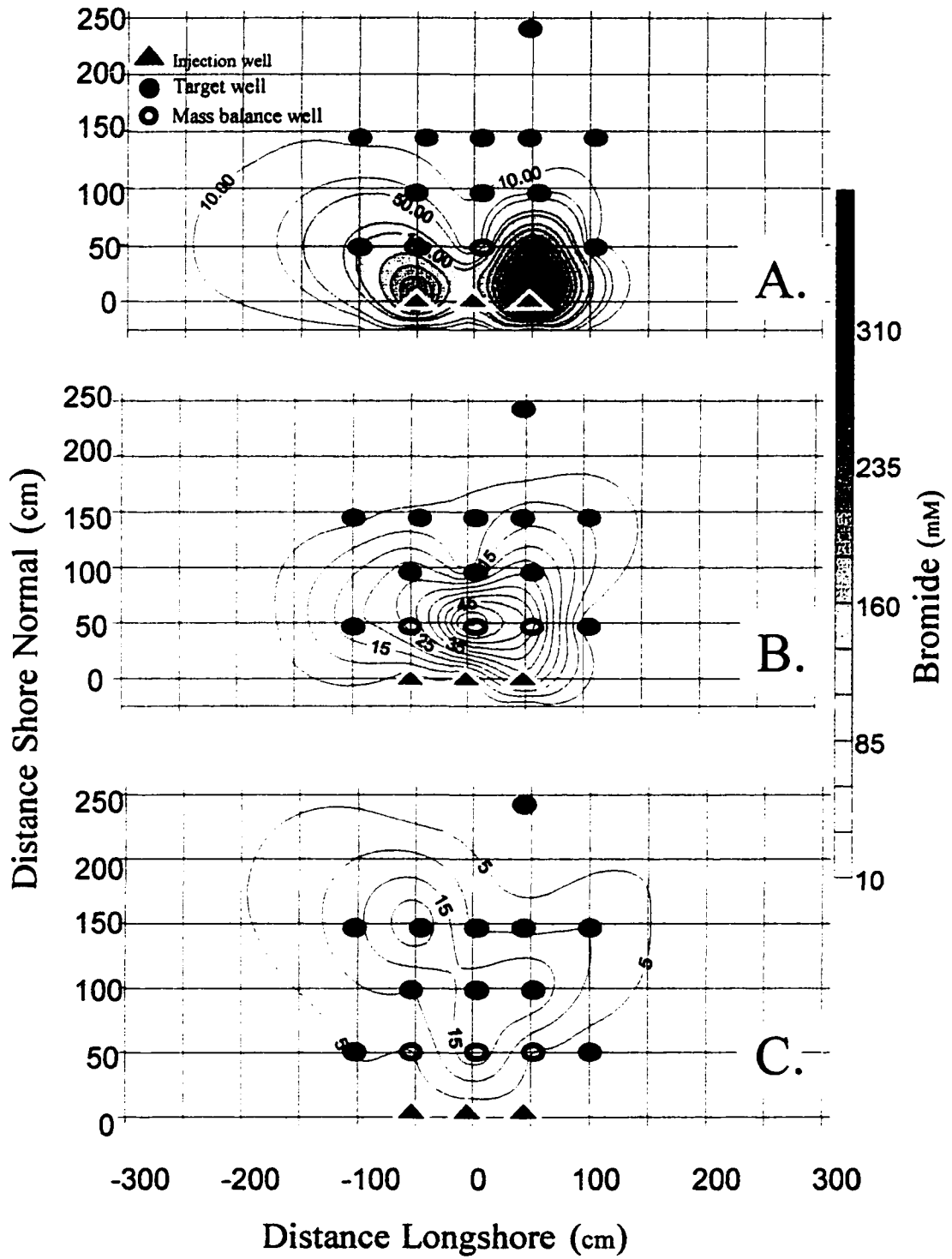
Figure 4. Breakthrough curves for Br^- and NO_3^-. C/C_0 equals the concentration of Br^- or NO_3^- at the sampling time t, divided by the initial concentration (Co) in the injection wells. The shaded area represents $N-NO_3^-$ loss during the study.
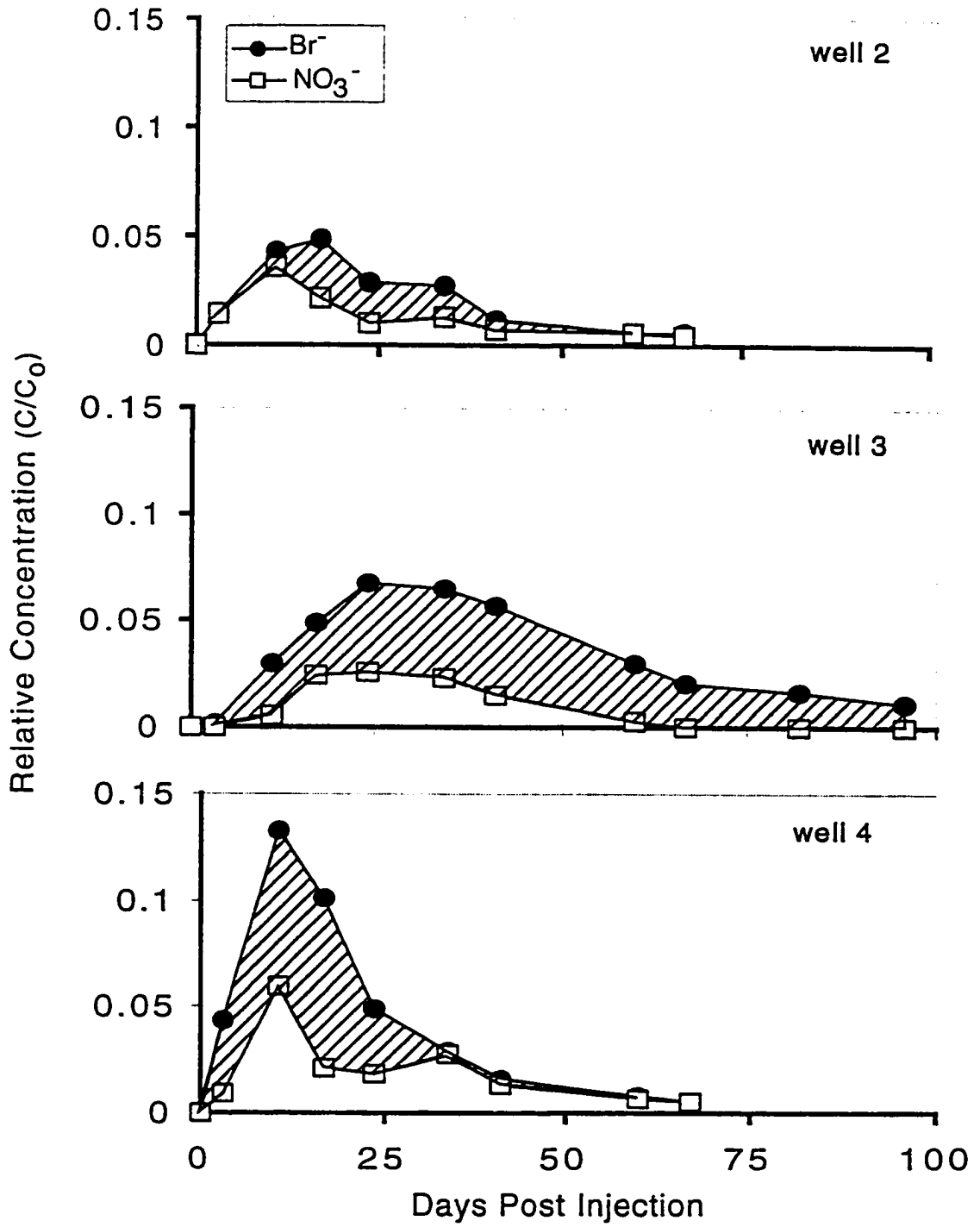
Table 1. Adjusted linear velocities (v) for wells used to calculate discharge volumes. Equations were derived from linear fits of average monthly change in hydraulic head observed in well transects adjacent to the tracer experiment calibrated to the initial (day 0) discharge velocity as determined from individual Br- breakthrough curves. (t) is the elapsed time (days) from the start of the injection.

Well #	Day 0 Velocity (cm day⁻¹)	Equation	R^2	Day 30 Velocity (cm day⁻¹)	Day 60 Velocity (cm day⁻¹)	Day 90 Velocity (cm day⁻¹)
2	3.0	$v = -0.020t + 3.0$	.99	2.4	1.8	1.2
3	2.1	$v = -0.015t + 2.1$	.99	1.7	1.2	0.8
4	4.5	$v = -0.032t + 4.5$	.99	3.6	2.6	1.7

140

4 (Fig.3) showed that the preferential flowpath is spatially constrained. Although the peak Br at well 3 lagged behind well 2 by one week, the maximum Br concentration attained in well 3 exceeded that in well 2 by two fold. Maximal nitrate concentrations encountered were 30 - 50 % of the C/C_o for Br at peak values (Fig. 4). Peak nitrate loss rates were calculated from the sizes of the shaded areas at peak bromide concentrations and normalized to travel time to yield magnitudes of 208 and 645 μM l^{-1} d^{-1} respectively.

Characterization of the N Pools

Maximal NO_3^- concentrations ranged between 3000 and 7172 μM and as a result of plume dilution and NO_3^- consumption, and declined to less than 90% of peak values within 67 days (Fig. 5). The isotopic enrichment ($^{15}N-NO_3^-$) for all wells averaged 7800 ‰ and varied within 10% of the mean for all periods except the last sampling dates for wells 2 and 3. The isotopic enrichment of 7800 ‰ is equal to the $^{15}N-NO_3^-$ of the injectate.

The NH_4^+ concentration and isotopic enrichment followed similar patterns in well 3, and to a lesser extent in wells 2 and 4, through the duration of the study (Fig. 6). NH_4^+ concentration ranged between 10.6 and 80.0 μM which is within the range observed in nearby monitoring wells of similar depth (Tobias 1999). Similar maximal ^{15}N enrichments were observed in all wells ranging between 2000 and 2400 ‰ or approximately 25 to 33% of the ^{15}N enrichment of the source NO_3^-. Peak values were reached between days 17 and 34 for all wells. Both concentration and enrichment decreased after reaching peak values to an average of 60% and 20% of their maximum values by day 100.

N_2O concentrations in all wells were undetectable at the start of the experiment and rose to maximal values (2000 - 4000 μM) on days coincident with peak Br values (Fig. 7).

Figure 5. Nitrate concentrations and isotopic enrichments. Error bars indicate the

precision of the isotopic analysis or the range of selected duplicate nitrate samples. Dilution

of high NO_3^- concentrations necessary for analysis caused most of the observed error in the

concentration measurements.
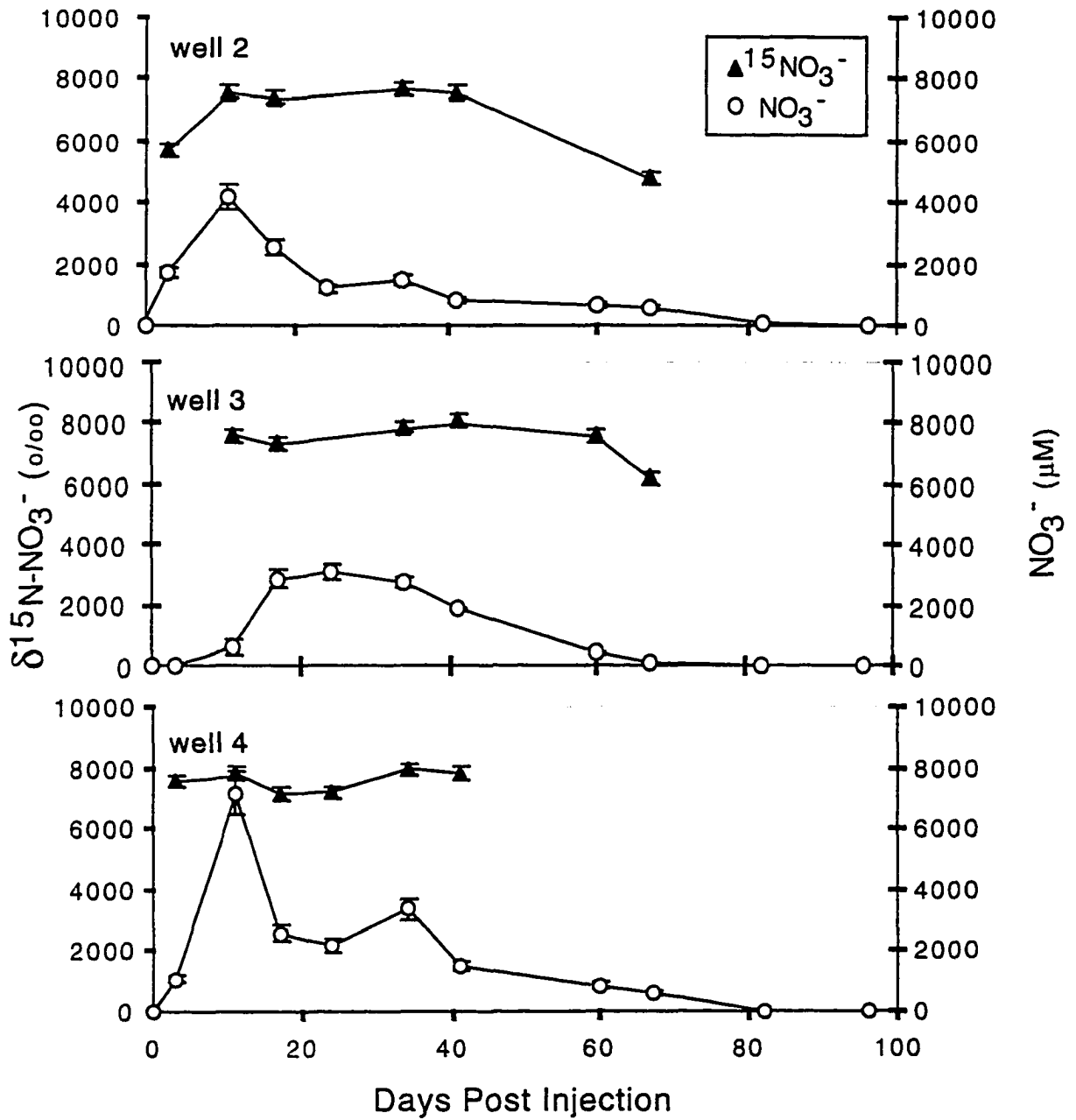
Figure 6. Ammonium concentrations and isotopic enrichments. Analytical precision for isotope analysis was within 1 ‰. Error bars for the ammonium concentrations represent the range of selected analytical duplicates.
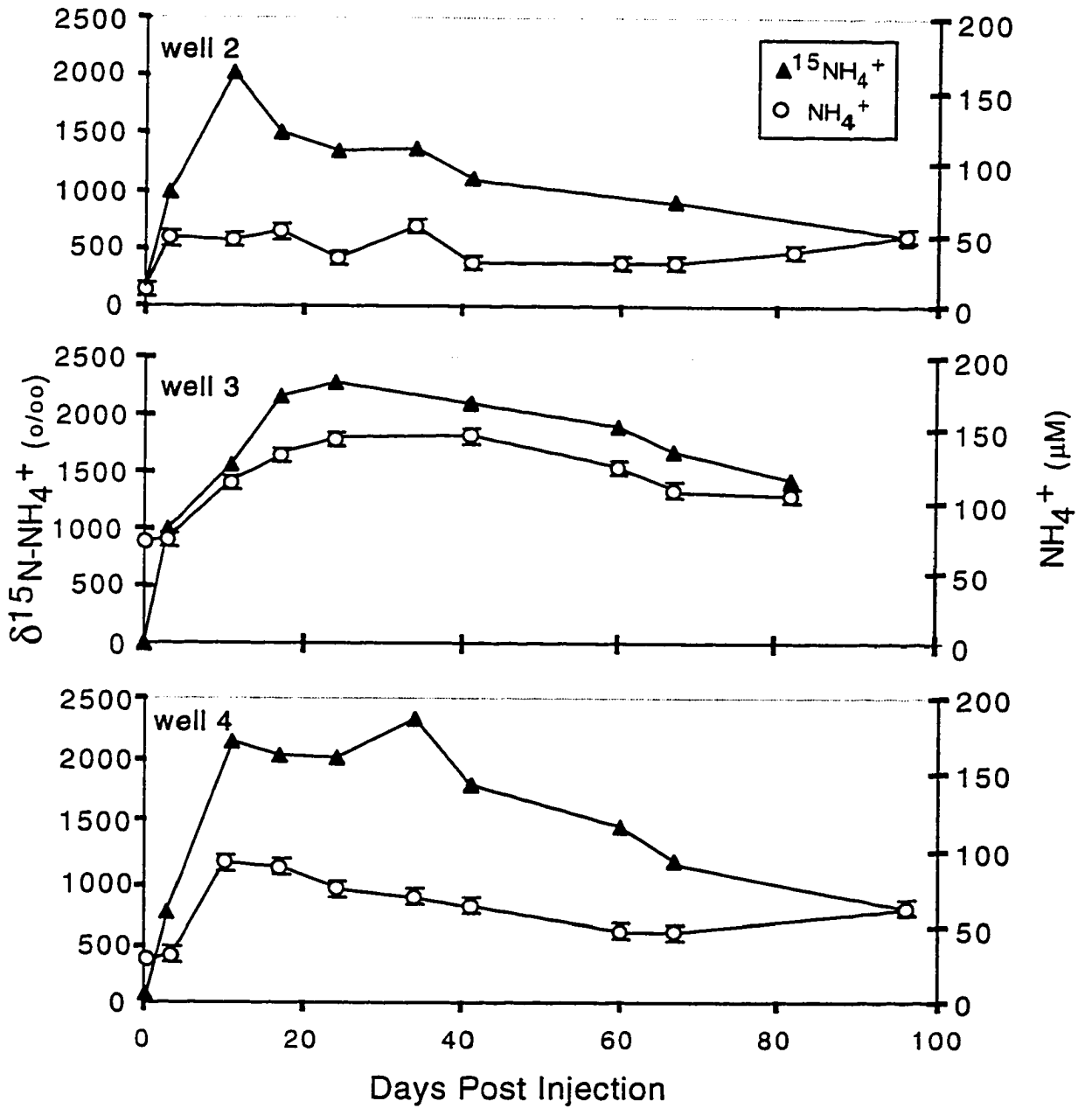
Figure 7. Dissolved nitrous oxide concentrations and isotopic enrichments. Analytical

precision for isotope analyses ranged between 28-200 ‰ and the error bars represent the

poorest analytical precision observed (200 ‰). Estimates of error for N_2O concentrations

were set at 20% of the mean. This value was derived from replicate standard headspace

equilibrations.
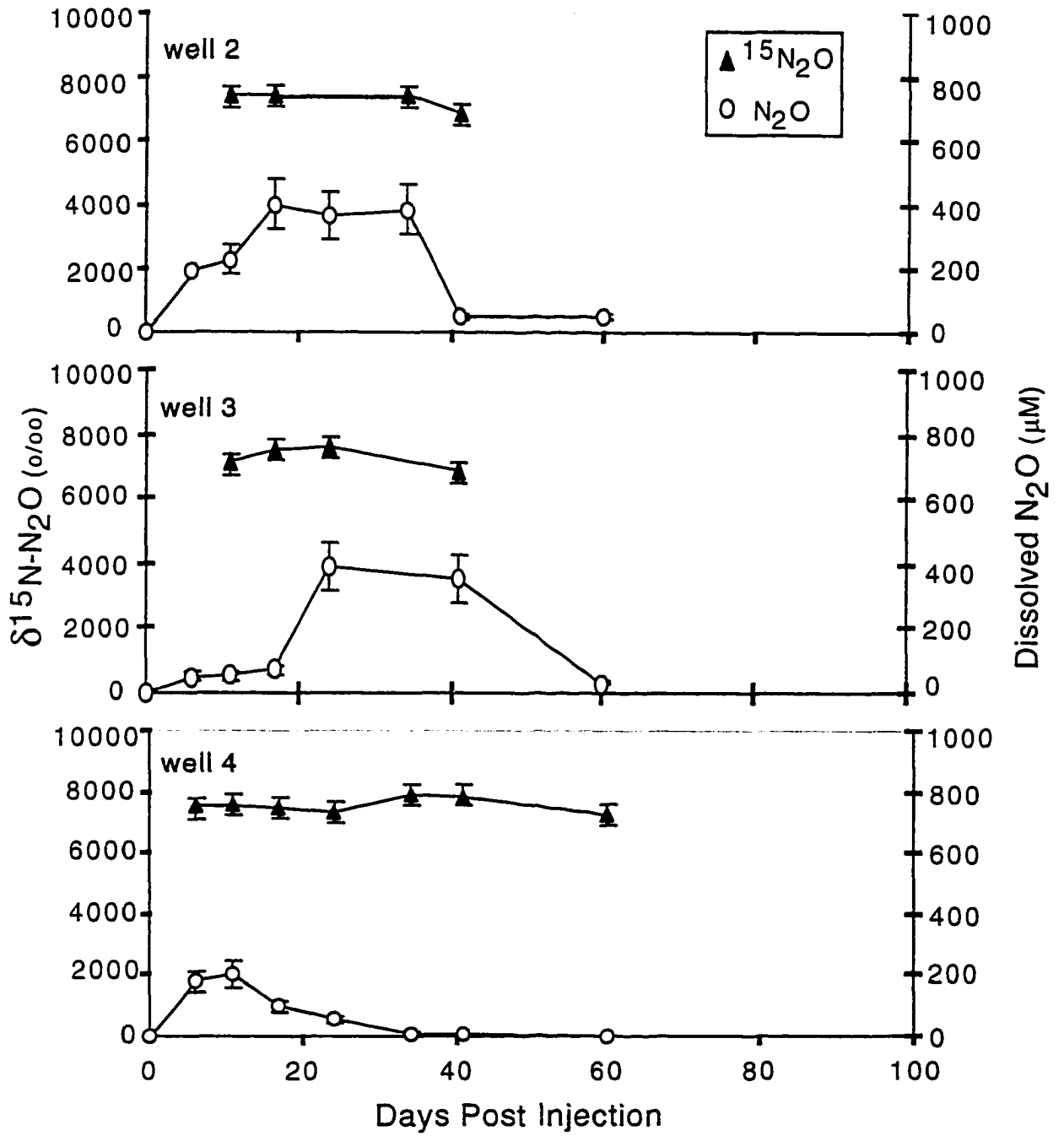
Concentrations returned to undetectable levels by day 82 after the injection. ^{15}N-N_2O levels were constant within the estimate of error at values on a par with the enrichment of the NO_3^- source (7800 ‰ ± 200 ‰).

The observed dissolved N_2, and predicted equilibrium N_2 concentrations, and the range of observed ^{15}N-N_2 enrichments are shown in Figure 8. N_2 increase did not show the same pattern as N_2O. There was only a maximum subsidy of approximately 100 μM dissolved N_2 relative to the dissolved N_2 concentration predicted at that sampling time based on the observed temperature and salinity. This is equivalent to an increase in dissolved N_2 of only 15% above background. This estimate of 15% is identical to that derived from an isotope mixing mass balance between N_2 derived from NO_3^- (7800 ‰) and ambient dissolved N2 (5 ‰). The N_2 subsidy disappeared by day 100 when the observed N_2 concentrations were at parity with or fell below predicted equilibrium concentrations. The ranges of ^{15}N- N_2 values show a slow rise followed by a plateau beginning around day 34 (Fig. 8). Values decline slightly after day 60 but did not rebound to near preinjection levels within the 100 days.

^{15}N-N_2 is reported as a range, owing to larger errors associated with measuring the isotopic enrichment of the N_2 pool. Isotopic values on selected duplicates varied between 10-80%. In nearly all cases, samples with higher quantities of N, as determined by the size of the ion beam on the IRMS, were correlated with more depleted isotopic values ($p < .05$) indicating atmospheric N_2 (δ $^{15}N_2$ = 0 ‰) as the probable source of variability. However no good fit regression equation was found that allowed for quantitative correction of isotopic values based on sample size determined during IRMS analysis. Nevertheless, the ranges of ^{15}N-N_2 reported in Figure 8 were derived from the observed values (minimums)

Figure 8. Observed and predicted equilibrium dissolved dinitrogen concentrations and isotopic enrichments. The dotted line and "X's" represent predicted N_2 equilibrium concentrations based on temperature and salinity (Weiss 1970). Open circles are the observed dissolved N_2 concentrations. Error bars represent an average error of 3% as determined from selected duplicates at all times. Triangles are the observed minimal $^{15}N_2$ values. Squares represent the maximal values and were calculated as described in the text: $[(0.8) \times (\text{observed } ^{15}N_2)] + (\text{observed } ^{15}N_2)$.
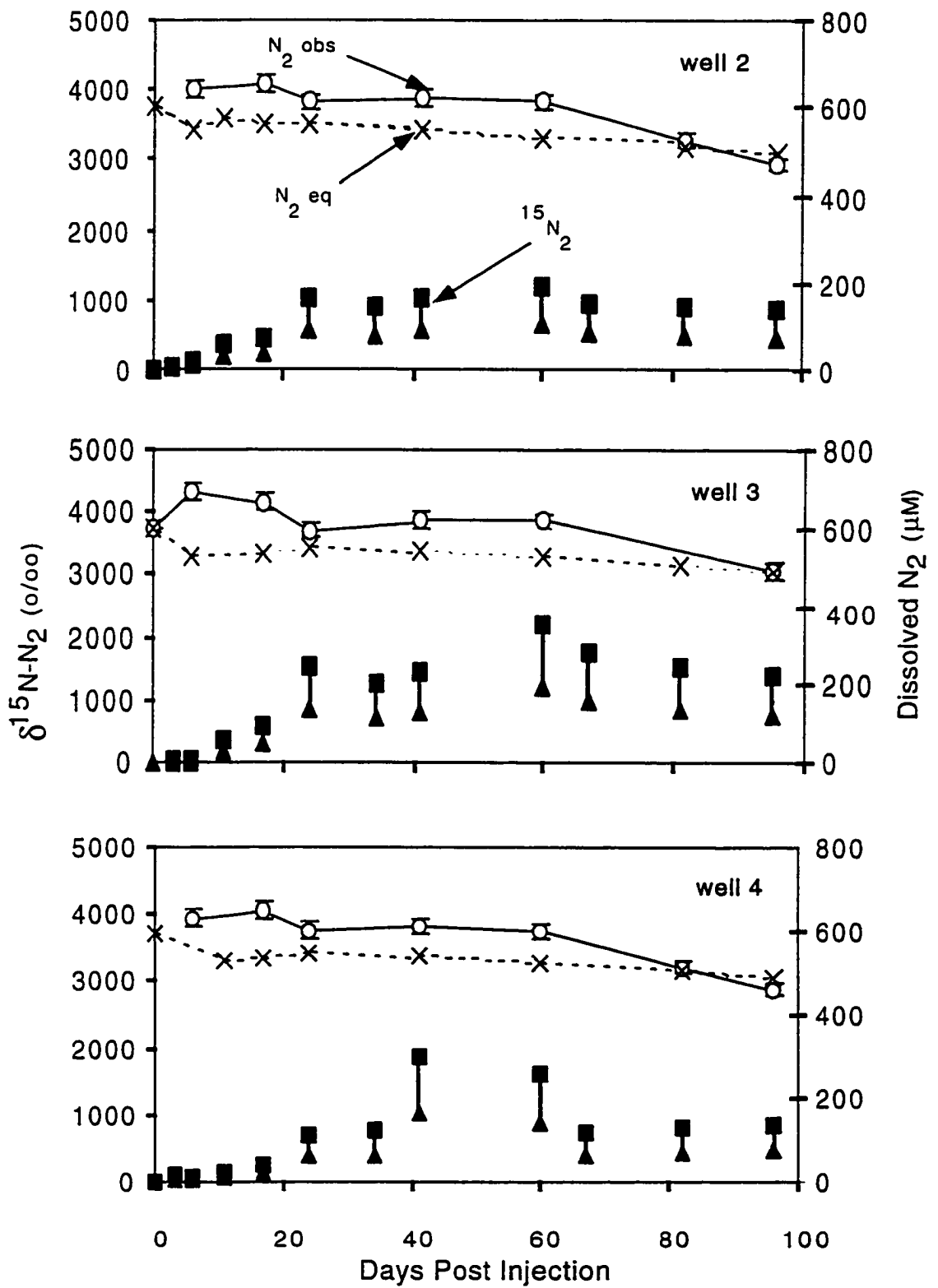
and the observed values plus the estimated maximal depletion of 80% of the observed values (maximums). The minimal estimates of ^{15}N-N_2 reported in Figure 8 were used in the mass balance.

The small N_2 subsidy was coincident with a deficit in observed argon concentrations relative to predicted equilibrium values (Fig. 9). The observed argon concentrations fell below the predicted equilibrium concentrations based on salinity and temperature by day 24 in all wells. The maximum argon deficit was 77% of the predicted equilibrium value and like the N_2 subsidy for wells 2 and 4 trended back towards equilibrium values in wells 3 and 4 near the end of the 100 day period.

Characterization of the sediment PON pool at 3 depths is given in Table 2. %N and C:N ratios for the 3 depths ranged from 0.002 - 0.277 and 13.4 - 20.3, respectively. With the exception of %N of the 40-50 cm interval, no difference between pre-injection and post-injection values of %N or C:N were detected in excess of the associated standard deviations. At the end of the study, the isotopic enrichment of 0-10, 20-30, and 40-50 cm deep sediment PON had increased by 25, 6 and 5 ‰, respectively.

Mass Balance

Estimates of N lost from the NO_3^- pool and NO_3^- derived N incorporated into the NH_4^+, N_2O and N_2 pools calculated from the isotope and concentration data are shown in Figure 10 as a function of time. The estimates were generated for each time step for the 67 days following the injection when > 90% of the NO_3^- had been consumed. Peak NO_3^- loss was observed the first 20 days for wells 2 and 4 and within 30 days for well 3. The amount of NO_3^- lost decreased as NO_3^- concentrations decreased due to both consumption and plume dilution. The magnitude of new N incorporated into the NH_4^+ was correlated

Figure 9. Predicted and observed dissolved argon concentrations. Errors ranged from

0.01 - 0.19 μM based on selected duplicates.

well 2

well 3

Dissolved Argon (μM)

well 4

Days Post Injection

---O--- Ar equilibrium
—■— Ar observed
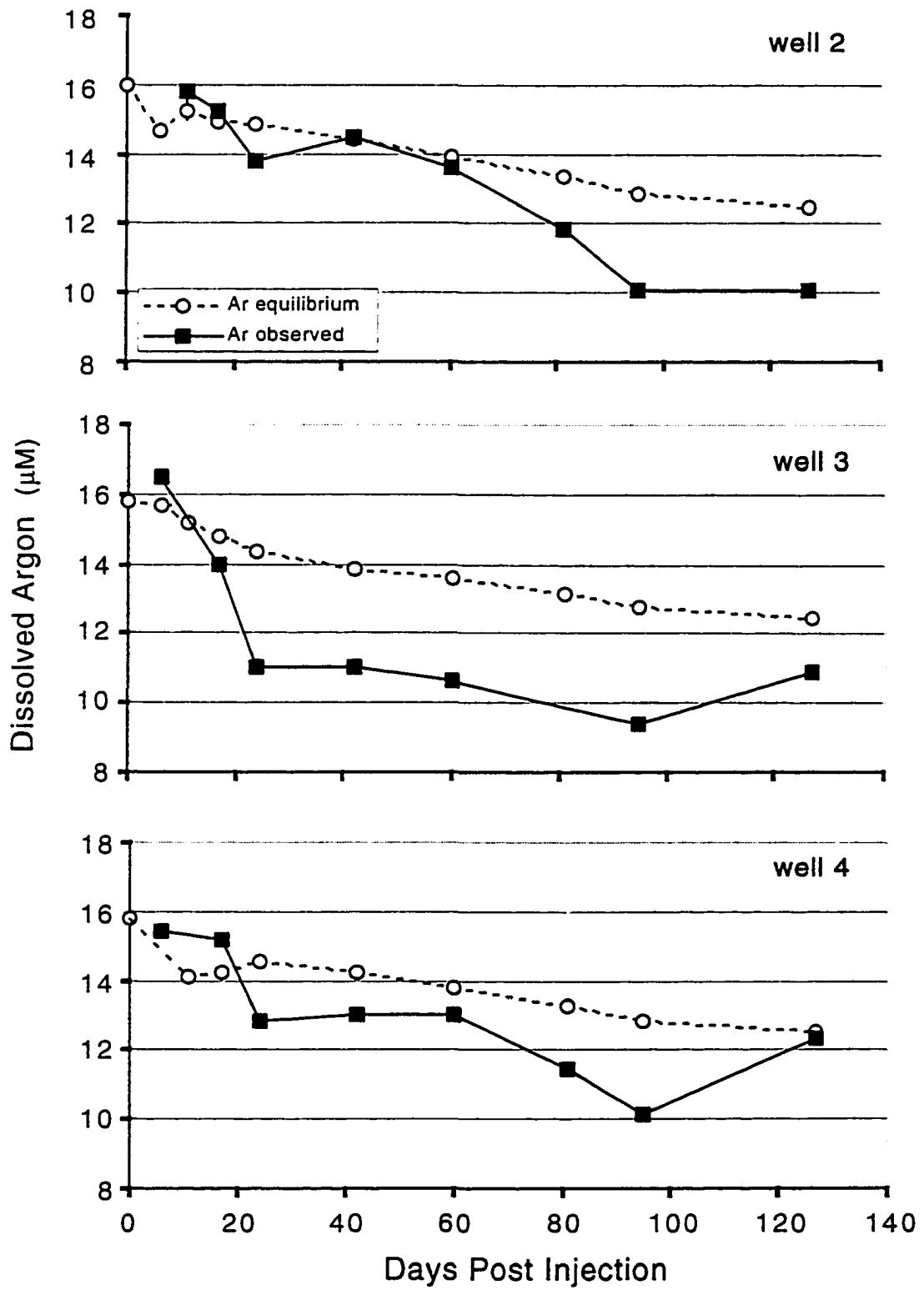
Table 2. Characterization of the sediment PON pool prior to the injection and on day 67 (post injection). Reported values are the average of measurements from duplicate cores at both samping periods located within one meter and 50 cm of the upland border for the pre injection and post injection cores respectively. δ^{15}N-PON values are reported as per mil. Range is reported in parentheses.

Depth (cm)	%N				C:N				δ^{15}N			
	Pre Injection		Post Injection		Pre Injection		Post Injection		Pre Injection		Post Injection	
0-10	.158	(.096)	.204	(.003)	17.2	(1.5)	17.4	(2.0)	3.2	(0.4)	28.3	(1.1)
20-30	.042	(.038)	.277	(.263)	16.3	(5.6)	13.4	(1.4)	3.8	(0.7)	9.8	(2.6)
40-50	.002	(.006)	.124	(.021)	20.3	(1.6)	19.9	(1.1)	3.7	(1.5)	9.0	(1.3)

Figure 10. Estimated N lost or gained for all dissolved pools vs time. Uncertainties in the estimates are discussed in the text.
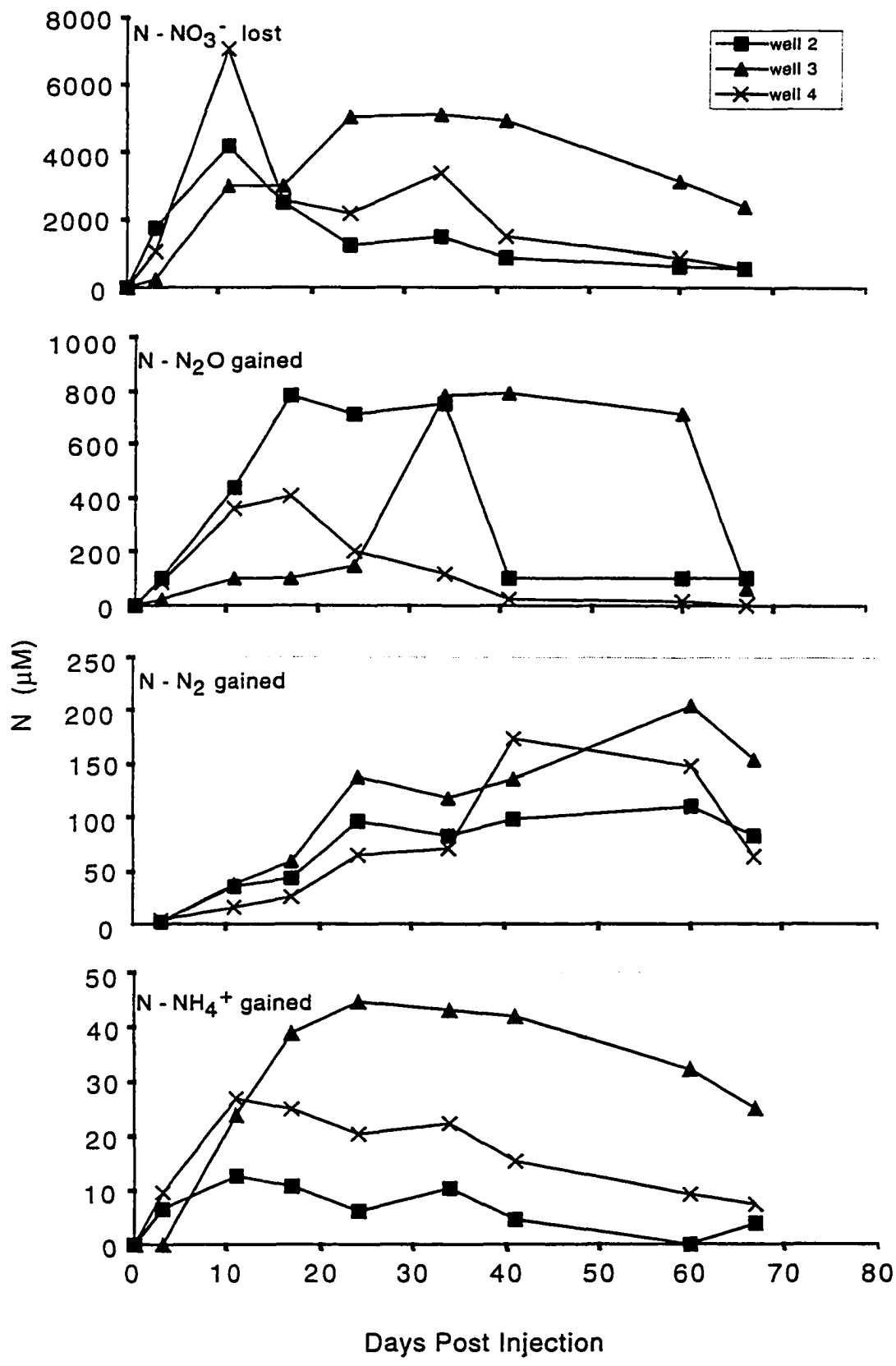
with the pattern of N loss from the NO_3^- pool (R^2 = 0.94, 0.99, 0.90 for wells 2, 3 and 4, respectively). With the exception of well 3, values returned to near zero by day 67. For each of the wells, the peak amount of new N incorporated into the N_2O pool lagged slightly behind peak N loss from the NO_3^- pool and returned to nearly undetectable levels at day 40 for wells 2 and 4, and day 60 for well 3. The incorporation of N into N_2 lagged behind N_2O production and did not show a decrease to initial values within the 67 day period All wells showed decreases at the final time measured, but do not return to pre-injection levels. The amount of new N incorporated into the N_2 pool steadily increased for most of the study period to peak values ranging between 100 - 200 μM N. Only a small decline from peak values was observed at the time the experiment was concluded.

Expression of the N lost or gained in μM N as a function of total volume of water discharged is shown in Figure 11. Integration of the area under the curves yielded estimates of the total mass of N lost or gained (μmoles) for the entire 67 day period. These estimates combined with an estimate of new N in PON derived from Table 2 are summarized in Table 3. The portion of the plume passing through well 4 lost the most N from the nitrate pool and had the poorest recovery in the mass balance. Wells 2 and 3 lost similar masses of NO_3^- but well 2 showed approximately a 30% better recovery of N in the measured products. Data from Table 3 were pooled and reported as a percent of total N lost in Figure 12a, will be discussed in the following section.

Figure 11. Estimated N lost or gained in all dissolved pools vs discharge volume. The

days post injection in Figure 10 were converted to discharge using an estimate of effective

area for each well (500 cm^2), sediment porosity of 0.79, and an estimate of decreasing

linear velocity calculated from the equations in Table 1. Uncertainties in the estimates are

discussed in the text.
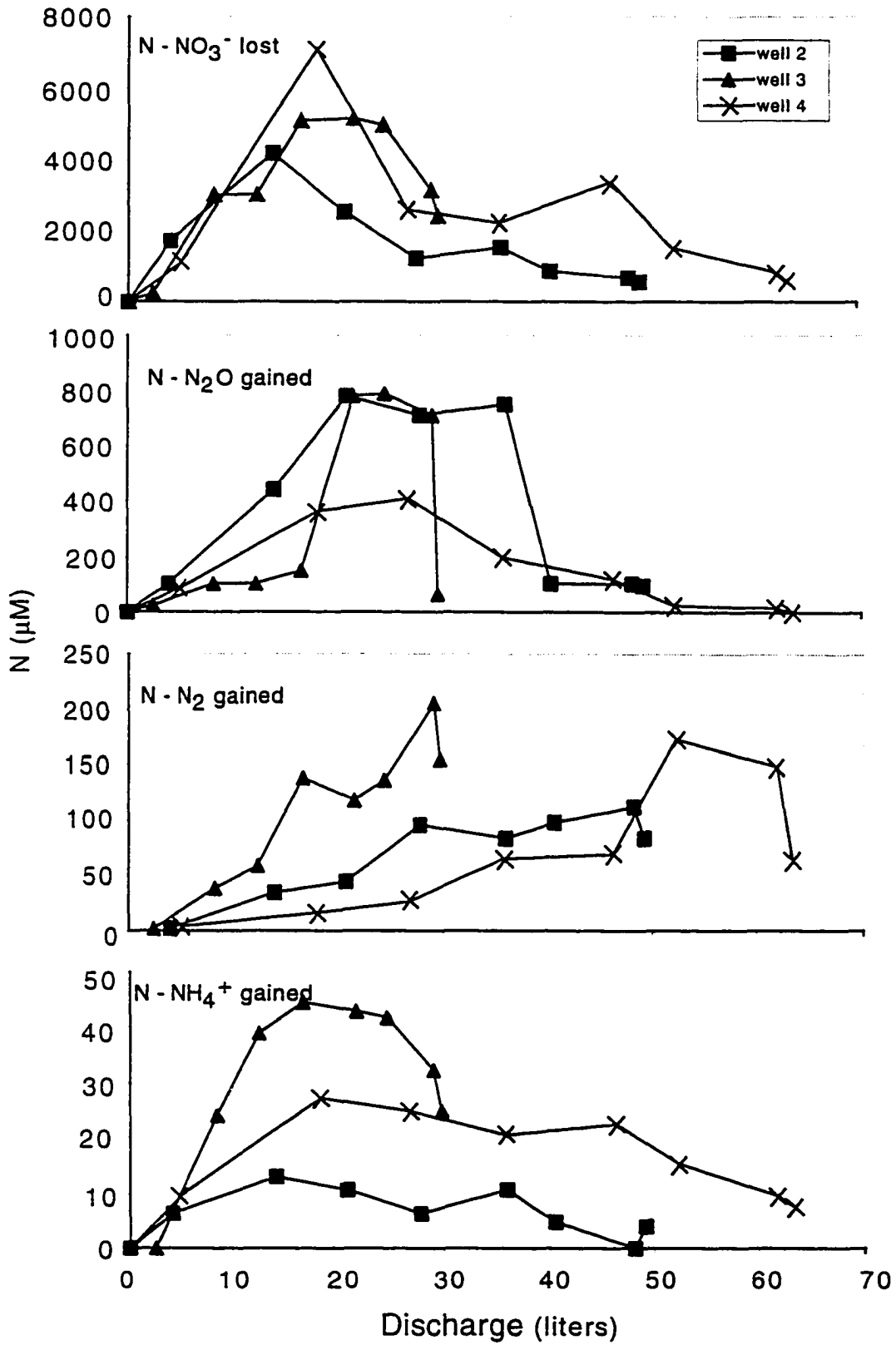
Table 3. Balance sheet of N loss and gains by well. All values are shown in mMoles. Bromide values indicate how much bromide passed through well 2, 3, and 4 during the 67 day experiment. Total Br (6002 mMoles) is 43% of total bromide added to the injection wells.

Well	Br	NO_3 (loss)	NH_4^+	N_2O	N_2	PON	Missing N
2	1233	91.1	0.4	20.9	3.0	8.4	58.4
3	1158	98.9	0.9	9.6	2.6	8.4	77.5
4	3611	174.6	1.2	11.4	3.9	8.4	149.8
Total	6002	364.6	2.5	41.9	9.5	25.2	285.7

Figure 12. Mass balance of all measured N products as a % of total N lost from NO_3^- for a 67 day period (A). Proportion of missing N in Fig. 12 A in each pool, as a % of the missing N. Determination of percents is based on estimated in situ dilution of incorporated ^{15}N or gas export, and is discussed in the text. Summary of NO_3^- - N denitrified or assimilated for the study (Fig. 12 C). Fig. 12 C was constructed by expressing data in Fig. 12 B relative to total N lost from NO_3^- and adding it to estimates from Fig. 12 A for each pool. Denitrification includes all N_2 and N_2O data as well as gas loss estimates. Assimilation includes NH_4^+, PON, and DON.

N$_2$O
(13.0%)

N$_2$
(2.7%)

NH$_4^+$
(0.7%)

PON
(7.5%)

Missing N

A. Observed Mass Balance

(% of N lost)

PON
(22.7%)

NH$_4^+$
(1.3%)

DON
(4.6%)

Missing
(DNF + Evasion?)
(21.1%)

N$_2$ stripped
(Ar deficit)
(20.3%)

Br$^-$ corrected
^{15}N$_2$ excess
(30.0%)

B. Fates of Missing N

(% of Missing N)

32 % Assimilated

68 % Denitrified

C. Overall Fate of Added NO$_3^-$ - N (adjusted)
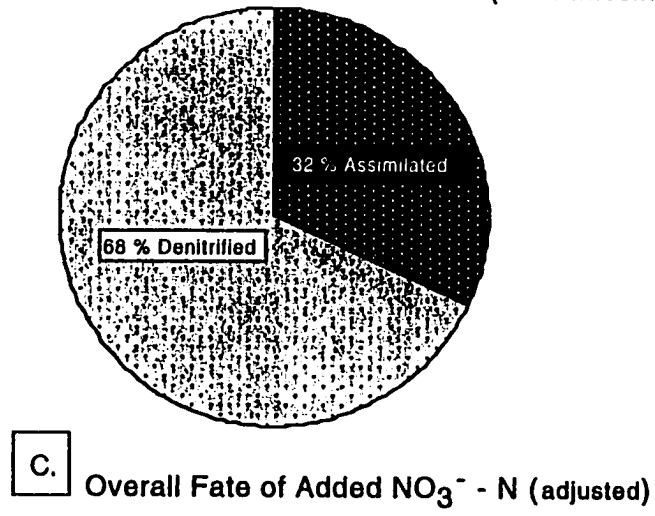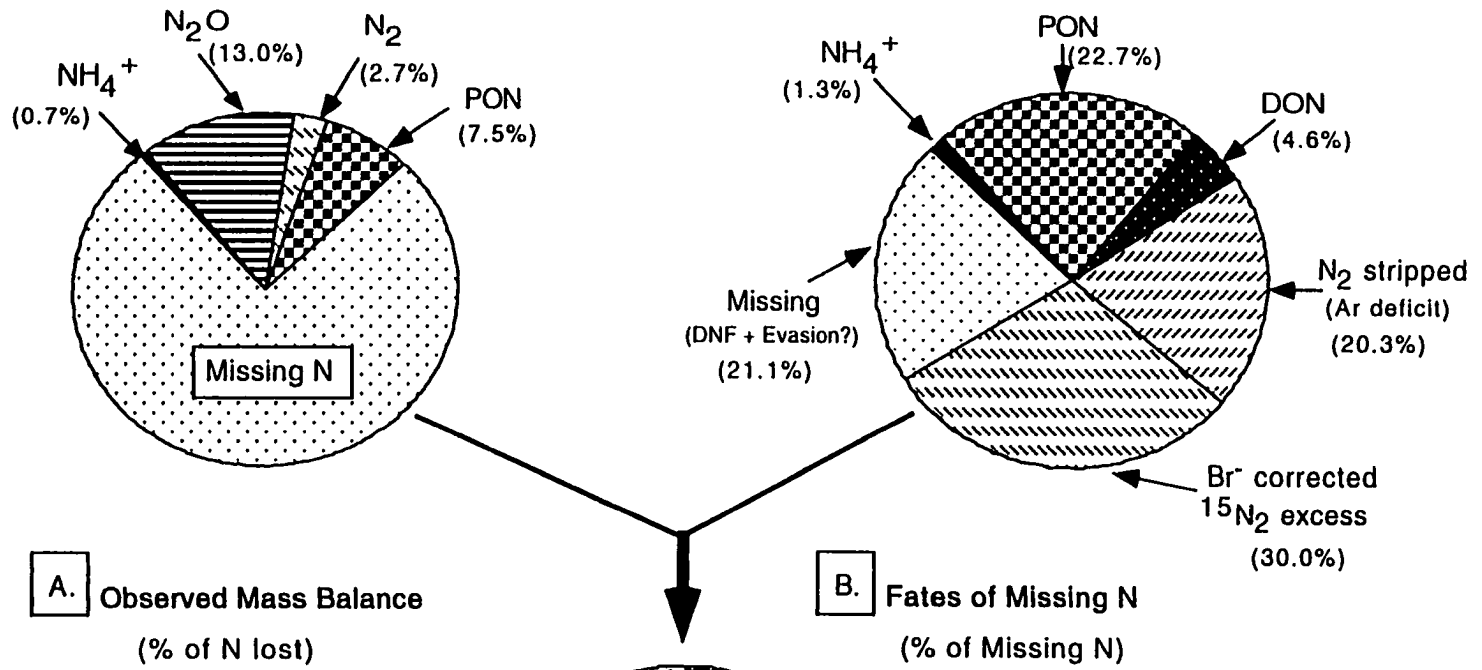
DISCUSSION

<u>Plume Characteristics</u>

Plume transport was subject to a high degree of dispersion and dilution upon discharge into the marsh. Plume transport through the marsh sediment decreases the linear velocity of discharging water and the microscale velocity differences arising from preferential flow paths may be primarily responsible for the large observed plume dispersion (Harvey and Odum 1990; Fetter 1988). Dilution of the plume was most likely caused by mixing with discharging groundwater and not tidal water. Tidal infiltration into the sediment was negligible during the first 60 days of the study (Tobias et al. 2000a). Several pieces of evidence suggest that the plume was confined within the upper 10 cm of the sediment: 1) during installation of the wells, most flow through the system was seen through macropores located within the upper 15 cm of sediment where hydraulic conductivity was highest (Tobias et al. 2000a); 2) shallow sediment pilot tracer studies showed no sinking of plumes of similar density, and strong vertical (up) gradients were encountered at the time of the study; 3) Br⁻ was detected in ponded surface water at several points within the sampling grid; 4) parallel "deep" injection study performed concurrently detected the transport of tracer from a depth of 225 cm to the surface within two weeks (Tobias unpublished data); and 5) nearly all the tracer incorporation into sediment PON (Table 2) was encountered within the uppermost 10 cm of sediment. Estimation of plume thickness and the vertical position of the plume in the sediment strata was critical for defining the control volume of sediment relevant in the mass balance, converting plume velocity into discharge volume, and likelihood of gas export to the atmosphere.

<u>N Loss from NO₃⁻</u>

Separation of the nitrate and bromide breakthrough curves occurred almost immediately indicating that nitrate loss was rapid and substantial prior to the tracer arriving

at the target wells. Loss rates calculated from peak concentrations ranged between 208 and 645 μM N d^{-1} or 684 - 2123 $\mu moles$ N m^{-2} hr^{-2} assuming a sediment thickness of 10 cm, and a porosity of 0.79. Compared to literature values for high nitrate or nitrate-amended marsh environments the total nitrate reduction rates are somewhat higher than denitrification rates reported for freshwater and salt marshes which typically range from 71-785 $\mu moles$ N m^{-2} hr^{-1} but close to the median of total NO_3^- reduction rates in estuarine and coastal sediments (Hattori 1983; Hee 1994; Kaplan et al.1979; Xue et al. 1999). Although DNF is typically nitrate limited in anaerobic sediments and is frequently governed by first-order kinetics due to low ambient NO_3^- concentrations, our system was most likely not first order for most of the study with respect to nitrate dissimilation. The mM NO_3^- concentrations generated are at the upper end of NO_3^- concentrations encountered in even the most anthropogenically impacted ground or surface waters (Bates et al. 1998; McMahon and Bohlke 1996; Smith and Duff 1988) and exceed most reported half saturation constant (K_s) values for nitrate reduction by a factor of 10-100 (Hattori 1983). Specifically, if DOC is the primary electron donor for DNF, the reaction requires a C:N ratio of 1.25 for complete conversion to N_2 (Bates and Spalding 1998). The highest DOC concentration observed at the site was 2500 μM (Tobias et al. unpublished data). The DOC:NO_3^- ratio was well below 1.25 for most of the study and zero order kinetics for denitrification have been observed in high nitrate aquifer microcosms even with C:N ratios at or exceeding 1.25 (Bates and Spalding 1998). Standing stocks of DOC, however, are likely supplemented by DOC production and may not be the sole source of electrons fueling nitrate reduction. High Fe^{++} concentrations (>500 μM) characterize the site and partially reduced iron oxides and ferrosulfur complexes can fuel denitrification (Bohlke and Denver 1995). Unless the rate of electron donor turnover was extremely fast, it remains unlikely that the reaction could be nitrate limited for all but the last month of the study when NO_3^- concentrations approached the reported K_s values, and/or the expected C:N may have exceeded 1.25.

During consumption of nitrate, the isotopic composition of the NO_3^- pool, with the possible exception of the final two sampling days remained reasonably constant. The lack of isotope dilution can be attributed to two things: a small ambient pool of NO_3^- or low *in situ* production rates of NO_3^- (i.e. nitrification) relative to the size of the labelled pool. Monitoring data from the site never recorded dissolved nitrate concentrations above 15 μM (Tobias in prep 2000b) and the peak isotopic enrichment of NO_3^- collected at target wells was equal to that of the injectate indicating a small ambient pool of NO_3^-. Laboratory determined nitrification rates for the upper 10 cm of sediment were 18 ± 2 ngN, a rate which is capable of affecting the isotope signal only over long time scales and under conditions of lower NO_3^- concentrations. Consequently, the depletion of ^{15}N-NO_3^- encountered between days 40 and 67 for wells 2 and 3 (Fig. 5) when NO_3^- concentrations were low likely reflects background nitrification.

Mass Balance of Products

Of the total N lost from NO_3^-, only 14-36% was accounted for. N_2O accounted for the majority of the recovered N (6.5-22.9%), followed by PON (4.8-9.2%), N_2 (2.2-3.2%), and NH_4^+ (less than 1%). Total N_2 estimated in the mass balance was approximately 20% of the estimated N_2O production. 64-86% of the total N lost from NO_3^- remained unaccounted for in the mass balance. The mass balance presented (Fig. 12 A) is intended to provide a first approximation of N transfer and incorporation. It is an observational framework from which we intend to construct an advection-dispersion based ^{15}N and ^{14}N transfer model at a future date. All final estimates of N incorporation were based on net estimates with respect to both stock size and isotope value. Compared with previous studies which have attempted to mass balance either labelled or unlabelled NO_3^- under *in situ* reducing conditions in aquifers or marshes, (Xue et al. 1999, Bates and Spalding 1998), our total recovery of released nitrogen (N reduced) is small. Our low

recovery of N may be attributable to several factors including but not limited to: a) incomplete characterization of all potential product pools, b) an underestimate of the enrichment of the measured pools, and c) an incomplete accounting of physical losses from the system. Factor "a" considers N transfer into unmeasured pools, while "b" and "c" may act independently or in concert to underestimate N incorporation into the measured pools.

Unsampled N Pools

Of the major N pools commonly measured in marsh N-cycling studies, three were not included in the mass balance: macrophytes, NO_2^-, and dissolved organic nitrogen (DON). Although marsh macrophytes can be considerable sinks for new N (White and Howes 1994; Dai and Weigert 1997), no above-ground macrophyte biomass was growing within the area bounded by the injection and target wells used to construct the mass balance. Little below-ground (alive) biomass was observed in cores collected for PON analysis and any contribution to label uptake by macrophytes would therefore be accounted for in the PON measurements. NO_2^- concentrations never exceeded a few μM. $NO_3^- ->$ NO_2^- is not usually the rate limiting step in denitrification and NO_2^- does not commonly accumulate under conditions (low Eh) encountered in this study (Kraynov et al. 1993). Consequently, storage of N in NO_2^- was determined to be negligible. Finally, DON concentrations were determined on select samples and found to be similar in magnitude to NH_4^+ concentrations (approximately 100 μM). Isotopic enrichment was not determined on this pool, however, even if the pool was at maximal enrichment (i.e., equal to the enrichment of the NO_3^- pool at 7800 o/oo), new N incorporation could account for no more than 5 % of the N lost from nitrate in the mass balance. We evaluate potential biases in our estimates of N losses in the following sections.

Ammonium-N (< 1% of total)

N transfer from NO_3^- into the NH_4^+ pool either directly through DNRA or indirectly through assimilatory nitrate reduction followed by mineralization was estimated to be small. Our estimate, however, is likely to be conservative due to the size and turnover of the NH_4^+ pool.

The ammonium pool in marshes turns over rapidly and may be maintained in steady state either by export to an adjacent water body or by immobilization (Anderson et al. 1997; Neikirk 1996). Mineralization is the dominant N cycling process in most marshes, and the observed isotopic enrichments of the NH_4^+ pool represent an integration of $^{15}NO_3^-$ reduction to $^{15}NH_4^+$ and ^{14}N-DON mineralization to $^{14}NH_4^+$. These factors, combined with a large initial pool of ammonium, yielded the $^{15}NH_4^+$ values which peaked at 25-30% of the substrate ($^{15}NO_3^-$) enrichment. Because of the long duration of the study, it is difficult to determine with certainty whether the labelled N entered the NH_4^+ pool directly from NO_3^- (DNRA) or whether the label was assimilated into PON directly from NO_3^-, and the subsequent rise in enrichment of the NH_4^+ pool resulted from mineralization of labelled, but less enriched, PON or DON. Ambient NH_4^+ concentrations as low 0.6 μM have been reported to inhibit assimilatory nitrate reductase in anaerobic groundwater microcosms, however the NH_4^+ concentration requirements for the suppression of nitrate assimilation remains largely unknown (Bengtsson and Annadotter 1989). If the NH_4^+ concentrations (10.6-80.0 uM) were sufficiently high throughout the study to inhibit direct assimilation of nitrate, all isotope appearance in NH_4^+ would presumably be due to DNRA. Bengtsson and Annadotter (1989) observed that reduction of NO_3^- to ammonium in anoxic groundwater microcosms was of similar magnitude as denitrification, and others have reported DNRA rates similar to DNF rates in anaerobic, sulfidic sediments. Because of high discharge, this normally mesohaline marsh assumed characteristics similar to

freshwater marshes with low porewater salinity (4 ppt), low sulfide, and high CH_4

concentrations during the study period (Tobias et al. 2000b). Although low amounts of

DNRA are consistent with results from other freshwater marshes and systems with low

$DOC:NO_3^-$ ratios (Bowden 1986; King and Nedwell 1985), our estimation of DNRA is

likely to be low.

We suggest that the estimate of N incorporation into NH_4^+ is biased on the

conservative side due to concurrent dilution of the pool by mineralization of relatively

unlabelled DON and by mixing with a large ambient pool of unlabelled NH_4^+ located

outside the plume. Gross mineralization rates determined in sediment cores averaged 225 ±

100 ngN gdw^{-1} hr^{-1}, and were three times larger than potential DNRA rates determined

from nitrate amendments (Tobias et al 2000b). Similarly, decreases in observed Br$^-$ during

the study predict a 60 - 84 % decrease in both mass and enrichment of NH_4^+ from peak

values. Because the observed mass decreases by 0-33% and the enrichment by 30-50 %

there must have been an additional transfer of labelled N into the NH_4^+ pool to satisfy the

deficit.. Although these independent estimates suggest that mineralization and ambient

NH_4^+ dilutes the DNRA signal in the NH_4^+ pool by a factor of three, the exact isotope

diluting effect is difficult to quantify because of uncertainties in the source and enrichment

of the mineralizable substrate. Nevertheless, mineralization must significantly lower the

observed enrichment of the NH_4^+ pool. Such high mineralization rates (in the absence of

large in situ nitrification rates), require that immobilization of NH_4^+ into the PON fraction

must be rapid; otherwise a huge subsidy of NH_4^+ in excess of what was observed would

have occurred (Anderson et al. 1997). Despite the potential underestimate of N transfer

into NH_4^+ it is unlikely that NH_4^+ itself is a significant sink for the new N, but instead may

serve to shuttle new N into the PON pool.

Particulate Organic Nitrogen (5 - 9% of total)

As the mass balance is presented (Fig 12 A), the amount of new N in PON is approximately the same as the amount of new N which was denitrified (N_2 +N_2O). The PON estimate assumed that N was assimilated directly from NO_3^- with an average isotopic signature of about 7800 ‰. However, high ammonium concentrations inhibit assimilatory NO_3^- reduction, and Smith et al. (1982) and Tiedje et al. (1981) demonstrated that peak N incorporation into sediment organic nitrogen (immobilization) from a labelled NO_3^- source flows initially either through NO_2^- or NH_4^+. The NH_4^+ pool enrichment in this study was only 25 to 33% of the $^{15}NO_3^-$ signal. While it is impossible in this study to determine what fraction of the immobilized nitrogen came from nitrate or ammonium, if NH_4^+ was the sole source, the amount of new N transferred into PON could be revised upward by 3 to 4 times its current estimate (i.e., between 13 - 30%) of the total N lost. Further, the pool size and isotopic enrichment of PON was not assessed during the course of the study, but rather at the experiment's onset and conclusion (t_0 and t_{70}). Because there is a constant rate of immobilization occurring in the marsh it is plausible that our estimates of new N incorporation are based on a PON pool that had already undergone significant isotopic depletion as a result of *in situ* immobilization and are consequently biased low. If one assumes that immobilization kept pace with mineralization (Anderson et al. 1997) and estimates of mineralization based on laboratory isotope dilution experiments (225 ngN gdw^{-1} hr-1) were accurate, it is possible that an additional 51 mmoles of N entered the PON pool through mineralization / immobilization over the course of the study. This represents 18% of the total measured PON fraction and consequently may have biased the observed isotopic enrichment by a commensurate amount. An increase in the C:N ratio would support this conclusion; however, because the active microbial population is probably a relatively small component of a spatially variable POM pool composed primarily of macrophyte detritus, no such shift in C:N could be discerned. The estimates of new N

incorporated into PON (Fig 12 A) should therefore be regarded as minimums.

N_2O (7 - 23% of total)

The dissolved oxygen and Eh values in the upper 10 cm of the marsh [for springtime periods] measured during the Spring prior to the injection were less than 10 μM and -125 to -210 mv, respectively. These conditions generally preclude either the production of N_2O from nitrification or the long term accumulation of N_2O as an intermediate product of denitrification. Because ambient N_2O stocks are nearly undetectable and *in situ* N_2O production under ambient conditions is negligible, there is little chance that we underestimated new N incorporation into N_2O because of isotope dilution effects. This is supported by the fact that the isotopic enrichment of N_2O came to parity with the enrichment of the substrate NO_3^-, thus clearly identifying the labelled nitrate as its source. There is, however, the possibility that we have underestimated the size of the N_2O pool as a result of gas export to the atmosphere. This is one possible explanation for the fact that the total N_2 produced does not equal the total N_2O produced (Fig 12, Table 3). Deficits in the mass balance of N_2O produced from NO_3^- during *in situ* aquifer C_2H_2 block studies suggest some N_2O loss from these types of systems (Bragan et al. 1997). Although N_2O export to the atmosphere has been observed in less reducing forest soils, it is seldom seen in wetland studies (Bowden et al. 1992; Xue et al 1999). In high nitrate-amended marsh microcosms, Xue et al. (1999) could account for less than 0.1% of the added nitrate in the gaseous N_2O pool despite high overall rates of denitrification. Consequently, we suspect that most of the gas loss from the system was in the form of N_2 and not as N_2O.

Because only a slight increase in the dissolved N_2 concentration was noted in the presence of significant isotope incorporation, N_2O may have been converted quickly to N_2,

but because of the lower solubility of N_2 relative to N_2O, and the proximity of the plume to the atmosphere (i.e.the upper 10 cm), N_2 was rapidly exported to the atmosphere. This explanation is supported by dissolved argon concentrations and discussed in the following section.

N_2 (2 -3%)

The estimated amount of new N which was incorporated into the N_2 pool is small compared to similar work using marsh or aquifer microcosms. Xue et al. (1999) was able to account for 58% of the NO_3^- lost to the gaseous N_2 pool following a surface application of $^{15}NO_3^-$ to the marsh surface in microcosms. Similarly, results from denitrifying aquifer microcosms show that 66 % of the NO_3^- lost could be accounted for by shifts in the ratio of Ar/N_2 (Bates and Spalding 1998). Despite the 1.6 meter depth of the microcosm, the remaining 34% of the N_2 was believed to have been lost to the atmosphere as a result of the supersaturation conditions. We suspect that our estimate of N incorporation greatly underestimates the amount of new N in this pathway because of both isotope dilution by a large unlabelled dissolved N_2 pool, and high rates of N_2 evasion to the atmosphere.

The rise in the isotopic enrichment of the N_2 pool was slower than the isotopic enrichment of the other pools indicating either a lagged process of N_2O to N_2 conversion (Firestone et al. 1980), or a greater background rate of dilution. The N_2 pool is subject to the greatest underestimate due to isotope dilution because it has the largest ambient pool size (450-700 μM). The maximum enrichment encountered in the N_2 pool was about 2100 o/oo (or about 25% of the NO_3^- isotope signal). There is only slight dilution of the isotope pool following peak values although changes in Br⁻ concentration indicate that there should be a 60 - 80% decrease due to mixing with non-plume water containing unlabelled dissolved N_2. As with the ammonium pool, the fact that the isotope signal becomes

depleted by less than 100 per mil in wells 2 and 3 while the mass remains essentially constant indicate that an additional source of labelled N must have been incorporated. Based upon the Br^- dilution and assuming an average equilibrium concentration of dissolved N_2 of 600 μM with an isotope value of 5 o/oo, approximately 300 $\mu moles\ l^{-1}$ of new N at 7800 o/oo must have been incorporated into the N_2 pool above that which was estimated. This would effectively elevate the amount of new N incorporated over the discharge period by approximately 88 mmoles or roughly 24 % of the total N lost as shown in the mass balance (Fig 12 A).

The observed (net) amount of ^{15}N incorporated into N_2 was sufficient to elevate the dissolved N_2 concentration to 1.3 times that measured, yet the observed increase in concentration was only 15% of the initial pool size. This difference is similar to the 50% loss of dissolved N_2 encountered by Bates and Spalding (1998) in a shallow aquifer, and illustrates that the inability to account for all the NO_3^- reduced by mass balance is most likely due to evasion of dissolved N_2 (and potentially N_2O) to the atmosphere. This mechanism is consistent with the observed stability of the $^{15}N_2$ signal and supported by the observed loss of argon from the system relative to predicted argon equilibrium concentrations (Fig. 9). We propose two mechanisms for N_2 export to the atmosphere: gas stripping through ebullition and evasion of N_2 under these supersaturated conditions.

Bubble formation and ebullition can be a dominant gas transport mechanism in freshwater marshes with high methane concentrations (Chanton et al. 1989). Our site is characterized by elevated methane concentrations (100 μM) and is supersaturated with respect to dissolved CO_2 (up to 5000 μM). Bubble formation in samples warmed to room temperature is rapid and extensive. Based upon the argon deficit, dissolved N_2 concentrations, and the solubility of argon and nitrogen (argon is 2.5 times more soluble

than N_2), we estimate that the total amount of N_2 stripped out of the system over the entire study was between 15 and 18 mmoles N. Based on this rough calculation, gas stripping could account for an additional 10-20% of the total NO_3^- -N lost at each well.

In addition to ebullition-mediated gas export, evasion at the water table-atmosphere interface driven by a high N_2 concentration gradient is suspected to generate a further loss of dissolved N_2. Because the water table was at or near the sediment surface for most of the study and vertical advective gradients confined the plume to the upper 10 cm of the water table, evasion potential should have been maximized. Evasion rates of gases from aqueous environments are variable and it is beyond the scope of this paper to derive a confident estimate of evasion of N_2 from this sedimentary environment. Nevertheless, an approximation of evasion based on Schmidt numbers and gas piston velocities of N_2 at the water table-atmosphere interface is more than sufficient by nearly two orders of magnitude to account for all the missing N in the mass balance (Wannikoff 1992; Hartman and Hammond 1984). However N_2 transport through the sediments, and not evasion itself, is most likely the rate limiting step for N_2 export to the atmosphere by this mechanism. Therefore, it is the gas flux rate to the atmospheric interface that is the relevant potential rate of N_2 export. Molecular diffusion is slow, but the diffusional distance to the atmospheric interface was reduced by the vertical transport of groundwater by both pressure head, and by evapotranspiration (Tobias et al. 2000a). Further, gas transport via convective flow through lacunal spaces in some emergent macrophytes accelerates the flux of dissolved gas from porewaters to the atmosphere (Chanton and Whiting 1996). We suggest that evasion (aided by vertical advection, and macrophyte mediated convection) was faster than the estimated N_2 production rate. Consequently, higher dissolved N_2 concentrations were never detected. Thus, much of the missing N may have been denitrified and exported to the atmosphere as N_2.

Revision of Mass Balance

Using the estimates of isotope dilution or gas export, each component of the original mass balance was revised to account for portions of the missing N fraction (Fig 12B). The two pools accounting for most of the missing N were N_2 and PON. Uncertainties in measuring the N_2 pool may account for 51% of the missing N. The estimate of N_2 loss by gas stripping (calculated from observed Ar deficits) was approximately 20 % of the missing N. The estimate of additional N incorporation into the N_2 pool (based on the observed Br$^-$ corrected $^{15}N_2$ and [N_2] excesses) was approximately 30% of the missing N. PON accounted for 23% of the missing N when NH_4^+ was assumed to be the sole N substrate for immobilization. DON's contribution to the missing N was estimated to be maximal at 4.6% when DON concentrations were assumed to be constant at 100 µM and its isotopic enrichment was assumed to be equal to that of NO_3^- (7800 ‰). Despite a possible 3 fold underestimate of the isotopic enrichment of the NH_4^+ pool, this fraction could account for only 1% of the missing N. While not a long term repository for N, we propose that NH_4^+ provided an important link between NO_3^- and PON. Following these revisions, approximately 21% of the missing N remained unaccounted for. However, because the estimated magnitude of N_2 evasion was believed to be high relative to the size of the missing N_2 pool, we suggest that this process was the likely fate of the remaining missing N.

When these fractions of missing N were incorporated into the original mass balance (Fig 12 A), the resulting proportion of N assimilated into the marsh vs. N denitrified is approximately 1:2 (Fig 12 C), with 84% of the denitrified N exported to the atmosphere within the 67-day study.

SUMMARY AND CONCLUSIONS

Denitrification followed by rapid export of N_2 to the atmosphere on short timescales (days to months) is the primary fate (at least 68%) of the groundwater derived nitrate load to this marsh. Assimilation of N into the sediment PON pool was the second largest sink, constituting up to 30% of the NO_3^- lost. The ammonium pool appears to be a highly active intermediate between DNRA and the ultimate immobilization of new N into PON, but does not represent a longer term storage compartment for N. Initial attempts to mass balance the N lost from NO3- and the observed incorporation of ^{15}N into N_2, N_2O, NH_4^+, and PON fractions proved to be underestimates (by 3-5 fold) as a result of *in situ* turnover of unlabelled N and rapid gas export out of the porewater.

To our knowledge, a study like this has not been attempted in these types of systems. This work illustrates the utililty of natural ^{15}N releases to simultaneously quantify multiple pathways under *in situ* conditions, and demonstrated that the use of conservative tracers in the aqueous (Br-) and gas (Ar) phases, as well as the hydrologic characterization of the discharge zone were critical in refining the final mass balance.

LITERATURE CITED

Alpkem. 1992. Nitrate/nitrite flow solution methodology. Document no. 00630. Perstorp Analytical Inc.

Anderson, I.C., C.R. Tobias, B.B. Neikirk, and R.L. Wetzel. 1997. Development of a process-based nitrogen mass balance model for a Virginia Spartina alterniflora saltmarsh: Implications for net DIN flux. Marine Ecology Progress Series. **159**: 13-27.

Bates, H.K., G.E. Martin, and R.F. Spalding. 1998. Kinetic isotope effecs in production of nitrite-nitrogen and dinitrogen gas during *in situ* denitrification. J. Enrivon. Qual. **27**:183-191.

Bates H.K., and R.F. Spalding. 1998. Aquifer denitrification as interpreted from *in situ* microcosm experiments. J. Environ. Qual. **27**:174-182.

Bengtsson, G., and H. Annadotter. 1989. Nitrate reduction in a groundwater microcosm determined by 15N gas chromatography-mass spectrometry. Applied and Environmental Microbiology. **55**: 2861-2870.

Bohlke, J.K., and J.M. Denver. 1995. Combined analysis of groundwater dating, chemical, and isotopic analyses to resolve the history and fate of nitrate contamination in two agricultural watersheds, Atlantic coastal plain, Maryland. Wat. Res. Res. **31**: 9, 2319-2339.

Bokuniewicz, H. J. 1982. Analytical descriptions of subaqueous groundwater seepage. Estuaries. **15**: 458-464.

Bowden, W.B. 1986. Nitrification, nitrate reduction, and nitrogen immobilization in a tidal freshwater wetland. Ecology. **67**: 88-99.

Bowden, W.B., W.H. McDowell, C.E. Asbury, and A.M. Finley. 1992. Riparian nitrogen dynamics in two geomorphologically distinct tropical rain forest watersheds: nitrous oxide fluxes. Biogeochemistry **18**: 77-99

Bowden, W.B., J. Merriam, J. Tank, R. Hall, K. MacNeale, P. Mulholland, J. Webster, and B. Sichol. 1998. The Hubbard Brook LINX Project: nitrogen transformations in a northern hardwood forest stream. Am. Soc. Limnol. Oceanog. - Aquatic Sciences Meeting - Abstract only.

Bragan, R.J., J.L. Starr, and T.B. Parkin. 1997. Shallow groundwater denitrification rate measurement by acetylene block. J. Environ. Qual. **26**:1531-1538.

Brooks, P.D., J.M. Stark, B.B. McInteer, and T. Preston. 1989. Diffusion method to prepare soil extracts for automated nitrogen-15 analysis. Soil Sci. Soc. Am. Proc. **53**:1707-1711.

Capone, D.G., and M.F. Bautista. 1985. A groundwater source of nitrate in nearshore sediments. Nature. **313**: 214-216.

Chanton, J.P., C.S. Martens, and C.A. Kelley. 1989. Gas transport from methan-saturated, tidal freshwater wetland sediment. Limnol. Oceanogr. 34: 807-819.

Chanton, J.P., and G.J. Whiting. 1996. Methane stable isotopic distributions as indicators of gas transport mechanisms in emergent aquatic plants. Aquatic Botany. 54: 227-236.

Dai, T., and R.G. Wiegert. 1997. A field study of photosynthetic capacity and its response to nitrogen fertilization in Spartina alterniflora. Estuarine, Coastal and Shelf Science 45: 273-283.

Fetter, C.W. 1993. Contaminant Hydrogeology. Macmillan Publishing.

Fetter C.W. 1988. Applied Hydrogeology, 2nd Edition. Merrill Publishing.

Finkelstein, K., and C.S. Haraway. 1988. Late Holocene sedimentation and erosion of estuarine fringing marshes, York River, Virginia. Journal of Coastal Research. 4:3, 447-456.

Firestone, M.K., R.B. Firestone, and J.M Tiedje. 1980. Nitrous oxide from soil denitrification: Factors controlling its biological production. Science 208:749-751.

Giblin, A.E., and A.G. Gaines. 1990 Nitrogen inputs to a marine embayment: the importance of groundwater. Biogeochemistry. 10: 309-328.

Hartman B., and D.E. Hammond. 1984. Gas exchange rates across the sediment-water and air-water interfaces in south San Francisco Bay. Journal of Geophysical Research 89:C3, 3593-3603.

Harvey, J.W., and W.E. Odum. 1990. The influence of tidal marshes on upland groundwater discharge to estuaries. Biogeochemistry. 10: 217-236.

Hattori, A. 1983. Denitrification and dissimilatory nitrate reduction. p. 191-233. In D.G. Capone and E.J. Carpenter [eds.] Nitrogen in the marine environment.

Hee, C., Howes. B.L., and P.K. Weiskel. 1995. the potential of denitrification for intercepting groundwater nitrate in a salt marsh ecosystem. In J.P. Grassle, A. Kelsey, E. Oates and P.V. Snelgrove [eds.] Twenty Third Benthic Ecology Meeting Conference Proceedings.

Holmes, R.M., B.J. Peterson,L.A. Deegan, J.E. Hughes, and B. Fry. 1999. Nitrogen biogeochemistry in the oligohaline zone of a New England estuary. Ecology. In press.

Howes, B.L., P.K.Weiskel,D.D. Goehringer, and J.M. Teal. 1996. Interception of freshwater and nitrogen transport from uplands to coastal waters: the role of saltmarshes. p. 287-310. In K.F. Nordstrom and C.T. Roman [eds.] Estuarine shores: evolution, environments and human alterations. John Wiley and Sons.

Hughes, J.E., L.A.Deegan, B.J. Peterson,R.M. Holmes, and B. Fry. 1999. Nitrogen flow through the food web in the oligohaline zone of a New England estuary. Ecology. In press.

Johannes, R.E. 1980. The ecological significance of the submarine discharge of groundwater. Mar. Ecol. Prog. Ser. 3: 365-373.

Kana, T.M., C. Darkangelo, M.B. Hunt, J.B. Oldham, G.E. Bennett, and J.C. Cornwell. 1994. Membrane inlet mass spectrometer for rapid high-precision determination of N_2, O_2, and Ar in enrivonmental water samples. Analytical Chemistry 66:23, 4166-4170.

Kaplan, W., I. Valiela, and J.M. Teal. 1979. Denitrification in a salt marsh ecosystem. Limnol. and Oceanog. 24: 726-734.

King, D., and Nedwell. 1985. The influence of nitrate concentration upon the end-products of nitrate dissimilation by bacteria in anaerobic salt marsh sediment. FEMS Microbial Ecol. 31: 23-28.

Knowles, R. 1990. Acetylene inhibition technique: development, advantages, and potential problems, p. 151-166. In N.P Revsbech and J. Sorenson [eds,], Denitrification in soil and sediment. Plenum Press.

Koike, I., and A. Hattori. 1978. Denitrification and ammonia formation in anaerobic coastal sediments. Appl. Env. Micro. 35: 278-282.

Koike, I., and J. Sorenson. 1988. Nitrate reduction and denitrification in marine sediments, p. 251-270. In T. Blackburn and J. Sorenson [eds.], Nitrogen cycling in the coastal marine environments. John Wiley and Sons.

Koroleff, F. 1983. Simultaneous oxidation of nitrogen and phosphorous compounds by persulphate. In K. Grasshoff, M. Ehrhardt, and K. Kreming [eds.], Methods of seawater analysis. Verlag Chemie.

Kraynov, S.R., G.A. Solomin, and V.P. Zakutin. 1993. Redox conditions for nitrogen-compound transformations in groundwater. Geochemistry International 6: 822-831.

Libelo, E.L., W.G. MacIntyre, and G.H. Johnson. 1990. Groundwater nutrient discharge to the Chesapeake Bay: Effects of near-shore land use preactices. Neww perspectives in the Chesapeake System: A research and management partnership. 613-622.

McMahon, P.B., and J.K. Bohlke. 1996. Denitrification and mixing in a stream-aquifer system: effect on nitrate loading to surface water. J. Hydrol. 186: 105-128.

Neikirk, B.B. 1996. Exchanges of dissolved inorganic nitrogen and dissolved organic carbon between salt marsh sediments and overlying tidal water. MA thesis, College of William and Mary, Gloucester Point, VA.

Nielsen L.P. 1992. Denitrification in sediment determined from nitrogen isotope pairing. FEMS Microbiology Ecology. **86**: 357-362.

Oberdorfer, J.A., M.A. Valentino, and S.A. Smith. 1990. Groundwater contribution to the nutrient budget of Tomales Bay, California. Biogeochemistry **10**: 199-216.

Peterson, B.J., M. Bahr, and G.W. Kling. 1997. A tracer investigation of nitrogen cycling in a pristine tundra river. Canadian Journal of Fisheries and Aquatic Sciences. **54**: 2361-2367.

Portnoy, J.W., B.L. Nowicki, C.T. Roman, and D.W. Urish. 1998. The discharge of nitrate-contaminated groundwater from a developed shoreline to a marsh-fringed estuary. Wat. Res. Res. **34**: 11, 3095-3104.

Reay, W.G., D.L. Gallagher, and G.M. Simmons. 1993. Sediment-water column nutrient exchanges in Southern Chesapeake Bay nearshore environments. Virginia Wat. Res. Bulletin. **181**: all.

Reilly, T.E., and A.S. Goodman. 1985. Quantitative analysis of saltwater-freshwater relationships in groundwater systems--A historical perspective. J. Hydrol. **80**: 125-160.

Simmons, G.M. 1989. The Chesapeake Bay's hidden tributary: submarine groundwater discharge. p. 9-29. *In* Proceedings of groundwater issues and solutions in the Potomac River Basin / Chesapeake Bay Region.

Smith, C.J., R.D. DeLaune, and W.H. Patrick Jr. 1982. Nitrate reduction in *Spartina alterniflora* marsh soil. Soil Sci. Soc. Am. J. **46**:748-750.

Smith, R.L., and J.H. Duff. 1988. Denitrification in a sand and gravel aquifer. Applied and Environmental Microbiology. **54**:5, 1071-1078.

Solorzano, L. 1969. Determination of ammonia in natural waters by the phenylhypochlorite method. Limnology and Oceanography **14**: 799-801.

Tiedje, J.M. 1988. Ecology of denitrification and dissimilatory nitrate reduction to ammonium. p. 179-224. *In* A. Zehnder [ed.] Biology of anaerobic organisms. John Wiley and Sons.

Tiedje, J.M., J. Sorenson, and Y.L. Chang. 1981. Assimilatory and dissimilatory nitrate reduction: perspectives and methodology for simultaneous measurements of several nitrogen cycle proceses. *In* F.E. Clark and T Rosswall [eds.] Terrestrial Nitrogen Cycles. Stockholm: Ecology Bulletin.

Tobias, C.R., J.W. Harvey, and I.C. Anderson. 2000a. Estimating groundwater discharge through fringing wetlands to estuaries: a comparison of methods and implications for marsh function. In prep.

Tobias, C.R., I.C. Anderson, and E.A. Canuel. 2000b. Nitrogen cycling through an aquifer - fringing marsh transition zone. In prep.

Valiela, I., K. Foreman, M. LaMontage, D. Hersh, J. Costa, P. Peckol, B. DeMeo-Andreson, C. D'Avanzo, M. Babione, C. Sham, J. Brawley and K. Lajtha. 1992. Couplings of watersheds and coastal waters: sources and consequences of nutrient enrichment in Waquoit Bay, Massachussettes. Estuaries. **15**: 443-457.

Valiela, I., and J.M. Teal. 1979. Nitrogen budget for a salt marsh ecosystem. Nature. **280**: 652-655.

Wannikoff, R. 1992. Relationship between wind speed and gas exchange over the ocean. Journal of Geophysical Research **97**:C5, 7373-7382.

Weiss, R.F. 1970. The solubility of nitrogen, oxygen, and argon in water and seawater. Deep-Sea Research. **17**: 721-735.

White, D.S., and B.L. Howes. 1995. Long term 15N-nitrogen retention in the vegetated sediments of a New England salt marsh. Limnol. Oceanog. **39**: 8, 1878-1892.

Xue, Y., D.A. Kovacic, M.B. David, L.E.Gentry, R.L.Mulvaney, and C.W. Lindau. 1999. *In situ* measurements of denitrification in constructed wetlands. J. Env. Qual. **28**: 263-269.

Appendix Ia. Raw Bromide and Nitrate Data

Well #2

Days Post Inject	Avg Br Co	Br obs mM	Avg NO3 Co	NO3 obs uM
0	959	0.06	119266	0.3
3	959	13.68	119266	1728.0
11	959	41.71	119266	4176.0
17	959	47.02	119266	2506.0
24	959	27.25	119266	1223.0
34	959	26.29	119266	1498.0
41	959	10.51	119266	848.0
60	959	6.02	119266	653.0
67	959	4.89	119266	567.0

Well #3

Days Post Inject	Avg Br Co	Br obs mM	Avg NO3 Co	NO3 obs uM
0	959	0.15	119266	0.2
3	959	1.49	119266	15.1
11	959	29.10	119266	604.0
17	959	47.02	119266	2835.0
24	959	65.40	119266	3094.6
34	959	62.83	119266	2712.0
41	959	54.63	119266	1845.0
60	959	28.18	119266	390.0
67	959	19.54	119266	67.5
82	959	15.35	119266	1.9
96	959	10.81	119266	3.1

Well #4

Days Post Inject	Avg Br Co	Br obs mM	Avg NO3 Co	NO3 obs uM
0	959	0.15	119266	0.2
3	959	41.45	119266	1069.0
11	959	127.82	119266	7172.0
17	959	96.59	119266	2565.0
24	959	47.57	119266	2191.0
34	959	28.46	119266	3380.0
41	959	15.71	119266	1519.0
60	959	7.05	119266	858.0
67	959	4.70	119266	582.0

Appendix Ib. Raw Nitrate Concentration and Isotope Data

Days Post Inject	Well #2 NO3- (uM)	15 NO3- (o/oo)	Well #3 NO3- (uM)	15 NO3- (o/oo)	Well #4 NO3- (uM)	15 NO3- (o/oo)
0	0.3		0.2		0.2	
3	1728.0	5719.6	15.1		1069.0	7570.7
11	4176.0	7570.7	604.0	7570.0	7172.0	7828.9
17	2506.0	7405.1	2835.0	7317.0	2565.0	7151.6
24	1223.0		3094.6		2191.0	7198.5
34	1498.0	7685.4	2712.0	7857.0	3380.0	7943.8
41	848.0	7570.7	1845.0	8064.0	1519.0	7828.9
60	653.0		390.0	7628.0	858.0	
67	567.0	4817.2	67.5	6258.0	582.0	
82	82.0		1.9		19.0	
96	5.6		3.1		2.2	

174

Appendix Ic. Raw Ammonium Concentration and Isotope Data

Days Post Inject	Well #2 NH4+ uM	15 NH4+ (o/oo)	Well #3 NH4+ uM	15 NH4+ (o/oo)	Well #4 NH4+ uM	15 NH4+ (o/oo)
0	10.6	6.0	80.0	6.0	32.2	6.0
3	46.9	997.1	72.3	1000.0	95.4	744.1
11	46.1	2030.5	111.7	1565.0	92.4	2136.3
17	51.7	1504.0	131.2	2158.0	88.9	2036.4
24	33.4	1341.2	142.8		74.3	2002.8
34	56.1	1363.7		2279.0	69.8	2328.1
41	30.1	1116.7	145.0	2095.0	63.5	1776.7
60	30.3		123.0	1908.0	46.9	1450.7
67	30.0	912.1	108.0	1677.0	46.3	1169.5
82	38.6		104.0	1436.0	151.1	
96	48.9	600.7			62.2	788.3

175

Appendix Id. Raw Nitrous Oxide Concentration and Isotope Data

Days Post Inject	Well #2 N2O (uM)	15 N2O (o/oo)	Well #3 N2O (uM)	15 N2O (o/oo)	Well #4 N2O (uM)	15 N2O (o/oo)
0	0.0		0.0		0.0	
6	188.0		50.4		177.7	7542.0
11	224.6	7398.8	51.0	7169.0	202.6	7570.7
17	400.5	7456.1	73.2	7513.0	98.2	7484.7
24	363.9		388.9	7599.0	57.3	7341.5
34	383.7	7398.8			10.7	7886.4
41	50.6	6884.4	352.0	6884.0	7.3	7828.9
60	51.3		32.0		0.9	7255.7

Appendix Ie. Raw Molecular Nitrogen Concentration and Isotope Data

Days Post Inject	Well #2 N2 (uM)	15 N2 (o/oo)	Well #3 N2 (uM)	15 N2 (o/oo)	Well #4 N2 (uM)	15 N2 (o/oo)
0		6.9	600.0	6.0		6.9
3		29.1		18.2		52.3
6	642.5	73.8	692.4	15.8	631.9	36.5
11		200.2		201.3		90.1
17	652.3	255.2	665.0	327.8	649.0	147.5
24	611.9	571.1	593.2	847.7	602.6	397.8
34		509.6		708.5		420.3
41	623.1	573.5	619.9	802.8	610.5	1037.2
60	612.2	658.9	618.1	1215.4	600.5	895.6
67		536.6		974.3		418.4
82	523.8	508.6		852.0	513.0	447.5
96	467.8	471.8	493.2	773.0	461.2	471.4

PROJECT SUMMARY AND SYNTHESIS

NITRATE REDUCTION AT THE GROUNDWATER - SALT MARSH INTERFACE

The overall objective of this project was to better define the interaction between groundwater discharge and a fringing marsh from two perspectives: 1) the potential influence on estuarine water quality (marshes as buffers), and 2) the effects on N cycling and retention within the marsh. Specifically we characterized the temporal pattern and magnitude of groundwater discharge into a fringing estuarine marsh, the influence of discharge on the cycling of autochthonous nitrogen within the marsh ecosystem, and the extent and mechanisms by which fringing marshes modify discharging groundwater nitrate loads.

Groundwater discharge to the marsh occurred seasonally from January to June. Construction of a non steady state mass balance for water and salt yielded the best estimates of the discharge magnitude during this period. Estimates of discharge during high flow based on hydraulic head and conductivity measurements (Darcy's Law) proved to overestimate the amount of discharge by nearly 3 fold. The majority of the discharge flowed horizontally through the upper one meter of marsh sediment where N cycling rates were highest. The groundwater flowing through the upper one meter of sediment is however likely to be a small percentage of the total groundwater discharged to the estuary. Thus, despite the discharge occurring where potential nitrate reduction rates were greatest, the overall effect of the marsh on attenuating groundwater nitrate loads would be small.

In contrast, the magnitude of discharge is large enough near the upland border to dominate the sediment water budget in those zones of the marsh. Discharge catalyzed a seasonal flushing of porewaters as was evidenced by decreasing porewater conductivity during the Spring discharge. In addition to driving an export of materials to the estuary, this flushing altered porewater geochemistry with respect salt, sulfide, and electron acceptors. Consequently, large differences N cycling rates were observed at high vs. low

discharge periods despite the lack of an increased groundwater N flux. The pattern of exponential decay in N cycling rates with sediment depth remained constant, but the depth integrated rates of mineralization, nitrification, and potential DNRA increased during high discharge. The increase in potential DNRA during high discharge was accompanied by a nearly 10 fold decrease in potential DNF such that 2.5 times as much of the N nitrified was reduced back to ammonium rather than exported out of the ecosystem through DNF. Nevertheless, during the Spring discharge, the marsh looses almost 3 times as much N through coupled nitrification - denitrification as during low discharge periods. Not only is this N not available for immobilization or macrophyte production, but the organic carbon oxidized during denitrification, is no longer available for accretion.

When groundwater containing high nitrate loads is introduced into these systems, most (at least 50%) of the nitrate is denitrified and exported to the atmosphere on short timescales (days - weeks). Depending on the size of the groundwater nitrate flux, denitrification may represent a sizeable sink for marsh carbon. Offsetting some of the N lost through DNF, was nearly 30 % of the nitrate loads which underwent DNRA followed by rapid immobilization into the sediment PON pool. Once in PON, the nitrogen is likely to be remineralized and reimmobilized several times (on timescales greater than months) prior to ultimate export out of the marsh. Nevertheless, DNF dominated the reduction of groundwater nitrate during discharge through this mesohaline marsh.
Consequently, marshes or zones of marshes, subject to large influxes of groundwater, particularly high nitrate groundwater, may be less apt to keep pace with rising sea level due to the loss of C and N through DNF, and ultimately less sustainable within the landscape.

Although ecotones are often considered active sites of biogeochemical transformation, traditional approaches to quantifying N cycling processes have been limited

because of disturbance the natural state of the system. Our application of a combined tracer test with the in situ use of ^{15}N isotope enrichment allowed the study of one such ecotone (the groundwater saltmarsh interface) with minimal disruption of in situ gradients. Despite the physical and biogeochemical complexity of the discharge zone, this technique, when used in conjunction with conservative tracers in the gas and aqueous phase, provided insight into the fate of groundwater nitrate during discharge. This method is a potentially powerful ecological tool to for quantifying the behavior of nitrogen under natural conditions, and insights gained from the use of this techniques should prove valuable for the application of this approach to a variety of marine, aquatic, and terrestrial ecosystems.

VITA

Craig Robert Tobias

Born in New York, NY, 28 September 1967. Earned a B.A. in Biology from the University of Delaware in 1989. Served as the Assistant Research Biologist, Virgin Islands National Park from 1990-1991, and as an Environmental Consultant with Tetra Tech, Incorporated, Wilmington, DE from 1991-1993. Entered the Ph.D. program in the Biological Sciences Department at the School of Marine Science, College of William and Mary in September 1993.